SYNTHESIS AND CHARACTERIZATION OF IRON-DOPED TITANIUM DIOXIDE THIN FILMS

Sigei Sharon Chemutai

A Thesis Submitted in Partial Fulfillment of the Requirements for the Degree of Master of Science in Physics of Murang'a University of Technology

August, 2026

DECLARATION

Student Declaration

I hereby declare that this thesis is my original work and, to the best of my knowledge, has not been presented with a degree award at this university or any other university. I understand what plagiarism is and I am aware of the university's policy in this. I understand that any false claim regarding this work shall result in disciplinary action in accordance with the University Anti-Plagiarism Policy.

_____ _____

Chemutai Sharon Date

AS402/5134/2024

Supervisors' Approval

The undersigned certify that they have read and hereby recommended for acceptance of Murang'a University of Technology a thesis entitled **"Synthesis and Characterization Iron-Doped Titanium Dioxide Thin Films."**

_____ _____

Dr. John Njagi Date

Department of Physical and Biological Sciences

Murang'a University of Technology

_____ _____

Dr. Jatani Ungula Date

Department of Physical Sciences

Rongo University

DEDICATION

I devote this work to my dear parents, Richard Cheruiyot Sigei and Jane Cherono Sigei whose constant guidance, motivation and selfless efforts have formed the cornerstone of my educational path. To my siblings Gladys, Caren, Winny, Brenda, Mercy, Faith and Benard who instilled in me the values of hard work and perseverance, thank you for always believing in me. To everyone who stood by me through the challenges, your kindness and strength have been my greatest motivation.

ACKNOWLEDGEMENT

First and foremost, I wish to convey my deep appreciation to Dr John Njagi (Murang'a University of Technology) and Dr Jatani Ungula (Rongo University), my project supervisors, for their priceless advice, assistance and encouragement throughout this study. Their knowledge, thoughtful guidance and patience were essential for the successful completion of this work. I am also thankful to Dr Sharon, the Department of Physical and Biological Sciences and the entire faculty at Murang'a University of Technology for their support and for fostering a positive learning environment. My sincere gratitude extends to my family and friends for their constant love, support and understanding during this endeavour. Their encouragement and confidence in me have been a continuous source of strength. Lastly, I would like to acknowledge everyone who, directly or indirectly, played a role in the achievement of this project.

ABSTRACT

Titanium dioxide (TiO_2) is a very promising thin film photovoltaic (PV) material since it is abundant, chemically stable and non-toxic. It has however, a comparatively large bandgap (3.0–3.2 eV), which only allows absorption within the ultraviolet region, making it less effective for use in solar energy conversion. The wide study of Fe is caused by its potential to enhance the optical characteristics of TiO_2 by the creation of impurity energy levels that aid in the absorption of visible light. In this work the 3 mol% iron doped titanium dioxide (Fe: TiO_2) thin films were deposited on clean soda-lime glass substrates by spin coating method. The influence of the volume of precursor solution, spinning time and number of deposited layers on the structural and optical properties were investigated and the stability of the optimized films were examined for 28 days. The X-ray diffraction (XRD), Fourier transform infrared (FTIR) spectroscopy and UV-Vis spectroscopy with Tauc plot analysis were used to characterize the deposited films, after annealing at 450 °C for 2 h. All samples showed the formation of mixed phases of anatase and rutile TiO_2 by XRD analysis. The best volume of precursor solution was 1.0 mL, which had the largest crystallite size of 4.107 nm and a smaller full width at half maximum (FWHM) value of 1.992°. By changing the spinning time, it was found that 30 s gives the optimum crystallinity, the crystallite size was 5.206 nm and the FWHM was 1.571° which is the best crystal growth from the uniform film formation. Optimum layer number was 5 and resulted in high crystalline films with better uniformity of the structure. FTIR spectra showed the presence of both Ti–O–Ti and Ti–O–Fe bonds, which confirmed the incorporation of Fe in the TiO_2 lattice. The results of the UV–Vis analysis revealed that the optical band gap depended on the deposition parameters. The band gap of 2.96 eV obtained for the optimum spinning time of 30 s was lower than the typical band gap of 3.2 eV of undoped TiO_2, which was attributed to the Fe induced impurity energy levels that narrowed the band gap and increased the visible light absorption. The optimized films showed only minor changes in the peak position, FWHM and crystallite size for the 28-day time period, which gave evidence of good structural stability. The results of this study show that the parameters of spin coating can be optimized to obtain the best structural and optical characteristics for 3 mol% Fe doped TiO_2 thin films. Specifically, films with improved crystallinity, lower band gaps and enhanced stability were generated after spinning for 30 s using 1mL precursor solution volume and 5 layers were deposited onto the surface, which are promising materials for use in better PV devices.

TABLE OF CONTENTS

DECLARATION ..... **ii**
DEDICATION ..... **iii**
ACKNOWLEDGEMENT ..... **iv**
ABSTRACT ..... **v**
LIST OF TABLES ..... **ix**
LIST OF FIGURES ..... **x**
ACRONYMS AND ABBREVIATIONS ..... **xii**
CHAPTER ONE: INTRODUCTION **1**
1.1 Background of the Study 1
1.2 Statement of the Problem 2
1.3. Research Objectives 3
1.3.1 General Objective 3
1.3.2 Specific Objectives: 3
1.4 Research Questions 3
1.5 Significance of the Study 4
1.6 Scope and Limitations 4
1.7 Contributions of the Thesis 5
1.8 Organization of the Thesis 5
CHAPTER TWO: LITERATURE REVIEW **7**
2.1 Introduction 7
2.2 Global Energy Demand and the Transition to Renewable Energy 7
2.3 Solar Cells 7
2.3.1 Operation of Solar Cells 8
2.3.2 Types of Solar Cells 9
2.4 Thin Film Photovoltaics 10
2.5 Titanium Dioxide 11
2.5.1 Polymorphism of Titanium Dioxide (TiO_2) 11
2.5.2 Electrical and Electronic Properties of TiO_2 12
2.5.3 Charge Carrier Dynamics in TiO_2 13
2.6 Properties of TiO_2 13
2.6.1 Optical Properties 13
2.6.2 Electrical Properties 14
2.6.3 Structural Properties 14
2.7 Metal Ion Doping Mechanism in TiO_2 15
2.7.1 Effect of Doping on Band Gap Engineering 15
2.7.2 Dopants 16
2.8 TiO_2 Doping 17

2.8.1 Iron Doping....18
2.8.2 Role of Annealing in Thin Film Formation....19
2.9 Deposition of Thin Films....20
2.9.1 Dip Coating....20
2.9.2 Vapor Deposition....20
2.9.3 Sputtering....21
2.9.4 Electroplating....21
2.9.5 Thermal evaporation....22
2.9.6 Chemical Bath Deposition....22
2.9.7 Spin Coating....22
2.9.8 Spin Coater....23
2.10 Factors Affecting Thin Film Quality in Spin Coating....25
2.11 Recombination Mechanisms in Thin Films and Efficiency Parameters of Solar Cells....26
2.12 Thermal Treatment Equipment....27
2.12.1 Laboratory Oven....27
2.12.2 Muffle Furnace....28
2.13 Analytical Techniques and Characterization of Coatings....29
2.13.1 Fourier Transform Infrared Spectroscopy....30
2.13.2 Ultraviolet-visible spectroscopy....32
2.13.3 X-ray diffraction....34
2.14 Research Gaps and Proposed Solutions....36
2.14.1 Material Selected: TiO_2....36
2.14.2 Choice of Dopant: Iron....37
2.14.3 Thin-Film Synthesis Techniques....37
2.14.4 Thin-Film Deposition Methods....38
2.14.5 Characterization Techniques....39
2.14.6 Overall Research Gap Addressed by the Study....39
2.15 Chapter Summary....40
CHAPTER THREE: MATERIALS AND METHODS....41
3.1 Introduction....41
3.2 Materials....41
3.3 Methods....41
3.3.1 Deposition of Fe:TiO_2 thin films of varying precursor volumes using spin coating technique....42
3.3.2 Variation of Spinning Time in the Deposition of Fe:TiO_2 Films....43
3.3.3 Formation of spin coated layers of Fe:TiO_2 Thin Films....43
3.3.4 Stability of Fe: TiO_2 Thin Films over Twenty Eight Days....43
3.4 Characterization of the Fe: TiO_2 Thin Films....43

3.4.1 X-ray diffraction Analysis 44
3.4.2 FTIR Analysis 44
3.4.3 UV–Vis analysis 45
3.5 Chapter Summary 45
CHAPTER FOUR: RESULTS AND DISCUSSION 46
4.1 Introduction 46
4.2 Fe: TiO_2 Thin Films Spin Coated Using Varying Precursor Solution Volumes 46
4.2.1 XRD Analysis of Fe:TiO_2 Thin Films Spin Coated Using Varying Precursor Volumes 46
4.2.2 FTIR Analysis of Fe:TiO_2 Thin Films Spin Coated Using Varying Precursor Volumes 51
4.2.3 UV-Vis Spectroscopy Analysis Of Fe:TiO_2 Thin Films Spin Coated Using Varying Precursor Volumes 53
4.3 Deposited Fe: TiO_2 Thin Films using Varying Spinning Times 55
4.3.1 XRD Analysis of Fe:TiO_2 Thin Films Deposited using Varying Spinning Times 55
4.3.2 FTIR Analysis of Fe: TiO_2 Thin Films Deposited using Varying Spinning Times 60
4.3.3 UV–Vis Analysis of Fe: TiO_2 Thin Films Deposited using Varying Spinning Times 62
4.4 Fe: TiO_2 Thin Films Coated using a Varying Number of Layers 63
4.4.1 XRD Analysis of Fe:TiO_2 Thin Films Coated using a Varying Number of Layers 64
4.4.2 FTIR Analysis of Fe: TiO_2 Thin Films Coated using a Varying Number of Layers 68
4.4.3 UV-Vis spectroscopy Analysis of Fe: TiO_2 Thin Films Coated using a Varying Number of Layers 70
4.5 Stability of Fe: TiO_2 Thin Films over Twenty-Eight Days 72
4.6 Chapter Summary 75
CHAPTER FIVE: CONCLUSION AND RECOMMENDATIONS 76
5.1 Conclusion 76
5.2 Recommendations 77
5.2.1 Recommendation from the study 77
5.2.2 Proposed future research 78
REFERENCES 79
APPENDICES 92

LIST OF TABLES

Table 4.1: Summary of the crystallite sizes, FWHM and the lattice parameters of Fe: TiO_2 thin films deposited using different volumes. 49
Table 4.2: Summary of the crystallite sizes, FWHM and the lattice parameters of Fe:TiO_2 thin films spin coated at different durations. 57
Table 4.3: Summary of the crystallite sizes, FWHM and the lattice parameters of Fe:TiO_2 thin films of varying number of layers. 65
Table 4.4: XRD Stability Analysis of Optimized Fe: TiO_2 Thin Film Over 28 Days. 74

LIST OF FIGURES

Figure 2.1: Evolution of solar photovoltaic technology through four main generations 8
Figure 2.2: Behavior of incoming light with a deposited film 10
Figure 2.3: Light transmission through a thin film 11
Figure 2.4: Polymorphs of TiO_2 (a) anatase (tetragonal), (b) rutile (tetragonal) and (c) brookite (orthorhombic 12
Figure 2.5: Effects of Fe as trapped states 19
Figure 2.6 A spin coater at Murang'a University of Technology 24
Figure 2.7: Spin coating technique 24
Figure 2.8 A laboratory oven at Murang'a University of Technology 28
Figure 2.9: A muffle furnace at Murang'a University of Technology 29
Figure 2.10 IR spirit Shimadzu Fourier Transform Infrared (FTIR) spectrophotometer at Murang'a University of Technology 32
Figure 2.11 Evolution one plus UV-Vis spectroscopy at Murang'a University of Technology 33
Figure 2.12 ARL Equinox 100 X-Ray diffractometer (XRD) at Murang'a University of Technology 35
Figure 3.1: Schematic flow chart of the preparation and deposition of Fe: TiO_2 thin films 42
Figure 4.1: XRD spectra of Fe: TiO_2 thin films of varying precursor volume (a) Full range XRD pattern (b) Magnified XRD pattern 47
Figure 4.2: Variation of FWHM and Crystallite Size of deposited Fe: TiO_2 thin films using varying volumes of the precursor. 50
Figure 4.3: FT-IR spectra of Fe:TiO_2 thin films deposited using different precursor volumes 52
Figure 4.4: (a) Absorbance spectra as a function of wavelength and (b) Tauc plots of $\alpha h\nu 1/2$ versus photon energy $h\nu$ for Fe-doped TiO_2 thin films deposited using precursor solution volumes ranging from 0.5 mL to 2.5 mL. 54
Figure 4.5: XRD patterns of Fe: TiO_2 thin films spin coated using different durations (a) full range XRD pattern, (b) magnified XRD pattern 56
Figure 4.6: Variation of FWHM and crystallite size as a function of the duration of spinning Fe-doped TiO_2 thin films. 59
Figure 4.7: FT-IR spectra of Fe: TiO_2 thin films deposited using varying spinning time 61
Figure 4.8: (a) the absorbance as a function of wavelength (b) the plots of $\alpha h\nu)1/2$ versus photon energy $h\nu$ for the different spinning durations 62

Figure 4.9: XRD patterns of Fe: TiO_2 thin films prepared with different numbers of deposited layers (a) full range XRD pattern (b) magnified XRD pattern 64
Figure 4.10 Variation of FWHM and crystallite size as a function of the number of deposited layers of Fe: TiO_2 thin films 67
Figure 4.11: FT-IR spectra of Fe: TiO_2 thin films with varying number of deposited layers..... 69
Figure 4.12: (a) the absorbance as a function of wavelength (b) the plots of $\alpha h\nu)1/2$ versus photon energy hν for the different layer numbers..... 71
Figure 4.13: A photograph of an optimized Fe:TiO_2 thin film..... 72
Figure 4.14: XRD patterns of the optimized Fe: TiO_2 thin film monitored over a period of twenty-eight days at intervals of one week..... 73

ACRONYMS AND ABBREVIATIONS

AFM	Atomic force microscopy
CdTe	Cadmium telluride
CIGS	Copper indium gallium selenide
CVD	Chemical vapor deposition
DSSC	Dye-sensitized solar cell
FTIR	Fourier transform infrared spectroscopy.
OSC	Organic solar cell
PSC	Perovskite solar cell
PV	Photovoltaic
PVD	Physical vapor deposition
SEM	Scanning electron microscopy
TFSC	Thin-film solar cells
TiO_2	Titanium dioxide
UV-Vis	Ultra violet-visible light spectroscopy
XRD	X-ray diffraction

CHAPTER ONE
INTRODUCTION

1.1 Background of the Study

The expanding international demand for eco-friendly energy sources has accelerated research into the development of high-efficiency, low-cost photovoltaic materials. Among the various materials studied for solar energy conversion**,** TiO_2 has drawn considerable recognition for its exceptional resistance to degradation , budget-friendly, biocompatibility and suitable electronic properties (Vaiciulis et al., 2012). TiO_2 is widely used as a window layer in thin-film solar cells because of its wide band gap, chemical stability, non-toxicity and excellent optical transparency. Iron doping and optimization of deposition parameters can further tailor its structural and optical properties for improved photovoltaic performance. However, the broad bandgap (~3.0–3.2 eV) severely limits its practical use in solar cells by limiting its uptake to the ultraviolet (UV) segment of the Sun's electromagnetic output that represents only a tiny fraction of the total incoming solar energy (Sobczyk-Guzenda et al., 2015).

Several studies have reported that TiO_2 thin films exhibit improved photocatalytic and photovoltaic performance when doped with transition metals. In visible and near infrared spectrum, TiO_2exhibits high optical transparency and charge carrier mobility. Thus, solar cells are the primary use for it. Researchers have demonstrated that doping TiO_2 with certain metal ions makes it simple to control its structural characteristics, optical parameters and magnetic properties. Attributable to its affordability and operational simplicity, iron is the best dopant for TiO_2. Additionally, the crystal radius of Fe^{3+} is close to that of Ti^{4+} (Kayani et al., 2020). Iron-doped TiO_2 (Fe:TiO_2) introduces impurity levels within the bandgap, allowing for sub-bandgap photoexcitation and improved utilization of the solar spectrum. Thin film technology is particularly advantageous in solar cell applications because of its promising ability to minimize material usage, decrease fabrication expenses and work well with flexible substrates (Lee et al., 2017). For obtaining superior Fe:TiO_2 films, factors like dopant concentration and annealing heat conditions, deposition technique and film thickness must be carefully optimized, all of which influence the film's microstructure and performance in solar cell architectures (Lourduraj et al., 2017). The Fe:TiO_2 has been recently shown to be a light-sensitive anode material in dye-driven photovoltaic

systems with significant enhancements in photo response and energy conversion efficiency.

The aim of this research is to address this gap by the preparation and analysis of thin films of Fe:TiO_2 with the ultimate goal of improving the suitability of these films for solar cell applications. This research will integrate Fe into TiO_2-based systems to determine the best doping conditions and elucidate the fundamental mechanisms that enhance the photovoltaic properties of such systems (Oviedo et al., 2023). Fe doping alters the electronic and structural environment of TiO_2, resulting in intermediate energy states that enhance charge separation and reduce electron-hole recombination. The introduction of Fe^{3+} may cause lattice distortion, which enhances the light absorption and carrier mobility, resulting in better optical and photocatalytic properties. In spite of these possible advantages, the results of the existing studies are ambiguous, due to the different synthesis conditions or to the fact that the films are not uniform, which means that film uniformity needs to be improved. This proposed study intends to fill this gap by systematically preparing and analysing Fe:TiO_2 thin films with different preparation conditions, explain the doping mechanism and its effects on the performance.

1.2 Statement of the Problem

The need for clean, sustainable and green energy sources has grown internationally, leading to a focus on improving PV material performance. TiO_2 is a material with many advantages, including its abundance, chemical stability, non-toxicity and low cost, making it a suitable material for use in photovoltaic devices. The large band gap (3.0–3.2 eV), however, means that it is only good at absorbing light at the ultraviolet region of the solar spectrum (around 5%). Thus, the practical photo-conversion efficiencies of pure TiO_2 are very low (about 0.1–0.2%) and rapid electron–hole recombination under visible-light illumination significantly hampers the photovoltaic performance of pure TiO_2.

Based on this mechanism, it has been reported that doping TiO_2 with a suitable impurity level can enhance its optical and structural properties by introducing the energy level of these impurities in TiO_2, which will improve its ability to absorb photons in the visible light region and decrease charge carrier recombination. However, the photovoltaic properties of Fe:TiO_2 thin films greatly depend on the deposition

parameters such as the volume of the precursor solution, spinning time and the number of layers of the thin films. The processing parameters have not yet been optimised and the effects of these parameters on the structural stability and optical properties of Fe:TiO_2 thin films have not been well understood. Consequently, films made under sub-optimal conditions can result in a poor level of crystallinity, a higher number of recombination centres and decreased photovoltaic response. Hence, it is important to study the effects of these deposition parameters on Fe:TiO_2 thin films in order to produce the materials that have higher crystallinity, lower band gap, higher absorption of visible light and better application to photovoltaic.

1.3. Research Objectives

1.3.1 General Objective

To synthesize and characterize Fe: TiO_2 thin films deposited using spin coating technique.

1.3.2 Specific Objectives:

1. To evaluate the effects of precursor solution volume on structural and optical analysis of Fe: TiO_2 thin films.
2. To investigate the effects of spinning time on the structural and optical properties of Fe: TiO_2 thin films.
3. To examine the impact of spin-coating layers on the structural and optical properties of the Fe: TiO_2 coatings.
4. To assess the structural stability of Fe: TiO_2 coatings over a period of twenty eight days.

1.4 Research Questions

1. How does varying the precursor solution volume influence the structural properties and optical properties of Fe: TiO_2 thin films?

2. In what ways does spinning time affect the structural and optical properties of Fe: TiO_2 thin films?

3. How does the number of spin-coating layers affect the structure and optical properties of Fe: TiO_2 thin films?

4. How does the structural stability of Fe: TiO_2 thin-film coatings change over a period of twenty-eight days?

1.5 Significance of the Study

This study contributes to the development of Fe: TiO_2 thin films for photovoltaic applications by providing a systematic evaluation of the effects of precursor solution volume, spinning time, number of coating layers and short-term stability on their structural and optical properties. The findings identify the optimum spin-coating conditions required to produce films with improved crystallinity, reduced optical band gap and enhanced structural stability, thereby providing a basis for optimizing the fabrication of Fe: TiO_2 thin films.

The results of this study provide useful information for researchers seeking to improve the performance of TiO_2 -based photovoltaic materials through controlled deposition conditions. They also serve as a reference for future studies on doped semiconductor thin films by demonstrating the relationship between deposition parameters and material properties. Furthermore, the optimized fabrication conditions established in this work can support the development of stable and efficient TiO_2 window layers for thin-film solar cells, contributing to ongoing efforts to enhance photovoltaic performance and promote sustainable energy technologies.

1.6 Scope and Limitations

In this present study, the synthesis of Fe:TiO_2 thin films by the spin coating technique is focused. It examined specifically how the crystallographic and light related characteristics of the coatings changed with respect to the precursor solution volume, spinning time and number of spin coating layers. In addition, the stability of Fe:TiO_2 thin films was studied for 28 days to understand their applicability in solar cell application in the long term. One drawback of the research was the fact that the technique of deposition employed was the spin coating technique and therefore a comprehensive comparison with the other deposition technique such as dip coating and vapor deposition was not carried out. In addition, other deposition parameters such as spin speed and solution viscosity were not investigated. Time constraints also limited the extent of stability and durability testing.

1.7 Contributions of the Thesis

This thesis contributes to ongoing research on the synthesis, characterization and stability assessment of Fe: TiO_2 thin films deposited using the spin coating technique, with the aim of developing low-cost and potentially efficient materials for solar energy applications. The main contributions of the study, in line with the specific objectives, are as follows:

i) Optimization of precursor deposition conditions

The study established suitable precursor solution conditions for the deposition of Fe: TiO_2 thin films using the spin coating technique. By varying the precursor solution volume, the study identified 1.0 mL as the optimum volume, based on the resulting structural and optical properties of the films.

ii) Optimization of spinning time

The study established the influence of spinning time on the structural and optical properties of Fe: TiO_2 thin films and identified 30 s as the optimum spinning time at a spin speed of 3000 rpm. XRD, FTIR and UV–Vis analyses demonstrated that changes in spinning time affected the crystallinity, bonding characteristics and optical band-gap behaviour of the films.

iii) Optimization of the number of coating layers

The study demonstrated the effect of increasing the number of coating layers on the structural and optical properties of Fe: TiO_2 thin films. Increasing the layers from one to five produced measurable changes in the films' optical behaviour, with the five-layer film identified as the optimum under the investigated conditions. The study therefore provides useful information on controlling film thickness through repeated coating for solar energy applications.

1.8 Organization of the Thesis

Chapter One presents the introduction of the study, including the background of the study, statement of the problem, research objectives, research questions, significance of the study, justification of the study, scope and limitations, contributions of the thesis and organization of the thesis.

Chapter Two presents the literature review, which discusses solar energy and solar cells, TiO_2 thin layerss, Fe doping in TiO_2, spin coating deposition technique, factors affecting thin film properties and the characterization techniques used in the study.

Chapter Three describes the materials and methods used in the study. It outlines the preparation of Fe:TiO_2 precursor solutions, deposition of thin films using the spin coating technique, annealing conditions and the characterization techniques employed to analyse crystallographic and light related characteristics of the films.

Chapter Four presents the results and discussion obtained from the characterization techniques, including XRD, FTIR spectroscopy and UV-Vis spectroscopy.

Chapter Five presents the conclusions drawn from the study and provides recommendations for future research related to Fe:TiO_2 thin films and their application in solar cell technology.

CHAPTER TWO
LITERATURE REVIEW

2.1 Introduction

This chapter summarizes the literature on thin film application and methods that have been used by different scholars to synthesize and characterize them. It also gives details on the effects of doping thin films for various application.

2.2 Global Energy Demand and the Transition to Renewable Energy

The unprecedented growth in the global population, coupled with rapid urbanization and industrial development, has contributed to a continuous rise in energy demand in recent years.

Even though fuels like coal, oil and natural gas remain the main sources of energy, they come with several problems, including air pollution, climate change, harmful greenhouse gas emissions and unstable market prices (N.s et al., 2022). Furthermore, the limited supply of fossil fuels raises concerns about sustainability for future generations. Beyond the industrial revolution, the shift to renewable energy represents a major transformation in both society and the economy. Access to energy is strongly linked to well-being and societal progress. The United Nations' seventh Sustainable Development Goal (SDG7) seeks to guarantee universal availability of modern, cost-effective, dependable and eco-friendly power by 2030, emphasizing the significance for this global priority (Hassan et al., 2024). A global shift to renewable energy sources has become necessary as a result of these constraints. Renewable energy sources that can lessen reliance on fossil fuels include solar, wind, hydro and biomass. They are also environmentally friendly and sustainable. Solar energy stands out among these and is currently a major focus of research aimed at increasing the affordability and efficiency of solar technologies because of its abundance, scalability and versatility (Bogdanov et al., 2021).

2.3 Solar Cells

Photovoltaic devices, referred to as solar cells, are systems that utilize sunlight to generate electrical power using the photovoltaic effect. The growing need for eco-friendly energy has led to significant advancements in solar cell technology over recent decades (Mohammad Bagher, 2015). Solar cells have been classified according

to generation. The present commercial market is dominated by first-generation solar cells made of crystalline silicon (cSi), which are known for their high efficiency and stability (Efaz et al., 2021). However, the high manufacturing costs and energy intensive production processes have prompted research into alternative materials. Thin-film photovoltaics, featuring deposited material layer technologies have several advantages including decreased material usage, flexibility and low production costs are low (Kant et al., 2022). However, concerns about toxicity and raw material scarcity have limited their widespread use. By investigating new materials and device architectures, third generation solar cells seek to get around these restrictions. Perovskite based photovoltaic devices, organic photovoltaic (OPV) cells, dye sensitized solar cells (DSSCs) and nanocrystal based solar cells are all included in this category (Giannouli,2021). Among these, perovskite solar cells have gained considerable attention because of their comparatively inexpensive manufacturing methods and rapidly rising efficiencies (Kumar et al., 2023). Figure 2.1 shows the evolution of solar photovoltaic technology through four main generations.

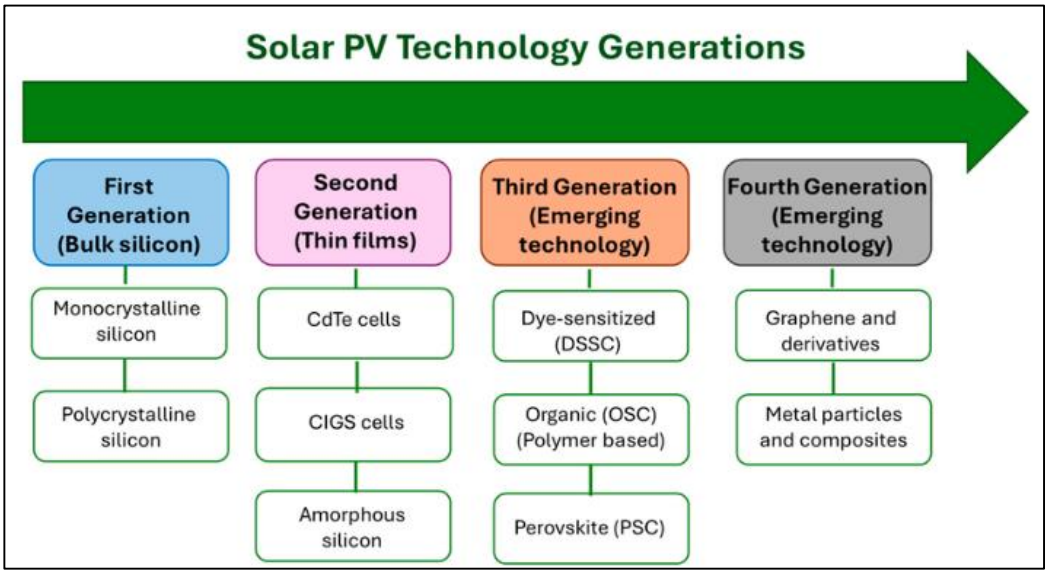


Figure 2.1: Evolution of solar photovoltaic technology through four main generations (Fricano et al., 2025)

2.3.1 Operation of Solar Cells

Solar cells operate on the principle of the photovoltaic effect, in which photons are absorbed by a semiconductor material, exciting electrons from the valence band to the conduction band. This generates electron–hole pairs that are subsequently separated by an internal electric field in the device, usually a p-n junction. This separation and

transport of charge carriers towards the electrodes induce an electric current when connected. This process is dependent on factors like absorption, charge separation and transport properties (El-Shafei et al., 2021). In thin film solar cells, wide band gap materials such as titanium dioxide are commonly employed as electron transport layers, owing to their suitable band edge positions. But TiO_2 absorbs mostly in the UV region, which reduces its capacity to absorb the entire spectrum of sunlight. Consequently, it is often doped and nanostructured to boost its absorption efficiency and facilitate charge transport. Thus, knowledge of the solar cell operation is crucial to assess the impact of material modifications on the device performance (Al-Ezzi et al., 2022).

2.3.2 Types of Solar Cells

Typically, solar cells can be classified into several classes based on the material or materials used and the processes used to make them. The types of solar cells primarily covered are crystalline silicon solar cells, thin film solar cells and emerging solar cell types. The crystalline silicon solar cell has been the most popular and most dominant type of solar cell for many years and has been popular for its superior performance and operational durability (Ballif et al., 2022). Despite these benefits, the manufacturing process is still relatively expensive and energy intensive, so that other technologies that can decrease the manufacturing process costs and yet keep in good performance are being explored. Thin film solar cells, however, have a number of practical benefits, including the use of cadmium telluride (CdTe) and copper indium gallium selenide (CIGS) (Adeyinka et al., 2023). These include lower material usage, mechanical flexibility and decreased production costs, which are ideal for large area applications and flexible devices. These are complemented by newer solar cell technologies like dye sun cell and perovskite solar cell, which, in recent years, have received much attention for their rapidly improving efficiencies and simple fabrication processes. Titanium dioxide (TiO_2) is an important electron transport material for many of these advanced systems due to its chemical stability and appropriate energy band alignment (Foo S et al., 2022). The ongoing development of various types of solar cells demonstrates the need for the improvement of materials such as doped TiO_2, which is crucial for the development of better light absorption and efficient charge transport within the solar cells for improved device efficiency (Fatima et al., 2024).

2.4 Thin Film Photovoltaics

Thin film solar cells are a type of second-generation technology that use single or multiple ultra-thin coatings of light-absorbing substances on surfaces like glass, plastic or metal. These films are extremely thin, ranging from several nanometers up to tens of microns, making them much thinner than conventional first-generation solar cells, which are formed from thick wafers about 200 micrometers thick. Because of their thinness, thin-film solar cells are lighter, easier to handle and less likely to be damaged by rubbing or scratching (Efaz et al., 2021). Figure 2.2 and 2.3 illustrate how incoming light interacts with a deposited film on a base material and how part of the light is transmitted through the film while multiple reflections occur within the film layer due to interference effects.

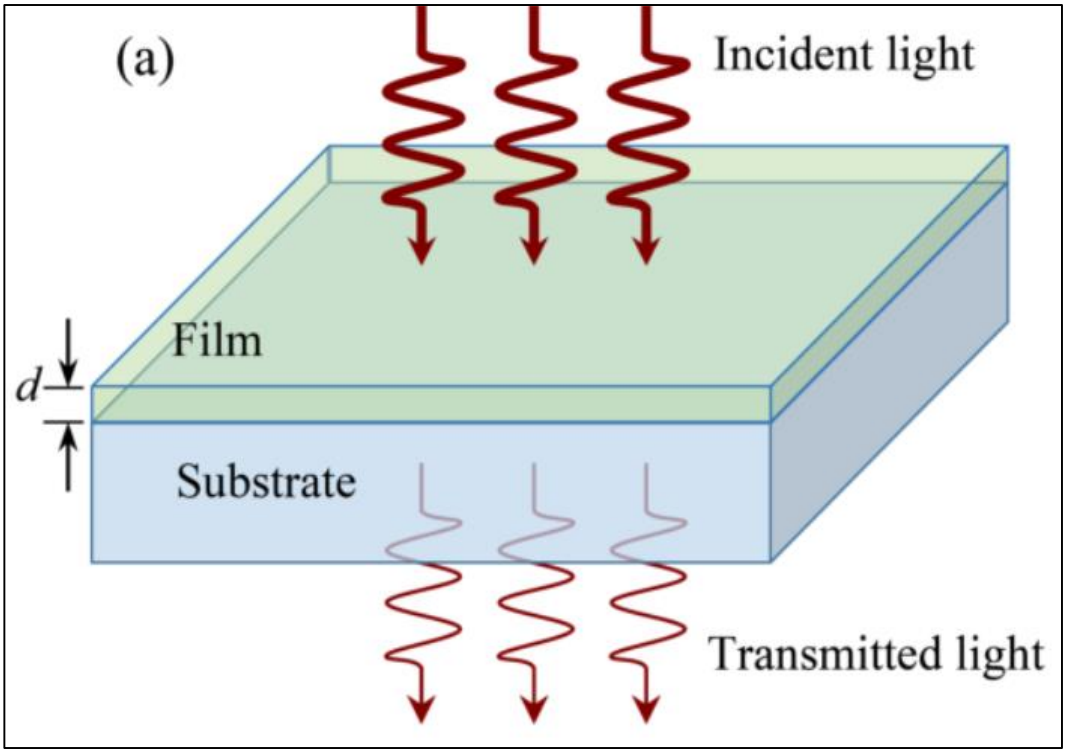


Figure 2.2: Behavior of incoming light with a deposited film

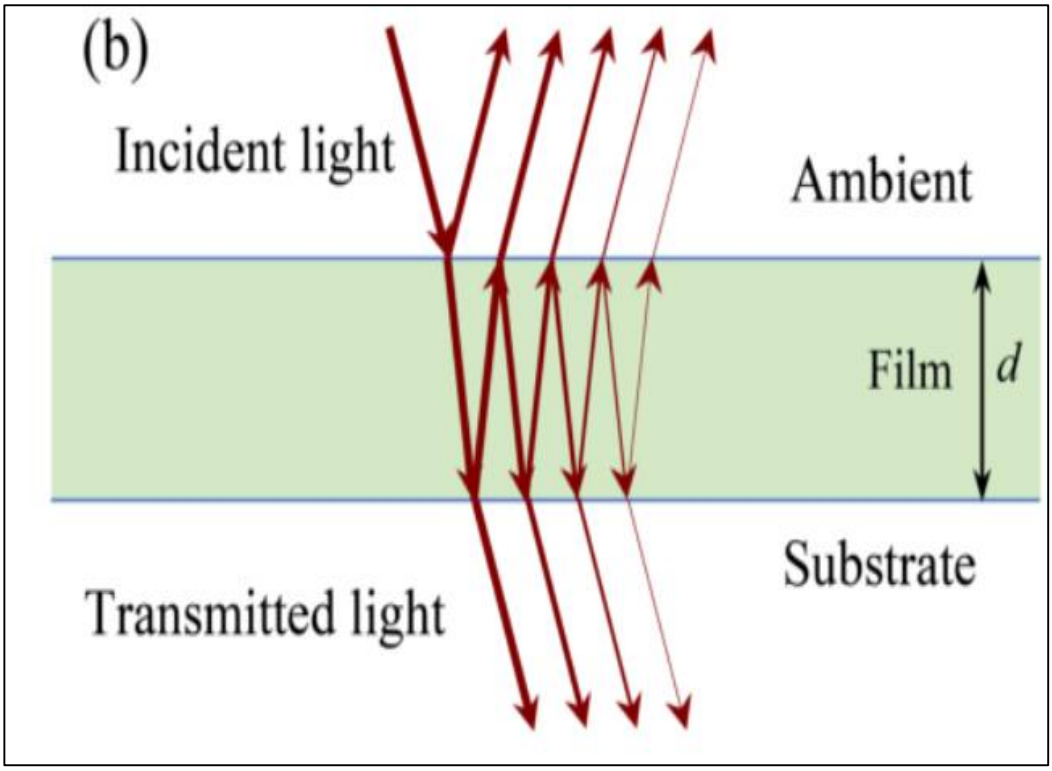


Figure 2.3: Light transmission through a thin film (Kesornkhup et al., 2021)

2.5 Titanium Dioxide

An extensively researched and utilized inorganic compound in material science is TiO_2, a naturally formed titanium oxide. It is extensively employed in many industrial, environmental and technological applications because of its remarkable chemical durability, safety, as well as high refractive index and potent UV light absorption (Racovita, 2022).

2.5.1 Polymorphism of Titanium Dioxide (TiO_2)

TiO_2 exhibits polymorphism, meaning it can exist in more than one crystalline form. The three primary polymorphs of TiO_2 are anatase, rutile and brookite, each possessing distinct crystal structures and properties that influence their suitability for different applications (Al, et al., 2024). Rutile, the most thermodynamically stable phase, is widely used in pigments and optical coatings because of its high refractive index and durability (Dai et al, 2024). It has a tetragonal structure and a forbidden energy gap of about 3.0 eV. Anatase, which is tetragonal but metastable, is typically formed at lower temperatures and transforms into rutile when heated, (Hiroi, 2022). Its wider band gap (~3.2 eV) and open crystal structure improve charge mobility and photocatalytic activity, making it suitable for dye-sensitized solar cells and environmental

remediation. Brookite, the least common and least stable of the three, has an orthorhombic structure and is more difficult to synthesize in pure form. It possesses a forbidden energy gap of 3.4 eV. The transformation of anatase and brookite into rutile is a critical area of research, particularly in high-temperature processes. Several factors influence the transformation, including particle size, dopants, synthesis method and annealing temperature (Rezaee et al., 2011)

Figure 2.4 below illustrates the three main polymorphs of TiO_2 which significantly affect their optical and photocatalytic properties.

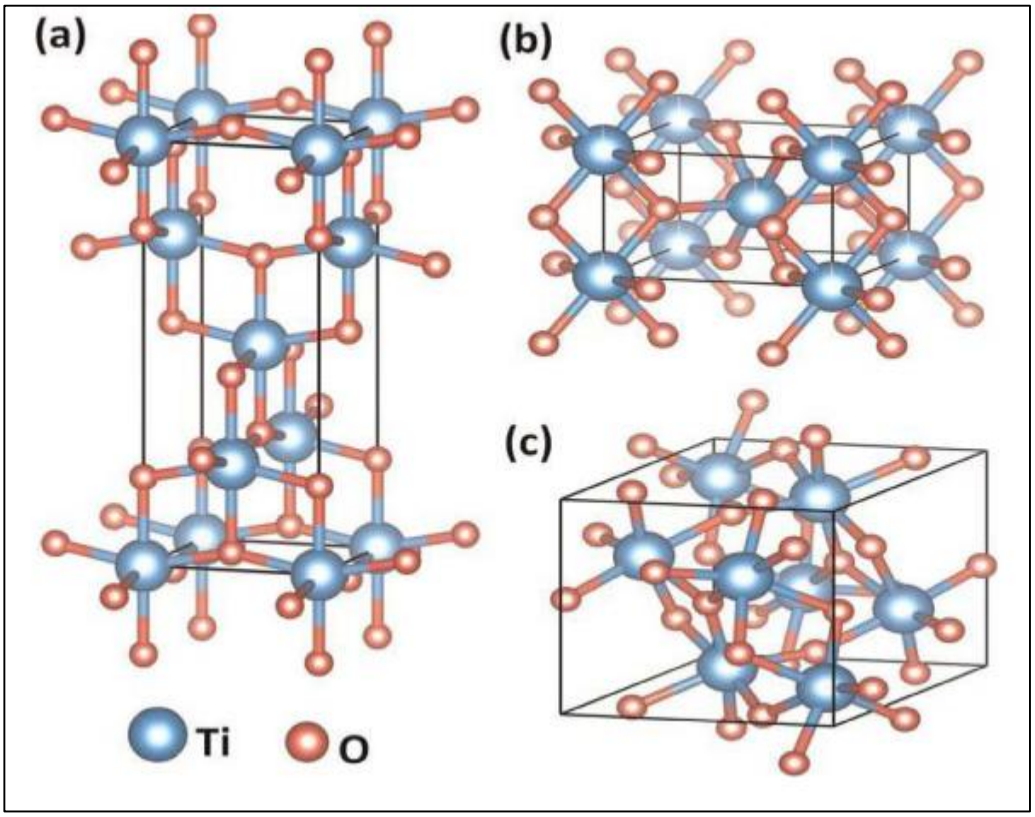


Figure 2.4: Polymorphs of TiO_2 (a) anatase (tetragonal), (b) rutile (tetragonal) and (c) brookite (orthorhombic) (Sadia, et al., 2024)

2.5.2 Electrical and Electronic Properties of TiO_2

Titanium dioxide is an n-type semiconductor, whose electrical properties are dominated by intrinsic defects such as oxygen vacancies and titanium interstitials. The defects provide free electrons and increasing conductivity. Pure TiO_2 generally has poor electrical conductivity because of its large band gap (3.0-3.2 eV), which limits

the thermal activation of electrons. This can have a negative impact on charge transport in photovoltaic devices, so its electronic structure must be modified (Kamoun et al., 2020a). Doping TiO_2 with transition metals, such as iron, can enhance its electronic properties thus creating new energy levels in the band gap, making it easier to excite electrons which effectively increases electrical conductivity, charge carrier mobility and decreases recombination loss. As a result, tuning the electrical properties of TiO_2 is essential for enhancing its efficiency in solar energy conversion and other optoelectronic applications (Arifin et al., 2024).

2.5.3 Charge Carrier Dynamics in TiO_2

In the case of TiO_2, charge carrier dynamics refer to the generation, transport and final recombination processes of electrons and holes in the material. When light energy is absorbed by TiO_2, electrons are promoted from the valence band to the conduction band leaving the valence band with holes. In order to ensure efficient operation of the photovoltaics, the charge carriers need to be effectively separated and transported to the different electrodes before they are able to recombine. However, this process is sometimes constrained by the swift recombination of photogenerated electron-hole pairs in pure TiO_2, depressing its efficiency for PV and PC applications. In order to overcome this limitation, transition metals like iron are doped into TiO_2 for purpose of changing its charge carrier behavior (Kamoun et al., 2020b). The addition of dopants forms energy states within the band structure that may serve as trapping sites that temporarily store charge carriers. This can extend their lifetime and minimize the chances of recombination for better charge separation. But it must be emphasized that over-doping can lead to opposite results: If too many defect states function as recombination centers these become a problem. Therefore, it is essential to carefully control dopant concentration to obtain optimal concentration balance for improving the efficiency of TiO_2 based solar cell material (Kochylas et al., 2021).

2.6 Properties of TiO_2

TiO_2 is a semiconductor with distinct optical, electrical and structural properties that affect its performance in scientific and industrial applications.

2.6.1 Optical Properties

TiO_2 is well-known for its excellent optical characteristics for example high refractive index together with strong absorption of ultraviolet (UV) light. Of all the materials,

rutile form of TiO_2 has the highest refractive index, which is approximately 2.614 and is the densest among them in respect of light interaction second only to diamond. Due to this, it is widely used in the production of white pigments and coatings for light. TiO_2 also has a large band gap that permits it to absorb UV light, but not visible light. For anatase, the forbidden energy gap is 3.2 eV and for rutile, it is 3.0 eV (Lettieri et al., 2021). It is useful in applications including sunscreen, photocatalytic processes and UV blocking coatings. The band gap can be altered through incorporation of impurity atoms or via nanostructure formation, allowing the material to absorb visible light and thereby improve its function in areas such as solar energy and photocatalysis.

2.6.2 Electrical Properties

The electron doped material is TiO_2 which has a wide band gap and is not particularly good at transporting electrons (Bonkerud et al., 2021). The electrical properties are dominated by charge carriers – oxygen vacancies and titanium interstitials. The addition of transition metals such as iron (Fe), niobium (Nb) or tantalum (Ta) or control of the defect concentration, can greatly improve the electrical properties of TiO_2 which otherwise has only low conductivity when undoped. These changes make donor states within the energy gap that enhances charge transport. TiO_2 is a common material used for electron conduction (ETL) in dye-sensitized solar cells and perovskite solar cells, as it is able to transport electrons effectively, while blocking holes and thus discouraging recombination loss (Lettieri et al., 2021). Additionally, TiO_2 possesses dielectric properties, making it suitable for use in capacitors and insulating layers in electronic applications.

2.6.3 Structural Properties

The thin film of TiO_2 has excellent structural properties, which make it useful in solar cells, photocatalysis and optoelectronic devices. TiO_2 is usually prepared as anatase or rutile crystalline structure, depending on the preparation conditions, including the temperature of the annealing process, the film thickness and the preparation method. XRD analysis has revealed that films of anatase TiO_2 tend to be more crystalline at moderate annealing temperatures and more crystalline to rutile at high temperatures. The coherent scattering domain size of the TiO_2 coatings is increased by increasing the calcination temperature which is attributed to the grain growth in the thin films, while the peak broadening is attributed to decrease of crystallinity and increase of

lattice strain. The presence of both anatase and rutile phases in mixed-phase films leads to better charge separation and less electron–hole recombination, yielding better photocatalytic or photovoltaic performance. Also, preferred orientations like anatase (101) and rutile (110) are frequently found and suggest a good crystalline ordering and tetragonal crystal structures (Kääriäinen et al., 2009).

2.7 Metal Ion Doping Mechanism in TiO_2

In the case of TiO_2, doping is the intentional inclusion of foreign ions into its crystal lattice, either through substitution of the Ti ions or by the presence of ions in interstitial sites. Fe^{3+} ions will replace Ti^{4+} ions by their similar ionic radius, resulting in lattice distortion and defect states in the material in the case of iron doping. The defect states create intermediate energy levels within the band gap, so that the energy gap is lowered and the visible portion of the electromagnetic spectrum can be absorbed. This results in strong optical absorption and charge carrier dynamics in TiO_2, which are highly favorable for a photocatalytic and photovoltaic use. Further, the metal ion doping impact extends beyond the optical properties of TiO_2 to the structural and electronic properties as well. It can alter the grain size, phase composition and crystallinity, which affect charge transport and recombination processes. However, if too highly doped, the doping may cause defect clustering which may reduce performance by providing recombination centres. So to maximize the concentration of dopants while maintaining a good balance between increased absorption and charge transport efficiency, a understanding of the doping mechanism is needed (Wang et al., 2020).

2.7.1 Effect of Doping on Band Gap Engineering

Band gap engineering is well-known to be one of the most effective methods of optimizing optical throughput of semiconductor materials in solar energy. The pure TiO_2 has a relatively large band gap and will only absorb light in the UV region, a small part of the solar spectrum. This limitation reduces its effectiveness in harvesting solar energy (Imran et al., 2021). Doping creates extra energy levels within the band gap, which reduces the band gap and allows the material to absorb light in the visible. The change in the band gap is highly dependent on the type and amount of the dopant. For example, if iron is doped, it causes the creation of localized energy states which facilitates the transition of electrons at lower energies of the photons. This results in a visible movement of the absorption edge toward longer wavelengths (also known as a

red shift) and can be seen in the results of UV-Vis spectroscopy. The reduction of the band gap, however, can be useful to improve the absorption of light but a very narrow band gap could result in higher recombination losses. Thus, it is crucially important to optimize the doping conditions carefully to ensure an optimum balance between enhancement of optical absorption and good charge transport properties (Cisternas et al., 2024).

2.7.2 Dopants

Doping is the intentional introduction of a small amount of impurities, known as dopants, into a pure material (typically a semiconductor) in order to change its electrical, optical or structural properties. Doping semiconductors such as TiO_2, involves adding atoms of a different element such as iron (Fe), zinc (Zn), copper (Cu) or vanadium (V) into the host material's crystal lattice. The dopant atoms are either donating additional electrons (n-type doping) or accepting electrons, creating holes (p-type doping). This process adds new energy levels to the semiconductor's band gap, altering how the material interacts with light and electricity (Scaccabarozzi et al., 2022).

2.7.2.1 Iron

Iron is a chemical element represented by the symbol Fe, (ferrum in Latin). It has an atomic number of 26. It is frequently added as a dopant to alter the magnetic and electrical characteristics of semiconductors and oxide materials. Iron is a transition metal that frequently functions as a deep-level trap by introducing localized electronic states within the band gap. Iron can counteract both n-type and p-type doping in semi conductors like gallium arsenide (GaAs), assisting in the achievement of semi-insulating behavior, which is advantageous in high-frequency and optoelectronic devices. Iron doping is used to improve the magnetic and photocatalytic properties of oxides such as zinc oxide (ZnO) and TiO_2 (Paul et al., 2021).

2.7.2.2 Zinc

Zinc is a chemical element represented by the symbol Zn, (zincum in Latin). It has an atomic number of 30. It is most commonly used as a host material in compounds such as ZnO, a wide band gap semiconductor with excellent optical and electronic properties. When doped with other elements such as aluminium, gallium, copper and

iron, ZnO can be tuned for specific functionalities, such as increasing n-type conductivity, causing ferromagnetism or improving photocatalytic activity. ZnO's versatility makes it useful in a variety of applications such as photocatalysis and antibacterial coating, (Alharshan et al., 2023).

2.7.2.3 Copper

Copper is a chemical element represented by the symbol Cu, (cuprum in Latin). It has an atomic number of 29. Copper is a versatile dopant that can be used in a variety of host materials to improve their electronic and functional properties. Copper introduces acceptor levels in semiconductors like zinc oxide and titanium dioxide, which promotes p-type conductivity and increases photocatalytic efficiency under visible light. However, copper's high mobility in materials such as silicon can cause contamination, resulting in deep-level traps that degrade device performance. As a result, copper doping must be carefully managed, particularly in sensitive electronic applications, (Chu et al., 2022).

2.7.2.4 Vanadium

Vanadium is a chemical element represented by the symbol V (vanadis in Latin). It has an atomic number of 23. It is a transition metal distinguished by its multiple oxidation states (+2, +3, +4 and +5) and strong ability to form stable compounds. Excellent optical, electrical and photocatalytic qualities make vanadium doped TiO_2 a good choice for solar energy and environmental applications. However, it is commonly avoided due to its tendency to form multiple oxidation states (V^{3+}, V^{4+}, V^{5+}), which create charge recombination centres and reduce photocatalytic efficiency (Sun et al., 2021).

2.8 TiO_2 Doping

This study uses iron (Fe) as the primary dopant for TiO_2. Iron, a transition metal with similar chemical properties to titanium, can easily substitute Ti^{4+} ions in the TiO_2 lattice. Its introduction is expected to create mid-level states within the conduction–valence band, enhancing absorption of visible light and improving the material's photocatalytic as well as optical characteristics. The discussion will focus on how iron incorporation alters the crystalline and electrical properties of TiO_2, (Sultana et al., 2023).

2.8.1 Iron Doping

Fe^{3+} has a crystal radius of 0.64 Å, while that of Ti^{4+} is 0.68 Å, which makes it readily substituted into the lattice. Fe doping is the intentional modification of a material's physical, chemical or electronic properties by introducing small amounts of Fe atoms into its crystal lattice, typically a semiconductor like TiO_2 (Shymanovska et al., 2022a). When Fe is doped into TiO_2, it usually replaces titanium atoms (Ti^{4+}) in the crystal structure There are several oxidation states for Fe (Fe^{2+}, Fe^{3+}) which can provide intermediate energy levels in a wide forbidden energy gap (anatase TiO_2: ~3.2 eV). The new levels are now trap states or stepping stone pathways for electrons that "short-cut" the band gap. With this modification, the material would not only absorb UV light but also absorb a larger amount of visible light, thus enhancing its potential applications in solar energy and photocatalytic processes (Dong et al., 2024a). Doping is a useful technique for materials such as TiO_2. The creation of intermediate energy levels within the TiO_2 forbidden energy gap increases the light absorption, which takes place in the visible spectrum, beyond that of UV light (M. Abdul et al., 2021). This enhances the photocatalytic and solar energy conversion efficiency of Fe:TiO_2. In addition, the potential of iron to increase charge separation by being an electron or hole trap can decrease the recombination rates and increase photocatalytic activity. Doping also can control the electrical properties, such as increasing the conductivity or changing the carrier concentration, as this is important in electronic and photovoltaic devices. In environmental applications like pollutant degradation and gas sensing sensing, iron can be used to enhance the surface reactivity of TiO_2 (Ruzgar et al, 2020). Chemical modification with iron is a powerful tool to enhance the properties of solid state materials in many advanced technologies. The trapped states effect of iron is shown in figure 2.5 below.

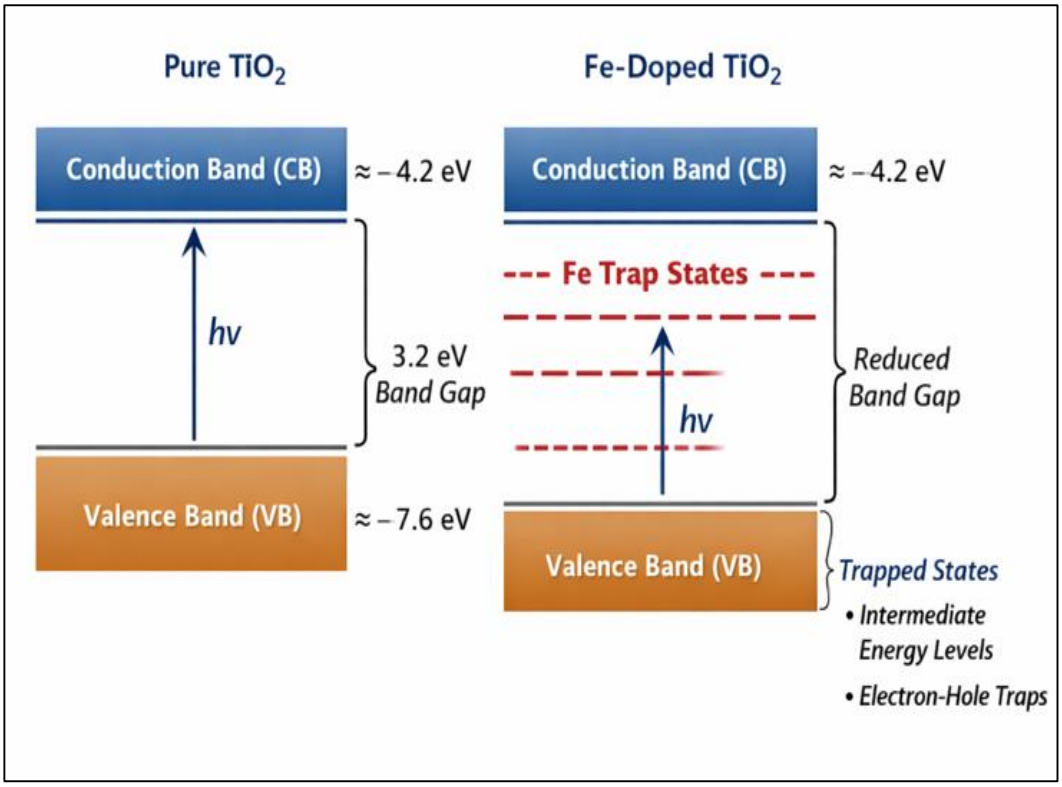


Figure 2.5: Effects of Fe as trapped states (Ruzgar et al., 2020)

2.8.2 Role of Annealing in Thin Film Formation

Annealing is an important post-deposition process that has a significant impact on the microstructural and light related characteristics of thin films. This process involves heating the deposited films at controlled temperatures to remove any remaining solvents, enhance crystallinity and promote the formation of well-defined phases (Rm et al., 2020). As for TiO_2 thin films, annealing can facilitate the structural transformation progressing from an amorphous phase to polymorphic crystalline phases such as anatase or rutile, depending on the annealing temperature and duration of the treatment.

Other important properties like grain growth, defect density and adhesion of film to substrate are also affected by the annealing. The crystallinity and number of defects in the films are generally improved with increasing annealing temperature, directly optimizing its optical and electronic efficiency. However, if the temperature is too high, then it could cause unwanted changes like cracking of films or unwanted phases. As a result, optimizing annealing conditions is crucial in order to deliver superior TiO_2 thin films exhibiting attributes that are suitable for solar cell applications (Gürakar et al., 2020).

2.9 Deposition of Thin Films

Thin film preparation involves the formation of a thin material coating on a substrate generally exhibiting a coating thickness from a few nanometers to several micrometers, to achieve a desired property. It is dependent on the desired characteristics, the material type and the film application. The wet chemical technique was used in combination with spin coating technique for the preparation of uniform films with controlled thickness and composition in this research because of its simplicity, low cost and capability of preparing uniform films with controlled thickness and composition. Common techniques for producing thin films include physical vapor deposition, chemical vapor deposition, electroplating, sol-gel processing, chemical bath deposition, spin coating, dip coating, sputtering and thermal evaporation (Moumen et al., 2022).

2.9.1 Dip Coating

Dip layer formation is a technique commonly employed to place a uniform film on a surface. The process begins by immersing the surface into a liquid mixture containing the desired material. The surface is then slowly withdrawn, allowing a thin and uniform layer to form. Dip coating is widely used in fields such as electronics, optics, coatings and nanotechnology (Manickam et al., 2020). However, immersion coating has some limitations. Lightweight components can lift or drop from the moving belt and the layer thickness may change along the height, a phenomenon referred to as the tapered layer effect. Excess material can accumulate at the bottom of the components as extra coating drips off and a portion of the applied layer can be stripped by rising solvent fumes from the reservoir.

2.9.2 Vapor Deposition

Vacuum evaporation is an approach in which materials are heated in a high vacuum to form a thin film on the base material. This is achieved by using an electron beam or lasers to heat the materials in a vacuum, resulting in the formation of a nanolayer on nearby surfaces such as glass or plastic. Vacuum evaporation is an important technique for producing coatings on different types of objects (Xu et al., 2021).

i. Physical vapor deposition

Physical vapor deposition (PVD) is a vacuum-assisted technique used to produce films and coatings. In this method, the material undergoes a physical transformation from a

solid or liquid state into a gaseous phase and then condenses back onto a base material to create a thin layer. The most frequently employed PVD techniques are sputtering and evaporation.

ii. Vapor-Phase Chemical Deposition Method

Vapor-phase chemical deposition method is a vacuum-based approach for creating thin films. During this process, a wafer is positioned in a chamber and subjected to specific gaseous materials that readily vaporize. These gases interact and break down on the wafer's surface, creating the targeted thin film layer.The gas stream in the reaction chamber removes volatile by-products produced during the process (Chaudhari, 2021) . However, the practicality of vapour deposition in certain applications is limited by a number of disadvantages. Depending on the precursor materials, it is usually applied at high temperatures, which may limit its application on substrates that are sensitive to temperature changes.

2.9.3 Sputtering

Sputter deposition is a process in which material is transferred from a source to a surface using ionized atoms in a vacuum. Ionized atoms are accelerated through a plasma voltage toward the target, causing atoms from the target to be ejected and deposited onto the substrate. These atoms accumulate on the base material, developing a fine coating composed of the same material as the target (Simon, 2025). In fact, sputter deposition can produce superior thin films and complex oxide superlattices. However, it has some drawbacks, including expensive and complex equipment, slower growth rates for certain materials and low target material utilization. Additionally, it can heat the substrate and ion bombardment may damage sensitive materials (Depla et al., 2010)**.**

2.9.4 Electroplating

Electroplating is a technique that uses applied current to create a thin coating on the surface of another material. Electrochemical deposition offers a promising approach for producing different thin films because of its benefits, such as inexpensive equipment and compatibility with large-scale manufacturing. The main disadvantages of electroplating are its environmental impact due to hazardous waste; the high costs of energy and equipment and the health and safety risks associated with handling toxic

chemicals. The process can also be time-consuming and may not result in a uniform finish, particularly for complex shapes (AAnand. et al., 2023).

2.9.5 Thermal evaporation

This technique involves evaporating the material under high to ultra-high vacuum conditions. The base material is aligned with the vaporized particles inside the enclosed chamber, enabling a conductive layer to develop atop its surface. A primary benefit of this technique lies in the precise regulation it provides over the deposition environment of the molecular coating, ensuring that the resulting layer on the base material is highly uniform and structured. However, evaporative deposition has several disadvantages including the fact that it is limited to materials with low melting points, it is difficult to maintain stoichiometry for compounds and alloys. There is also a risk of material decomposition at high temperatures, certain materials have poor adhesion and some applications require long deposition times. The process can also be energy intensive (Yunus et al., 2022).

2.9.6 Chemical Bath Deposition

Chemical bath deposition (CBD) is a low cost and simple method to make a thin film from a solution of metal ions and an appropriate source of anions. This is a chemical bath method in which a substrate is dipped into a chemical solution that takes time to release reacting species to create a controlled nucleation and growth of a solid film on the surface of the substrate. It typically takes place at relatively low temperatures and needs no complicated apparatus, which makes it possible for coating large area materials and substrates. The thickness of the films can be manipulated by changing various parameters like deposition time, concentration, pH and temperature. The FDA has noted, however, that CBD products suffer from several drawbacks such as poor uniformity of the film, weak adhesion in some cases and inadequate control of exact thickness and the production of chemical wastes which may have environmental implications (Amudhavalli et al., 2022).

2.9.7 Spin Coating

Spin coating is a method for applying even thin layers of organic compounds onto flat surfaces. A droplet of the solution is placed on the central part of the substrate, which can remain still or rotate slowly. The substrate is subsequently rotated at the target speed, causing the applied material to move outward under centrifugal force. The

process continues until the layer reaches the intended depth. The properties and uniformity of the resulting film are influenced by the rotation rate (in revolutions per minute, rpm) and the spinning time (Mustafa et al., 2021).The main advantages of the spin-coating approach are its convenience and ease of setup, as well as its thinness and homogeneity (Butt, 2022). It is a popular method for creating thin oxide films like titanium dioxide on flat substrates owing to its economical nature, user-friendliness and excellent reproducibility (Priyalakshmi Devi et al., 2022). It is widely used in applications requiring precise film thickness and surface uniformity, such as solar cells, optical coatings, sensors and microelectronics.

2.9.8 Spin Coater

A spin coater is a laboratory instrument used to deposit a thin and uniform layer of a liquid precursor or solution onto a flat substrate. It operates by rotating the substrate at a controlled speed while a measured amount of the coating solution is placed on its surface. The centrifugal force generated during rotation spreads the solution across the substrate, while excess solution is expelled from the surface. The resulting film thickness and uniformity are influenced by parameters such as spin speed, spinning time, solution viscosity, precursor volume and the properties of the substrate. In this study, a spin coater was used to deposit the Fe:TiO_2 precursor solution onto soda-lime silica glass substrates.

2.9.8.1 Working Principle of a Spin Coater

The operation of a spin coater begins with placing and securing the substrate on a rotating platform, commonly referred to as the spin chuck. A predetermined volume of the Fe: TiO_2 precursor solution is then applied to the surface of the substrate. When the motor is activated, the substrate rotates at a specified speed, generating centrifugal forces that cause the liquid to spread radially from the centre toward the edges of the substrate. As rotation continues, excess solution is removed from the substrate and the liquid layer becomes progressively thinner. Solvent evaporation also occurs during spinning, contributing to the formation of a thin and relatively uniform coating. The final thickness and uniformity of the deposited film depend on the spinning speed and duration, precursor volume, viscosity, solvent evaporation rate and solution properties. Figure 2.6 and 2.7 show a spin coater and the steps in spin coating respectively.

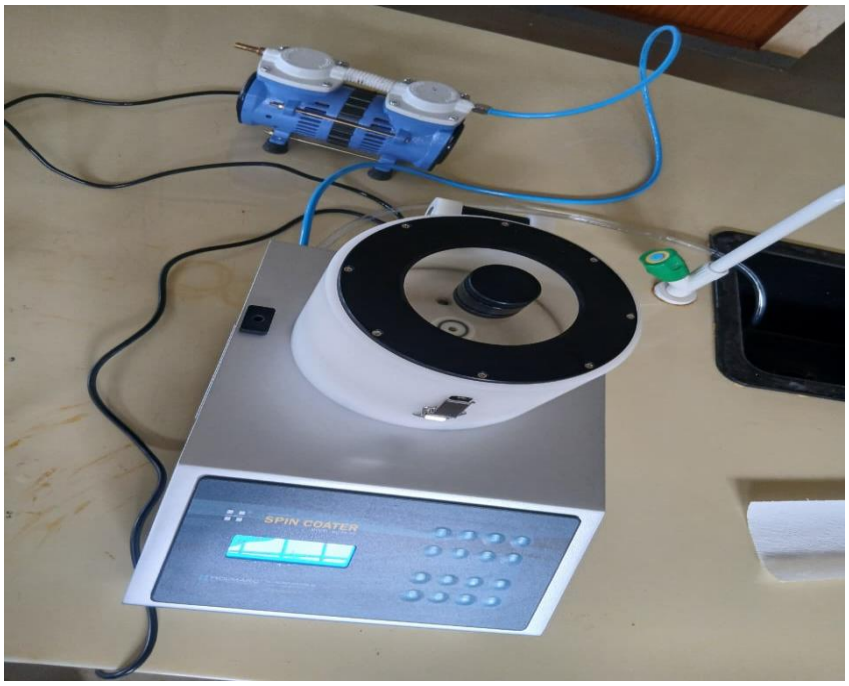


Figure 2.6 A spin coater at Murang'a University of Technology

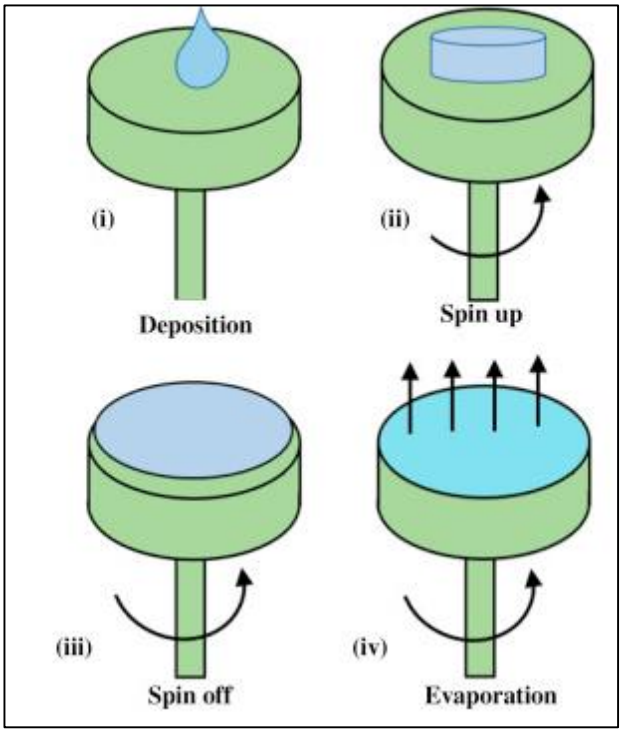


Figure 2.7: Spin coating technique

(i) Deposition

At this stage, a measured volume of the precursor solution is dropped onto the centre of the base material. The goal is to ensure enough solution is present to fully cover the surface during spinning. The volume deposited is important because it directly influences the final film thickness, too little may lead to incomplete coverage, while too much can cause non-uniformity.

(ii) Spin-up

The substrate is rapidly accelerated to a high rotational speed. This sudden motion spreads the liquid outward due to centrifugal force. During this phase, the initially thick droplet begins to flatten and expand across the substrate surface. The acceleration rate and final speed play a key role in determining how uniformly the film will form.

(iii) Spin-off

Once the desired speed is reached, excess solution is flung off the edges of the substrate. This stage helps to thin the film and improve uniformity. The viscosity of the solution and the spinning speed determine how much material is removed. A balance is needed here, too much spin-off can make the film too thin, while too little can leave it uneven.

(iv) Evaporation

As spinning continues, the solvent in the film begins to evaporate, leaving behind a solid thin layer. This stage is critical for film formation because it determines the final thickness, density and microstructure. Faster evaporation generally leads to thinner films, while controlled evaporation helps improve film quality and uniformity.

2.10 Factors Affecting Thin Film Quality in Spin Coating

Some of the parameters that affect thin film quality produced by spin coating are spin speed, spin time, precursor concentration and solution viscosity. The centrifugal force to the solution is based on the spin speed, which will influence the thickness and uniformity of the film. Faster speeds will give thinner films, slower speeds will give thicker films, but may not be as uniform in thickness (Min, 2021). Likewise, the spin time will influence the evaporation of the solvents, which can affect the process to an

incomplete film formation if spent and to defects if over-spun.As well as these parameters, the number of layers deposited and the annealing conditions are important for determining the final film properties. Several layers can be used to increase thickness of the film and provide better coverage of the surface, but can lead to stress and cracking if too many layers are used. The crystallinity and phase formation depend on the annealing temperature and time, especially for TiO_2 films, in which anatase-to-rutile phase transition can take place. These factors therefore must be carefully optimized to obtain high quality films for PV applications (Chaudhary, 2021).

2.11 Recombination Mechanisms in Thin Films and Efficiency Parameters of Solar Cells

One of the primary factors that greatly affect the efficiency of semiconductor materials in solar cell applications is recombination. This happens when excited electrons release their energy as they form a bond with a hole which prevents them from participating in electrical current generation. The recombination can occur in different ways in TiO_2 thin films: radiative recombination, defect-assisted recombination which are usually described by Shockley–Read–Hall processes and surface recombination at the grain boundaries. The recombination is greatly affected by the level of doping and the presence of structural defects. Controlled doping can increase the charge separation and decrease the recombination rate, but when the density of defects will be too high because of doping and/or synthesis the recombination rate will increase. Thus, recombination should be avoided in PV devices as much as possible in order to achieve high efficiency in PV devices. This can be achieved by controlling the material composition, increasing the crystallinity and optimizing the manufacturing process (Zerrouk et al., 2026a) (Bojtor et al., 2024).

Several parameters are used to assess the performance of solar cells, mainly open-circuit voltage (Voc), short-circuit current density (Jsc), fill factor (FF) and overall power conversion efficiency (PCE). Each of these parameters is important and gives information on the efficiency of the device in converting incident light to electrical energy. The efficiency of this system is decided by comparing the electrical power produced by the solar cell with the solar power received by the solar cell. The intrinsic properties of the material (band gap, charge carrier mobility, recombination rates, etc.) directly affect these performance parameters. Therefore, increasing the absorption of

light and reducing the recombination is crucial for increasing the efficiency of TiO_2-based systems. In this context, it is essential to establish the correlation between the intrinsic characteristics of materials and these performance parameters when designing and developing high performance thin film solar cells (Auf der Maur et al., 2019).

2.12 Thermal Treatment Equipment

Thermal treatment equipment was used during the preparation of the Fe: TiO_2 thin films to control the drying and heat treatment processes. The laboratory oven was used for drying the coated substrates, while the muffle furnace was used for calcination of the deposited films. The two processes served different purposes: oven drying promoted the removal of volatile solvents from the deposited precursor layer, whereas calcination at elevated temperature promoted decomposition of residual organic components and the formation and stabilization of the TiO_2 crystalline structure.

2.12.1 Laboratory Oven

A laboratory oven is a temperature-controlled equipment used for heating and drying samples under controlled conditions. In this study, the oven was used to dry the Fe: TiO_2-coated glass substrates at 120 °C for 2 hours after spin coating. During drying, the heat supplied by the oven promoted evaporation of volatile components, particularly solvents, from the deposited precursor layer. This process helped to remove excess solvent and consolidate the coating before the subsequent high-temperature calcination step. Figure 2.8 shows the oven that was used.



Figure 2.8 A laboratory oven at Murang'a University of Technology

2.12.2 Muffle Furnace

A muffle furnace is an electrically heated furnace designed to provide controlled high-temperature treatment of materials while minimizing direct contact between the sample and combustion products. In this study, the dried Fe: TiO_2 thin films were calcined in the muffle furnace at 450 °C for 2 hours. During calcination, the elevated temperature promoted the decomposition and removal of residual organic compounds from the precursor, enhanced the conversion of the deposited precursor into TiO_2 and promoted crystallization and stabilization of the Fe: TiO_2 thin-film structure. The calcination temperature was therefore important in obtaining the desired structural and optical properties of the deposited films. Figure 2.9 shows a muffle furnace.



Figure 2.9: A muffle furnace at Murang'a University of Technology

2.13 Analytical Techniques and Characterization of Coatings

Complementary characterization techniques are commonly used to gain information about the structural, chemical and optical properties of Fe: TiO_2 thin film and each characterization technique provide specific information about the quality and performance of the thin film. The combination of XRD, FTIR spectroscopy and UV–Vis spectroscopy are also commonly used to gain a full picture of how the thin film properties change with fabrication parameters.

XRD is one of the most crucial techniques available to investigate crystalline materials. It uses the diffraction of X-rays from the atomic planes in a crystal in accordance with Bragg's law. The following features are used to identify the crystalline phases present, to determine crystal structure, to evaluate crystallinity, to estimate crystallite size using the Debye - Scherrer equation and to detect changes in lattice structure that occur when dopants are incorporated. XRD can be especially useful for Fe: TiO_2 thin films for distinguishing anatase and rutile phases and for evaluating the effect of deposition parameters (precursor solution volume, spinning time, number of coating layers) on crystal growth and the structural quality of the films.

FTIR spectroscopy is used to detect the chemical bonds and functional groups in the thin films by measuring the absorption of infrared radiation at wavelengths where molecular vibrations produce absorption. FTIR can be used to confirm the presence of Ti–O–Ti bonds that are characteristic of the TiO_2 network in sol–gel derived TiO_2 films and can also identify the presence of Ti–O–Fe bonding, which is indicative of successful incorporation of Fe into the TiO_2 lattice (Zerrouk et al., 2026a). In addition, FTIR can detect the presence of residual hydroxyl groups or organic species and/or solvent related compounds that can be present in the films after synthesis and annealing, thus giving important information on the chemical composition and purity of the films.

The optical properties of semiconductor thin film are usually studied by using UV–Vis spectroscopy. The method is based on the absorption and transmission of light in the ultraviolet and visible part of the electromagnetic spectrum. The absorption spectra can be used to determine the optical band gap by analyzing with the Tauc plot method. The band gap is important since it dictates the range of wavelengths for which absorption of light and creation of charge carriers can occur. For Fe: TiO_2 thin films, UV–Vis spectroscopy is crucial for assessing the effect of Fe doping and spin-coating parameters on the optical absorption, band-gap energy and as such the suitability of the resulting thin films for photovoltaic applications.

The XRD, FTIR and UV–Vis spectroscopy results complement each other, giving information about the structural, chemical and optical properties of Fe: TiO_2 thin films. These techniques allow one to perform a detailed analysis of the impact of the deposition parameters on the quality of the films and to optimize thin films in order to enhance their photovoltaic performance (Arunmetha et al., 2024).

2.13.1 Fourier Transform Infrared Spectroscopy

FTIR is a very useful analytical tool that can be used to identify the chemical bonds, functional groups and molecular interactions of a material. In the layers of Fe:TiO_2 that are deposited, FTIR confirms the formation of Ti-O and Ti-O-Fe bond vibrations. It also detects residual organic or precursor compounds from the synthesis process, such as hydroxyl groups, alcohols or carbonates. Typically this spectrum is measured in the mid-infrared region (4000-400 cm^{-1}), with each type of functional group absorbing certain frequencies. Absorption bands around 400-800 cm^{-1} are generally

characteristic of the Ti-O-Ti stretching vibrations in TiO_2 films. These bands may be suppressed or broadened slightly by the presence of Fe, which signifies that the doping was successful or that there is a lattice distortion. FTIR can also be used to identify water molecules that are still present on the material surface as hydroxyl (-OH) groups and confirm the elimination of any remaining organic residues after annealing. This makes FTIR particularly useful for sol-gel or spin coating processes, where it is crucial to monitor the chemical evolution of the precursor to the oxide (Dong et al., 2024b) (Foyshal et al., 2025).

2.13.1.1 Working Principle and Mechanism of FTIR spectrophotometer

FTIR spectroscopy is a vibrational spectroscopic technique used to identify chemical bonds and functional groups present in a material. Its principle is based on the absorption of infrared radiation by chemical bonds when the frequency of the incident radiation corresponds to the natural vibrational frequency of the bond. The absorbed energy causes molecules or lattice bonds to undergo vibrational motions such as stretching and bending. Because different bonds have characteristic vibrational frequencies, the absorbed infrared radiation produces distinct bands in the FTIR spectrum, which are presented as a function of wavenumber. For the Fe: TiO_2 thin films, the interaction of infrared radiation with the Ti–O–Ti lattice and possible Ti–O–Fe bonding produces characteristic absorption bands, while additional bands may arise from hydroxyl groups and residual organic species. FTIR was therefore important in this study for confirming the formation of metal–oxygen bonds, identifying the characteristic vibrational modes of the TiO_2 lattice and providing evidence of chemical interactions associated with Fe incorporation into the TiO_2 matrix (Giechaskiel et al., 2021). Figure 2.10 shows IR spirit Shimadzu Fourier Transform Infrared spectrophotometer.

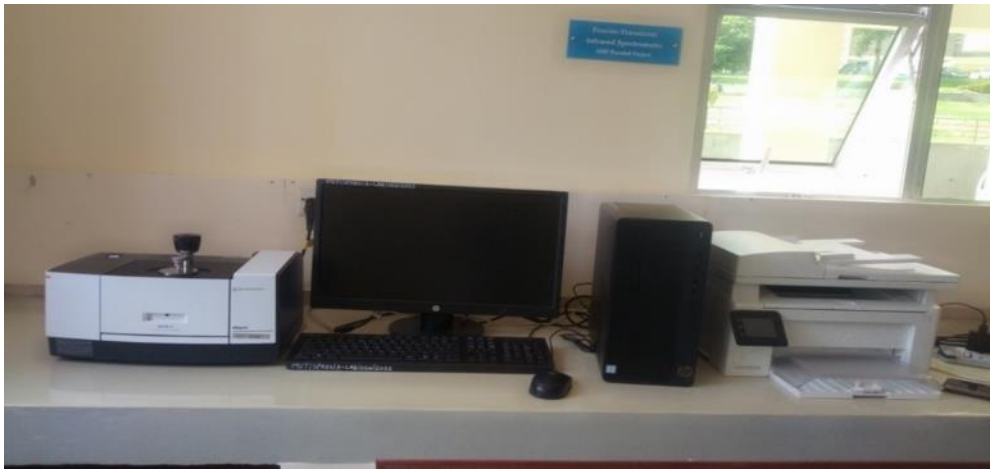


Figure 2.10 IR spirit Shimadzu Fourier Transform Infrared (FTIR) spectrophotometer at Murang'a University of Technology

2.13.2 Ultraviolet-visible spectroscopy

UV-Vis spectroscopy is a commonly used technique to investigate the optical properties of thin films, like Fe:TiO_2.The technique allows the assessment of how well a film can absorb and transmit light in the optical region of the spectrum. In photocatalytic and photovoltaic applications, the forbidden gap of the coating material Fe:TiO_2 influences the function, hence it is essential to determine the light absorption energy gap by using UV-Vis spectroscopy. Iron doping of TiO_2 normally moves the absorption edge towards the visible spectrum, resulting in a reduced semiconductor energy gap than in pure TiO_2. This enhancement in visible light absorption boosts the material's effectiveness in solar energy utilization. The absorption spectrum can be used to determine the band gap energy and its impact on the optical behaviour by using the Tauc plots, which can be used to estimate the band gap energy and its effect on optical behaviour as the function of the doping concentration or film thickness. Moreover, UV-Vis spectroscopy can detect changes in transparency and light scattering as a result of changes in or crystallinity. The technique is useful for optimizing the Fe:TiO_2 thin films for use in solar cells and photocatalytic applications (Nair et al., 2014) (Chandra Paul et al., 2022).

2.13.2.1 Working Principle and Mechanism of UV-Vis spectroscopy

UV–Vis spectroscopy is an optical characterization technique based on the absorption of ultraviolet and visible electromagnetic radiation by a material, resulting in

electronic transitions between different energy states. When radiation with photon energy equal to or greater than the energy difference between allowed electronic states interacts with a semiconductor, electrons can be excited from lower-energy states to higher-energy states. In a semiconductor thin film, photons with sufficient energy can promote electrons from the valence band to the conduction band, producing increased optical absorption near the fundamental absorption edge. During measurement, the intensity of radiation incident on the Fe: TiO_2 film and the intensity transmitted through the sample are compared over a selected wavelength range, producing an absorption spectrum as a function of wavelength. The absorption data can subsequently be converted into photon energy and used with the Tauc relation to estimate the optical band-gap energy. In this study, UV–Vis spectroscopy was therefore important for evaluating the optical absorption behaviour of the Fe: TiO_2 films and determining their optical band-gap energies, which are important parameters for assessing their suitability for solar-cell applications (Thomas et al., 2019). Figure 2.11 shows the Evolution one plus UV-Vis spectroscopy.



Figure 2.11 Evolution one plus UV-Vis spectroscopy at Murang'a University of Technology

2.13.2.2 Determining Band Gaps with Tauc Plots

Photon energy in relation to the absorption coefficient is commonly known as the Tauc plot method for calculation of the optical band gap of semiconductor thin films. This is a plot of $(\alpha h\nu)^n$ against photon energy, hν and n identifies the electronic transition and α is the absorption coefficient. The allowed transition of TiO_2 is usually indirect and therefore n is assumed to be ½. The value of the optical forbidden energy gap is estimated by extending the linear region of the graph to the energy axis. Accurate measurement of the forbidden energy gap is important to study the suitability of TiO_2 nano film for solar energy conversion. Increased absorption in the visible spectrum is indicated by a smaller optical band gap, which is advantageous for raising photovoltaic efficiency. The changes of forbidden energy gap of doped TiO_2 systems can be directly correlated with the structural changes and impurity levels added. Consequently, the Tauc plot is a very important analytical tool to relate material performance and optical properties (Ghobadi, 2013; Ghosh et al., 2025).

2.13.3 X-ray diffraction

XRD is an analytical technique for studying the crystalline structure of thin films, such as Fe: TiO_2. X-ray diffraction identifies the film's phase composition, distinguishing TiO_2 polymorphs like anatase, rutile or brookite and detecting secondary phases caused by iron doping. Evaluation of crystallite growth and lattice distortion in the film can also be done using peak broadening analysis, which is often used with the Scherrer equation. Therefore, XRD is also a crucial technique for studying the structural integrity and phase purity of doped films that have major implications on their light-related and electronic behavior (Zerrouk et al., 2026).

2.13.3.1 Working Principle and Mechanism of XRD

XRD is a non-destructive characterization technique used to investigate the crystallographic structure, phase composition and structural properties of crystalline materials. The technique is based on the interaction of incident X-rays with regularly arranged atomic planes in a crystal. When monochromatic X-rays strike the crystal planes, the X-rays are scattered by the atoms and constructive interference occurs when the path difference between the scattered waves satisfies Bragg's law, $n\lambda = 2d\sin\theta$. During an XRD measurement, the angle of incidence is varied and the intensity of the diffracted X-rays is recorded as a function of 2θ, producing a

diffraction pattern consisting of characteristic peaks. The position of each peak is related to the interplanar spacing and therefore enables identification of crystalline phases, while peak width provides information about crystallite size and structural disorder. In this study, XRD was important for identifying the anatase and rutile phases of Fe:TiO_2, examining changes in crystallinity associated with the deposition parameters and estimating crystallite size using the Debye–Scherrer equation (Al-Amin et al., 2025). Figure 2.12 shows ARL Equinox 100 X-Ray diffractometer.



Figure 2.12 ARL Equinox 100 X-Ray diffractometer (XRD) at Murang'a University of Technology

2.13.3.2 Analysis of Crystallite Size and Structure

Using XRD data, the Scherrer equation is usually used to assess the structural characteristics of thin films, such as crystallite size and lattice parameters. This technique connects the size of the material's crystalline domains to the broadening of diffraction peaks. Broader peaks are frequently the result of smaller crystallite sizes, suggesting nanoscale structures that can have a major impact on optical and electronic characteristics. The device efficiency of TiO_2 layers in solar applications is significantly dictated by crystallite size. Increased surface area from smaller grains can improve charge separation and light absorption. On the other hand, excessively small crystallites could increase charge recombination by introducing more grain

boundaries. Therefore, to increase device efficiency, an ideal balance between crystallite size and crystallinity is required (Chandra Paul et al., 2022) .

2.14 Research Gaps and Proposed Solutions

The literature reviewed shows that TiO_2-based thin films have been extensively investigated for photovoltaic and related applications. However, several aspects remain insufficiently addressed, particularly regarding the selection and modification of TiO_2, the synthesis of Fe: TiO_2, the deposition conditions used to form thin films and the comprehensive characterization and stability assessment of the resulting films. The major research gaps identified from the reviewed literature and the approaches adopted in the present study to address them are discussed below.

2.14.1 Material Selected: TiO_2

TiO_2 is one of the widely investigated semiconductor materials for photovoltaic and other optoelectronic applications because of its chemical stability, non-toxicity, relatively low cost, optical transparency and suitable electronic properties. It has also been widely employed as an electron-transport or window-layer material in photovoltaic devices. However, its relatively wide band gap limits its intrinsic absorption mainly to the ultraviolet region of the solar spectrum, thereby restricting its utilization of the available solar radiation.

Although TiO_2 possesses several properties desirable for photovoltaic applications, its wide band gap and consequently limited visible-light absorption remain important limitations. Various approaches have therefore been explored to modify TiO_2 and improve its optical and electronic properties. However, further investigation is required to establish suitable modifications and processing conditions that can improve the properties of TiO_2 thin films while retaining its inherent advantages.

The present study selected TiO_2 as the base material because of its favourable chemical, optical and electronic properties and investigated its modification through Fe doping. The study further examined how controlled fabrication parameters influence the resulting Fe: TiO_2 thin-film properties, thereby providing an approach for improving the suitability of TiO_2 for potential photovoltaic applications.

2.14.2 Choice of Dopant: Iron

Doping TiO_2 with transition-metal ions has been investigated as a means of modifying its structural and optical properties. Among the transition metals, iron is an attractive dopant because the ionic radius of Fe^{3+} is relatively close to that of Ti^{4+}, allowing Fe ions to interact with the TiO_2 lattice. Fe incorporation can modify the electronic structure of TiO_2 by introducing impurity-related energy states and can consequently influence its optical absorption and structural characteristics.

Although Fe-doped TiO_2 has been investigated in previous studies, the reported structural and optical properties vary depending on the Fe concentration, synthesis conditions, heat-treatment conditions and deposition parameters employed. This variation makes it difficult to establish a generally applicable set of conditions for obtaining Fe: TiO_2 thin films with desirable properties. In addition, studies have not always systematically examined the influence of the deposition conditions while maintaining the Fe concentration constant.

The present study selected iron as the dopant and maintained its concentration at 3 mol% while systematically investigating selected deposition parameters. This controlled approach allowed the study to focus on how fabrication conditions influence the structural and optical properties of Fe: TiO_2 thin films rather than introducing the additional variable of changing dopant concentration.

2.14.3 Thin-Film Synthesis Techniques

Several techniques have been used to synthesize TiO_2-based thin films, including sol-gel processing, chemical vapour deposition, physical vapour deposition, sputtering, spray pyrolysis and related chemical deposition approaches. The synthesis route can influence the composition, crystallinity, phase formation and optical characteristics of the resulting thin films. Sol-gel processing is particularly attractive for thin-film preparation because of its relatively simple procedure, low equipment requirements and ability to provide control over precursor composition.

Despite the availability of different thin-film synthesis routes, variations in precursor chemistry, stabilizing agents, synthesis conditions, ageing and heat treatment can produce differences in the properties of Fe: TiO_2 thin films. There is therefore a need for a controlled and reproducible synthesis procedure in which the precursor

composition and preparation conditions are consistently maintained before investigating the subsequent deposition parameters.

The present study employed a sol-gel synthesis route to prepare the Fe: TiO_2 precursor solution. Titanium(IV) isopropoxide was used as the titanium precursor, ferric nitrate as the Fe source, ethanol as the solvent and diethanolamine as a stabilizing/chelating agent. The precursor preparation, stirring, ageing and heat-treatment conditions were controlled to obtain a consistent Fe: TiO_2 precursor for thin-film deposition.

2.14.4 Thin-Film Deposition Methods

Different deposition methods have been used to deposit TiO_2 and doped TiO_2 thin films, including spin coating, dip coating, spray pyrolysis, sputtering and chemical vapour deposition. These techniques differ in their equipment requirements, deposition mechanisms, film-thickness control, uniformity and scalability. Spin coating is particularly suitable for laboratory-scale thin-film fabrication because it is relatively simple, economical and allows several deposition parameters to be controlled.

Although spin coating has been used to deposit TiO_2-based thin films, the properties of the resulting films depend strongly on deposition conditions. Variations in precursor solution volume, spinning time, spin speed and number of coating cycles can influence film thickness, crystallinity, optical absorption and band-gap behaviour. However, the effects of precursor solution volume, spinning time and number of coating layers on Fe: TiO_2 thin films have not been sufficiently investigated under a consistent set of experimental conditions. This creates a need for systematic optimization of these parameters.

The present study employed spin coating to deposit Fe: TiO_2 thin films on soda-lime silica glass substrates. A constant spin speed of 3000 rpm was maintained while the selected deposition parameters were systematically varied. The study first investigated precursor solution volume, followed by spinning time and number of coating layers. The optimum conditions were subsequently identified based on the structural and optical properties of the deposited films.

2.14.5 Characterization Techniques

The properties of TiO_2-based thin films are commonly investigated using complementary characterization techniques. XRD provides information on crystal structure, phase composition, crystallinity and crystallite size, while FTIR spectroscopy provides information on chemical bonding and vibrational characteristics. UV-Visible spectroscopy provides information on optical absorption and enables estimation of the optical band gap. Other advanced techniques, such as scanning electron microscopy, transmission electron microscopy, Raman spectroscopy and X-ray photoelectron spectroscopy, can provide additional information on morphology, microstructure and surface chemistry.

Previous studies have characterized TiO_2 and Fe: TiO_2 thin films using different combinations of characterization techniques, but the relationship between deposition parameters and the resulting structural, bonding and optical properties requires further systematic investigation. Furthermore, characterization is often concentrated on the properties of freshly prepared films, while the short-term structural stability of optimized Fe: TiO_2 thin films receive less attention.

The present study employed XRD, FTIR and UV-Vis spectroscopy as complementary characterization techniques. XRD was used to investigate the crystalline structure, phase composition and crystallite characteristics; FTIR was used to examine the bonding and vibrational characteristics; and UV-Vis spectroscopy was used to evaluate optical absorption and band-gap behaviour. In addition, the optimized Fe: TiO_2 thin film was monitored using XRD over 28 days to evaluate its structural stability.

2.14.6 Overall Research Gap Addressed by the Study

From the reviewed literature, the major gap is not the absence of research on TiO_2, Fe doping, thin-film deposition or characterization individually, but the limited systematic integration of these aspects for Fe: TiO_2 thin films under controlled deposition conditions. The present study addresses this gap by using TiO_2 as the base material, Fe as the dopant at a fixed concentration of 3 mol%, sol-gel processing for precursor synthesis and spin coating for thin-film deposition. The study systematically investigates precursor solution volume, spinning time and number of coating layers and evaluates their effects using XRD, FTIR and UV-Vis spectroscopy. Finally, the structural stability of the optimized film is assessed over 28 days using XRD. This

approach provides a controlled framework for establishing the relationship between deposition conditions and the structural and optical properties of Fe: TiO_2 thin films for potential photovoltaic applications.

2.15 Chapter Summary

This chapter reviewed the literature on TiO_2-based thin films, with emphasis on their potential for photovoltaic applications. TiO_2 was identified as a chemically stable, non-toxic and relatively inexpensive semiconductor material with suitable optical and electronic properties, although its wide band gap limits its absorption mainly to the ultraviolet region. The review further established that Fe is a suitable dopant for modifying the structural and optical properties of TiO_2 because of its ability to influence the electronic structure and introduce impurity-related energy states within the TiO_2 band gap.

The chapter also examined the different synthesis and thin-film deposition approaches used for TiO_2 and Fe: TiO_2 coatings. Although several methods have been reported, variations in precursor chemistry, synthesis conditions and deposition parameters have resulted in differences in the properties of Fe: TiO_2 thin films. Spin coating was therefore identified as a suitable deposition technique for the present study because of its simplicity, cost-effectiveness and ability to provide controlled thin-film deposition. The reviewed literature further showed the importance of controlling parameters such as precursor solution volume, spinning time and number of coating layers in determining the structural and optical characteristics of the resulting films. The chapter also reviewed the characterization techniques applicable to TiO_2-based thin films, particularly X-ray diffraction, Fourier-transform infrared spectroscopy and UV-Visible spectroscopy. The literature indicated that these techniques provide complementary information on the crystallographic, bonding and optical properties of the films. However, the review revealed a need for more systematic investigation linking controlled deposition parameters to the structural and optical properties of Fe: TiO_2 thin films, together with assessment of their structural stability after deposition. Based on these identified gaps, the present study focuses on optimizing precursor solution volume, spinning time and number of coating layers and assessing the 28-day structural stability of Fe: TiO_2 thin films using XRD, FTIR and UV-Vis spectroscopy.

CHAPTER THREE
MATERIALS AND METHODS

3.1 Introduction

This chapter presents the materials and experimental methods used in the synthesis and characterization of Fe: TiO_2 thin films. It describes the preparation of the precursor solution, deposition of the films using the sol-gel spin coating technique and subsequent drying and heat treatment. The chapter also outlines the experimental parameters investigated, including precursor volume, spinning time, number of coating layers and film stability. The characterization techniques and data analysis methods used to evaluate the structural, chemical and optical properties of the films are also presented.

3.2 Materials

The following chemicals were used: Titanium (IV) isopropoxide [$Ti[OCH(CH_3)_2]_4$] (purity 97.0%), iron (III) nitrate nanohydrate [$Fe\ (NO_3)_3\ ]\cdot 9H_2O$ (purity 99.0%), Diethanolamine (DEA) (purity 99.9%), absolute ethanol [C_2H_6O] (purity 99.9%) and acetone (purity 99.8%), silica glass substrates. All chemicals were obtained from Sigma Aldrich.

The following equipment and instruments were used: Digital analytical balance, magnetic stirrer with hot plate, spin coater, laboratory oven, muffle furnace, ARL Equinox 100 X-Ray diffractometer, Fourier Transform Infrared spectrometer, UV–Visible spectrophotometer, measuring cylinders, micropipettes, beakers and laboratory glassware.

All the equipment and instruments used in this study were available at Murang'a University of Technology (MUT). The laboratory work, including sample preparation, thin-film deposition, heat treatment and characterization, was conducted in the Research Laboratory at MUT, Murang'a, Kenya.

3.3 Methods

Iron doped titanium dioxide thin films were deposited using modified sol-gel spin coating technique adapted from (Lin et al. 2014).

3.3.1 Deposition of Fe:TiO_2 thin films of varying precursor volumes using spin coating technique

In two separate 100 mL beakers, 10 mL of titanium (IV) isopropoxide was mixed with 20 mL of absolute ethanol (Solution A) and 5 mL of DEA was mixed with 5 mL of absolute ethanol (Solution B) respectively. 3 mol% iron (III) nitrate nanohydrate ($Fe(NO_3)_3 \cdot 9H_2O$) was added to 5 mL of absolute ethanol in a 50mL beaker (Solution C). To prepare the Fe: TiO_2 sol-gel, solution B was added to solution A and the mixture stirred using a magnetic stirrer at 250 rpm at room temperature for 10 minutes (Solution D). Solution D was then added to solution C to form Solution E. The resultant solution was stirred continuously at 250 rpm at 75 °C for 90 minutes to form a homogeneous solution, which was aged for 24 hours. The prepared gel was spin-coated onto clean soda-lime silica substrates at 3000 rpm for 30 seconds and the coating process was repeated until 0.5 mL,1.0 mL,1.5 mL,2.0 mL and 2.5 mL of Solution E depleted to obtain five different uniform films. The films were dried in the oven at 120 °C for 2 hours and then calcined in an electric furnace at 450 °C for 2 hours to form thin films of Fe: TiO_2. Figure 3.1 shows a schematic flow chart of the procedure described in section 3.2.1 above.

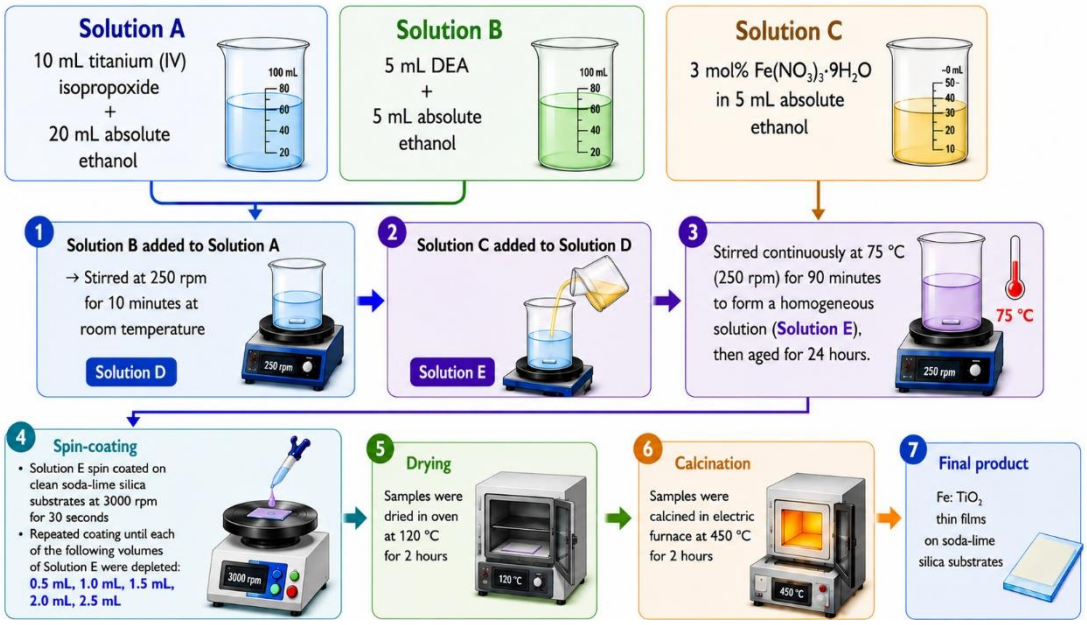


Figure 3.1: Schematic flow chart of the preparation and deposition of Fe: TiO_2 thin films

3.3.2 Variation of Spinning Time in the Deposition of Fe:TiO_2 Films

To investigate the effects of spinning time on the structural and optical properties of Fe:TiO_2 thin films, sol-gel synthesis was carried out as described in 3.2.1. The spinning time was varied from 10 s to 60 s at 3000 rpm. At 10 s interval, 1.0 mL of Solution E was spin coated onto clean soda-lime substrates to isolate the effect of spinning time. The samples were dried at 120 °C for 2 hours and calcined at 450 °C for 2 hours.

3.3.3 Formation of spin coated layers of Fe:TiO_2 Thin Films

To investigate how the number of spin-coated coatings influenced the structure and light-interaction characteristics of Fe:TiO_2 films, 1.0 mL of solution E was spin coated onto clean glass substrates at 3000 rpm for 30 s per layer, while the number of coating layers was varied as 1, 2, 3, 4 and 5 layers. After the deposition of each layer, the films were dried at 120 °C for 2 hours prior to the application of the subsequent layer. Upon completion of the desired number of layers, all samples were calcined at 450 °C for 2 hours.

3.3.4 Stability of Fe: TiO_2 Thin Films over Twenty Eight Days

To assess the stability of Fe:TiO_2 thin films, 1 mL of solution E was used to deposit 5 layers at 3000 rpm for 30 s, dried at 120 °C for 2 hours and calcined at 450^0C for 2 hours. The films were stored in a dark room. Structural characterizations were performed once in 7 days for 28 days.

3.4 Characterization of the Fe: TiO_2 Thin Films

The deposited Fe:TiO_2 thin films were characterized to evaluate their structural, chemical and optical properties, which are critical in determining their suitability for photovoltaic applications. XRD was used to investigate the crystalline structure, phase composition and crystallite size of the films. FTIR spectroscopy was employed to identify the chemical bonds and confirm the incorporation of Fe into the TiO_2 lattice, while UV–Vis spectroscopy was used to determine the optical absorption characteristics and band gap energy of the films. The combined use of these complementary techniques provided a comprehensive assessment of the effects of precursor solution volume, spinning time, number of coating layersand storage period on the properties of the synthesized the Fe:TiO_2 thin films.

3.4.1 X-ray diffraction Analysis

The crystal structure and phase composition of the Fe:TiO_2 thin films were characterized using ARL Equinox 100 X-Ray diffractometer at MUT research laboratory. Prior to sample analysis, a background scan was performed to eliminate diffraction contributions from the instrument and the environment, thereby improving the accuracy of the diffraction patterns. The coated glass substrate was then mounted on the sample holder with the coated surface facing the incident X-ray beam. The diffraction patterns were recorded over θ-2θ scanning range, current set to 0.9A, a voltage of 40kV, using Cu Kα radiation (λ = 1.5406 Å).

The obtained diffraction peaks were compared with standard JCPDS reference cards to identify the crystalline phases present. Bragg's law was used to determine the lattice spacing of thin films (Doan et al., 2020)

$$n\lambda = 2d\sin\theta \quad \text{..... (3.1)}$$

Where n is the order of diffraction (1), λ is the X ray wavelength (1.5406 Å), θ is the Bragg's angle, which is half of the diffraction peak position 2θ, d is the interplanar spacing.

The average crystallite size of the thin films was calculated using the Scherrer equation (Muniz et al., 2016).

$$D = \frac{K\lambda}{\beta\cos\theta} \quad \text{..... (3.2)}$$

Where D is the average crystallite size, λ is the X ray wavelength, θ is the Bragg's angle, which is half of the diffraction peak position 2θ, β is the full width at half maximum and K is Scherrer constant (0.9).

3.4.2 FTIR Analysis

IR spirit Shimadzu FTIR spectrophotometer at MUT research laboratory was employed to investigate the chemical bonding and functional groups present in the Fe_2 thin films. Before sample analysis, a background spectrum was collected to remove the contribution of atmospheric gases and the instrument. The coated glass substrate was then placed in the sample compartmentand the infrared spectrum was recorded

over the wavenumber range of 4000–400 cm^{-1}. The absorption bands obtained were analysed to identify the characteristic Ti–O–Ti and Ti–O–Fe vibrations, as well as hydroxyl groups and any residual organic species remaining after synthesis and annealing. The observed absorption bands were compared with values reported in the literature to confirm the chemical composition of the deposited films.

3.4.3 UV–Vis analysis

The optical properties of the Fe:TiO_2 thin films were investigated using Evolution one plus UV–Vis spectrophotometer at MUT research laboratory. A clean uncoated glass substrate was used as the reference (blank) before analysing the coated samples. The coated films were placed in the sample holder and the absorbance spectra were recorded over the wavelength range of 300–900 nm. The absorbance data were converted into absorption coefficient values and Tauc plots were constructed to determine the optical band gap energy of the films. Band gap of the thin films was calculated using Tauc's relation (Dhruv et al., 2023) (Baishya et al., 2018).

$$\alpha h\nu = A(h\nu - E_g)^n \quad \text{..... (3.3)}$$

Where α is the absorption coefficient of the material, A is the proportionality constant, hv is the photon energy, E_g is the band gap and n is $\frac{1}{2}$ for indirect allowed transmission. The variation in the optical band gap with precursor solution volume, spinning time and number of coating layers was then evaluated to determine the optimum deposition conditions for photovoltaic applications.

3.5 Chapter Summary

This chapter described the experimental procedures used to prepare and characterize Fe: TiO_2 thin films deposited on glass substrates by the sol-gel spin coating method. The preparation of the precursor solution, film deposition, drying and calcination procedures were presented. The experimental variables and characterization techniques, including XRD, FTIR and UV–Vis spectroscopy, were also discussed. The methods used to determine crystallite size and optical band gap were outlined, providing a basis for the presentation and discussion of the experimental results in the following chapter.

CHAPTER FOUR
RESULTS AND DISCUSSION

4.1 Introduction

This chapter presents the results obtained from synthesis and characterization of iron-doped titanium dioxide thin films. The results discusses the effect of spinning time, number of spin coated layers and film stability over a 28-day period on the structural and optical properties of Fe:TiO_2 thin films.

4.2 Fe: TiO_2 Thin Films Spin Coated Using Varying Precursor Solution Volumes

Fe: TiO_2 uniform coatings were effectively coated on silica glass substrates via the spin coating technique using varying precursor solution volumes to investigate their influence on film formation and structural properties.

4.2.1 XRD Analysis of Fe:TiO_2 Thin Films Spin Coated Using Varying Precursor Volumes

The structural characterization of the thin films was conducted using ARL Equinox 100 X-Ray diffractometer. Figure 4.1 following displays the XRD patterns of Fe-doped TiO_2 thin layers formed through spin coating with precursor volumes ranging from 0.5 ml to 2.5 ml volume (a) full range XRD pattern and (b) magnified XRD pattern. The prominent diffraction peaks observed at $2\theta \approx 27.4°$ and $2\theta \approx 49°$ correspond to the (110) plane of the rutile phase and (200) plane of the anatase phase of TiO_2 respectively. These are consistent with the standard JCPDS cards (21-1276) and (21-1272) respectively.

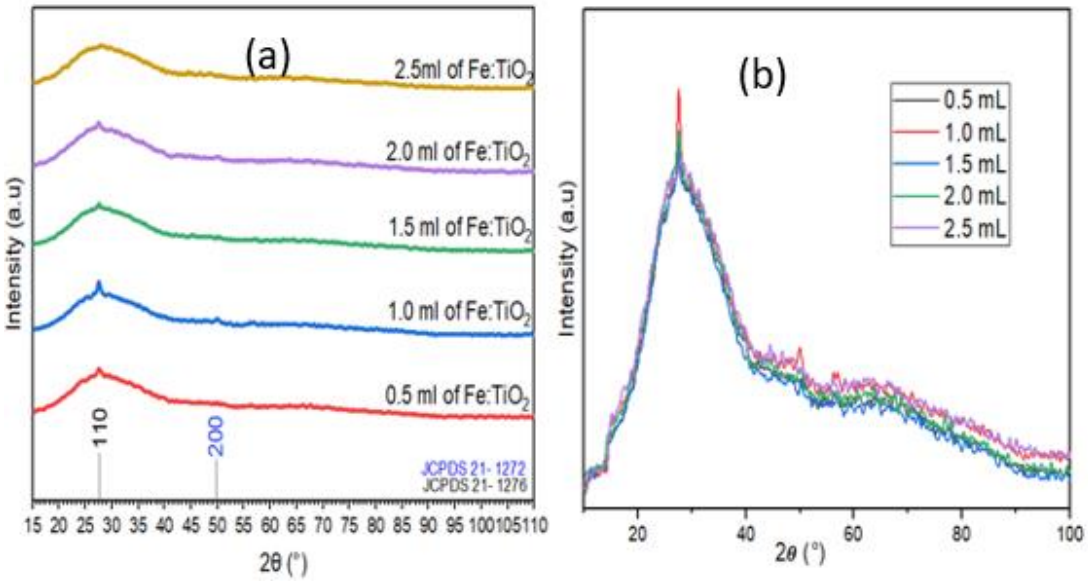


Figure 4.1: XRD spectra of Fe: TiO_2 thin films of varying precursor volume (a) Full range XRD pattern (b) Magnified XRD pattern

The XRD pattern confirms the coexistence of both rutile and anatase phases in the Fe TiO_2 thin films. This mixed-phase formation occurs because annealing at 450 °C falls within the temperature range where anatase begins transforming into rutile but the conversion is not fully completed. In addition, Fe doping introduces lattice distortions and oxygen vacancies that stabilize the coexistence of both phases by hindering full phase transformation. The anatase to rutile phase transition is facilitated by Fe doping in conjunction with the annealing temperature. This result aligns with prior studies (Dong et al.,2024). The XRD patterns show no secondary phases related to iron oxides, suggesting that Fe ions are incorporated into the TiO_2 lattice. This confirms the structural purity of the films within the XRD detection limits and is consistent with previous work (Lin et al., 2012).

It can be observed that the films made with 0.5 mL and 1.0 mL precursor volume have relatively sharp and well-defined diffraction peaks, suggesting good crystallinity and effective crystal growth in these two volumes. The intensity of plane (110) is seen to be sharp and most intense in the 1.0mL sample, indicating a good balance between the availability of suitable precursors and the process of nucleation which results in highly ordered grains. The findings demonstrate that peaks become increasingly wide and

less sharp as the volume of the precursor is increased, as seen from the films prepared with higher precursor volume 1.5-2.5 mL. This can be explained by the internal strain of the film and possible agglomeration effect which makes the crystal growth not uniform. The peaks are also broader at higher volumes, which indicates that the crystallite size is decreased and there is an increase in structural disorder.

The average crystallite size of thin films was calculated using Debye Scherrer equation (Ravi et al., 2021).

$$D = \frac{K\lambda}{\beta \cos \theta} \quad 4.1$$

Where D is the average crystallite size (usually in nm), K is the Scherrer shape factor (0.9), **λ** is the X-ray wavelength 0.15406 nm for Cu Kα used, β is full width at half maximum (FWHM) in radian**s** and θ is Bragg's angle which is half of 2θ. The crystallite sizes of Fe:TiO_2 thin films were observed in Table 4.1 to range between 3.89 nm at 27.79^0 and 4.11 nm at 27.73^0 across all samples. The crystallite size showed only slight variation with increasing precursor volume, indicating that the changes in precursor volume did not produce a consistent increase in the estimated crystallite size under the deposition conditions used. The consistent small crystallite sizes substantiate the nanocrystalline architecture of the films and are ascribed to the presence of Fe dopants, which introduce lattice strain and defects that inhibit crystal growth.

Bragg's law was used to calculate the interplanar d spacing of Fe:TiO_2 thin film (Dinnebier et al., 2019)

$$n\lambda = 2d\sin\theta \quad 4.2$$

Where X-ray wavelength λ used was of Cu Kα = 1.5406 Å, n is an integer 1, d is the inter-planar spacing and θ is the diffraction angle from XRD pattern. The lattice parameters were determined from the XRD data by assuming a tetragonal structure and applying the relation (Sahadat et al., 2023)

$$\frac{1}{d^2} = \frac{h^2+k^2}{a^2} + \frac{l^2}{c^2} \quad 4.3$$

using the measured d-spacing values and corresponding Miller indices. The lattice constant a was specifically determined using the (110) diffraction plane. Table 4.1

following summarizes the crystallite size, FWHM and the lattice parameters of Fe: TiO_2 thin films deposited using different volumes.

Table 4. 1: Summary of the crystallite sizes, FWHM and the lattice parameters of Fe: TiO_2 thin films deposited using different precursor volumes.

Sample (mL)	Plane (hkl)	2θ (°)	FWHM (°)	Crystallite size (nm)	d_{hkl} (Å)	Lattice parameter a (Å)
0.5	110	27.79	2.101	3.893	3.208	4.537
1.0	110	27.73	1.992	4.107	3.214	4.545
	200	49.60	2.078	4.211	1.836	3.672
1.5	110	27.71	1.997	4.097	3.216	4.548
2.0	110	27.70	2.031	4.028	3.218	4.550
2.5	110	27.55	2.091	3.911	3.235	4.575

The influence of precursor volume on the crystallographic characteristics of the coatings shows a clear trend in crystallinity and crystallite size. For the sample prepared using 0.5 mL precursor volume, the diffraction peak at 2θ = 27.79° corresponding to the (110) plane exhibits a relatively high FWHM value of 2.101°, indicating broader peaks and thus lower crystallinity, which is supported by the small crystallite size of 3.893 nm, suggesting limited crystal growth due to insufficient precursor material. Previous studies have demonstrated that precursor concentration or molarity can influence the crystallinity and crystallite size of TiO_2 thin films, with changes in precursor availability affecting the structural development of the deposited films (Shuhadah et al., 2018). The FWHM value at 1.0 mL is slightly narrowed (decreased) to 1.992° and the crystallite size is increased to 4.107 nm; a similar trend is observed at 1.5 mL (1.997° and 4.097 nm) where the crystal structure around this precursor volume is stabilized. The FWHM of the 2.0 mL sample slightly increases to 2.031° with a slight reduction in crystallite size to 4.028 nm and at 2.5 mL, the FWHM increases to 2.091° with the corresponding reduction in crystallite size to 3.911 nm indicating that there was a minor decrease in crystallinity and possible structural imperfections. Similar dependence of TiO_2 crystallite characteristics on precursor concentration has been reported, indicating that changes in precursor conditions can

modify the structural development and crystallite size of TiO_2 films (Khetta et al., 2022). The variation of full width at half maximum (FWHM) and crystallite size with the volume deposited on the base material is illustrated in figure 4.2 for the Fe:TiO_2 thin coatings annealed at 450 °C.

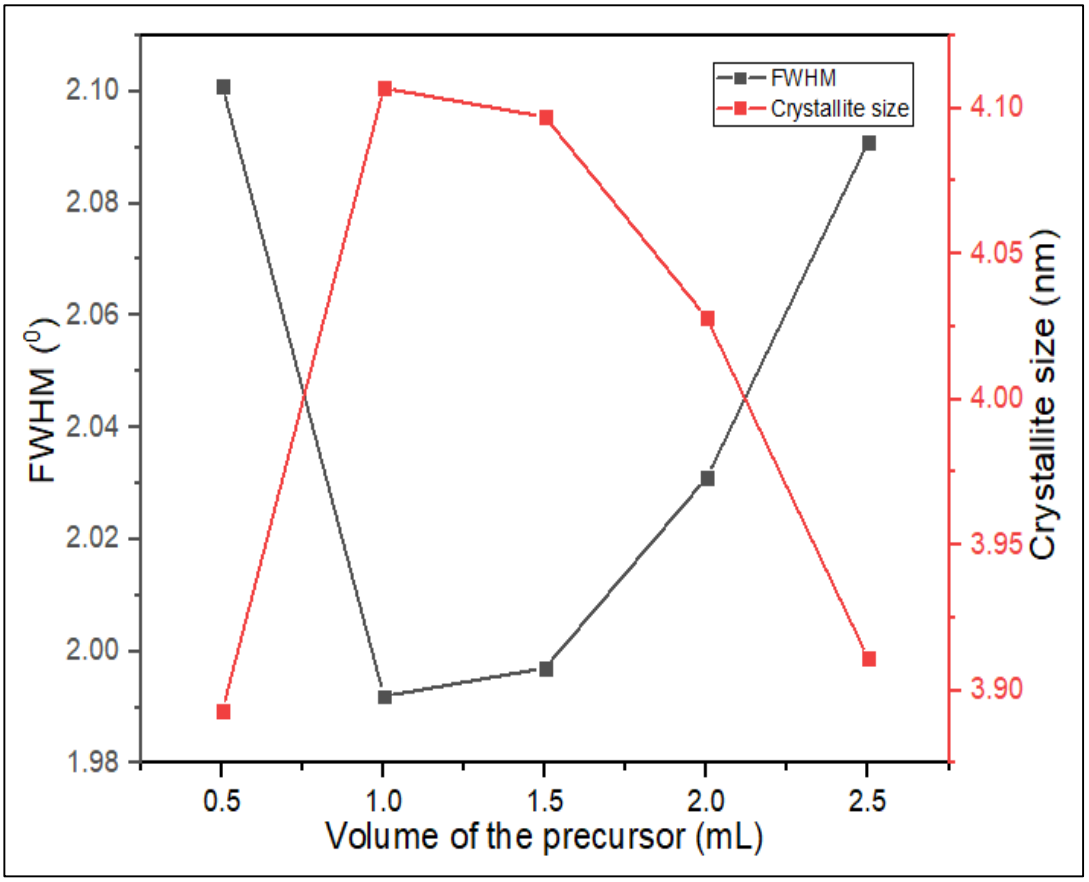


Figure 4.2: Variation of FWHM and Crystallite Size of deposited Fe: TiO_2 thin films using varying volumes of the precursor.

Based on the structural analysis, a precursor volume of 1.0 mL was identified as the optimum deposition condition for the Fe: TiO_2 thin films. At this volume, the film exhibited the highest diffraction peak intensity, the lowest FWHM of , an average lattice parameter of 4.545 Å and a crystallite size of approximately 4.107 nm. The lower FWHM indicates reduced peak broadening and is consistent with the relatively larger crystallite size estimated at this volume. This behaviour agrees with reports that precursor conditions can strongly influence the crystallization and crystallite development of TiO_2 thin films. reported that increasing Ti precursor concentration improved the crystallization of TiO_2 films and increased crystallite size from 30 to 47 nm (Khetta et al., 2022). Similarly, it was observed that increasing precursor

concentration affected crystallite size and was accompanied by a reduction in microstrain and dislocation density (Gapale et al., 2018). The present study did not demonstrate that crystallites size increases linearly with the volume of the precursor. On the contrary, the peak was found to be at 1.0 mL and then the crystallite sizes slightly decreased and the FWHM increased. This result contradicts previous reports of a gradual increase in precursor volume and may be related to the following factors: the volume of the precursor in the spin coating process does not necessarily relate directly to the concentration of the precursor in the solution as well as to the spreading, solvent evaporation, film thickness and the fixed spinning and annealing conditions. The present results, therefore, indicate 1.0 mL to be a more advantageous ratio of the deposited material and the conditions for crystallite formation when the conditions used in this study are applied. The slight increase in FWHM and decrease in crystallite size with the increase in precursor amount indicates that the crystallographic properties did not improve further with the addition of more precursor at high volume. The same non-linear dependency of the crystallite properties on precursor parameters was also observed for TiO_2 thin films.

4.2.2 FTIR Analysis of Fe:TiO_2 Thin Films Spin Coated Using Varying Precursor Volumes

The functional groups and bonding properties of the Fe:TiO_2 thin films were identified by IR spirit Shimadzu FTIR spectrophotometer. Figure 4.3 following presents the resulting spectra for the various samples.

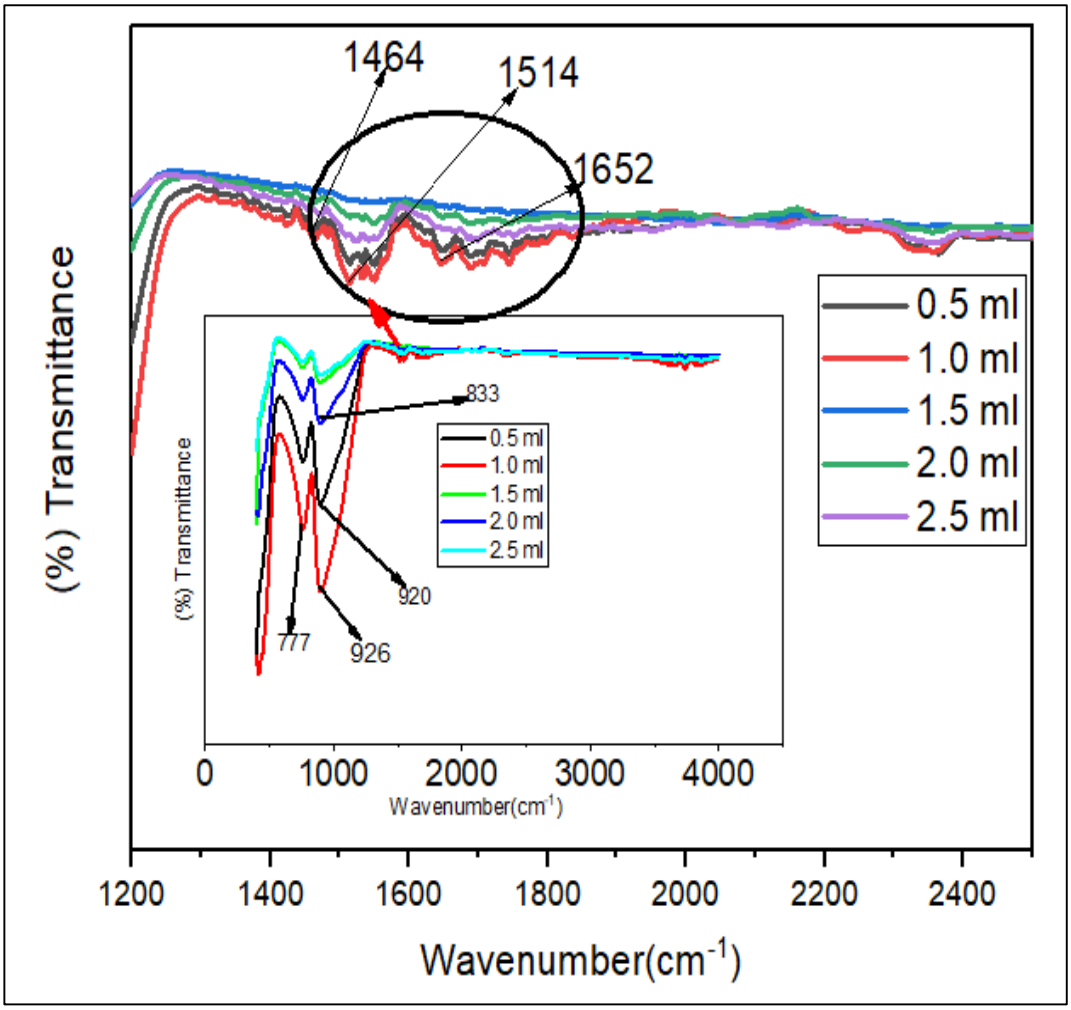


Figure 4.3: FT-IR spectra of Fe:TiO_2 thin films deposited using different precursor volumes

The absorption bands at 777 cm^{-1} and 833 cm^{-1} are identified to be of Ti -O -Ti lattice vibrations, which proves the existence of the TiO_2 network. The peaks of 920 cm^{-1} and 926 cm^{-1} are related to Ti–O-Fe and Ti-O-Ti stretches, which confirms the effective incorporation of Fe ions into the TiO_2 framework. The bands at 1464 cm^{-1} and 1514 cm^{-1} are C-H bending and potential C-C stretch vibrations, which indicate the existence of remaining organic species. The H–O–H bending vibrations of the adsorbed water molecules are attributed to the absorption peak of 1652 cm^{-1} which was observed earlier (Mercy et al., 2026a). The weak bands between 2800- 3000 cm^{-1} are ascribbed to C -H stretching vibrations in the higher wavenumber region and the broad absorption band in the 3200-3500 cm^{-1} range is indexed to the O-H stretching vibrations of hydroxyl groups agreeing to earlier reports (Estrada-Flores et al., 2020).

In general, the precursor volume changes affected the vibrational behavior of the functional-group bands for the Fe: TiO_2 thin films and affected the relative intensity of the functional-group bands in the films. The characteristic Ti–O–Ti and Ti–O–Fe stretching vibration frequencies were still present throughout the precursor volumes studied, suggesting that the basic TiO_2 bonding network was retained with the incorporation of Fe. These changes in the intensity of the bands with the precursor volume can be correlated with changes in the quantity of material deposited and, therefore, the number of bonds that cause an infrared absorption. Other changes in the relative intensities of the C–H, H–O–H and O–H bands may relate to the differing amounts of precursor-derived organic species, adsorbed moisture and hydroxyl groups that may be present after drying and calcination. Thus, changing the precursor volume had a greater impact on the relative abundance and vibrational response of the existing functional groups and not in the introduction of entirely new bonding species. In summary, the FTIR results suggest that the amount of precursor affects the bonding environment and relative abundance of remaining functional groups, but does not affect the characteristic Ti–O–Ti and Ti–O–Fe bonds of the Fe: TiO_2 thin-film network.

4.2.3 UV-Vis Spectroscopy Analysis Of Fe:TiO_2 Thin Films Spin Coated Using Varying Precursor Volumes

The optical properties and band gap of the Fe:TiO_2 thin films prepared using different amounts of precursors were investigated using Evolution one plus UV–Vis spectrophotometer. Absorbance spectra were obtained at 300-900 nm and forbidden energy gaps were estimated based on Tauc plots of the absorption data. Quantitative evaluation of the forbidden energy gap (E_g) was carried out using Tauc methodology through graphical Tauc plot construction. Equation 4.4 gives the Tauc relation (Dolgonos et al., 2016).

$$(\alpha h\nu)^n = A(h\nu - E_g) \quad \text{.....4.4}$$

Where α is the absorption coefficient, $h\nu$ is the photon energy, E_g is the optical bandgap, A is the proportionality constant, while n depends on the number of

electronic transitions i.e. n=$\frac{1}{2}$ for direct allowed transitions, while n =2 for indirect allowed transitions. Figure 4.4 following presents (a) the absorbance spectra as a function of wavelength and (b) the Tauc plots of $(\alpha h\nu)^{1/2}$ versus photon energy ($h\nu$) for films deposited using precursor volumes ranging from 0.5 ml to 2.5 ml. The extracted band gap values for each sample are also indicated in the figure.

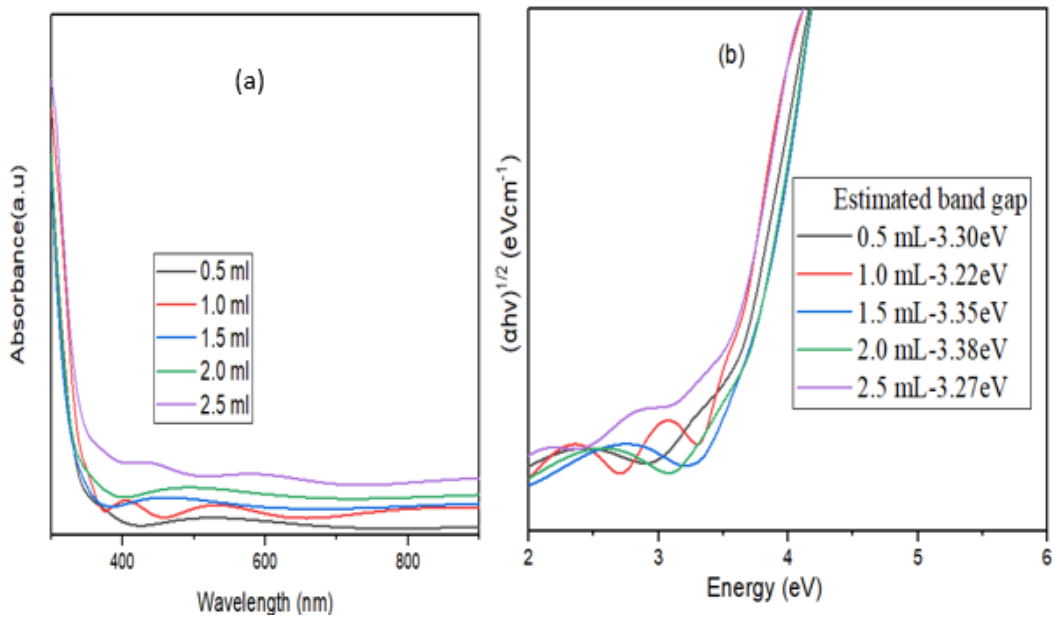


Figure 4.4: (a) Absorbance spectra as a function of wavelength and (b) Tauc plots of $(\alpha h\nu)^{1/2}$ versus photon energy $(h\nu)$ for Fe-doped TiO_2 thin films deposited using precursor solution volumes ranging from 0.5 mL to 2.5 mL.

As can be seen from figure 4.4, the volume of the precursor solution has a significant effect on the optical properties of the Fe: TiO_2 thin films. The absorbance spectra reveal a characteristic optical response of TiO_2 with strong spectral absorption in the ultraviolet region for all samples. Absorbance intensity changes and changes in the position of the absorption edge occur with changes in precursor volume, demonstrating alterations in the electronic profile and microstructural architecture of the ultrathin layer. The optical band gap values obtained from Tauc plot demonstrate that it ranges from 3.22 eV to 3.36 eV with respect to precursor volume. The lowest forbidden energy gap estimate of 3.22 eV is found for the 1.0mL sample, whereas the band gap values of the 1.5mL sample and the 2.0mL sample are 3.35eV and 3.36eV, respectively. A marginal decrease to 3.27 eV is subsequently seen for the 2.5 mL film.

This non-uniform variation implies that the volume of the precursors has an influence on crystallinity, grain-growth and defect-concentration as well as film thickness. The decrease in the band gap from 3.30 eV (0.5 mL) to 3.22 eV (1.0 mL) could be explained by the better incorporation of the Fe ions and the creation of localized impurity states near the band gaps, resulting in easier electronic transitions at lower energy. The larger band gap may be correlated with better crystal quality and decreased defect levels as the precursor material is increased further. The small reduction in band gap at the highest precursor volume might stem from the presence of extra structural defects and localized states with thicker films. The results show precursor volume to be a key parameter for controlling the optoelectronic response of Fe:TiO_2 thin films, both by its effect on the film microstructure and on its effect on the electronic energy levels which is in line with earlier reports (Mesoudy et al., 2023).

4.3 Deposited Fe: TiO_2 Thin Films using Varying Spinning Times

Fe:TiO_2 thin films were successfully deposited using the spin-coating technique with varying spinning times and their crystallographic and light related characteristics were systematically investigated to evaluate the influence of spinning duration on the quality and functionality the films.

4.3.1 XRD Analysis of Fe:TiO_2 Thin Films Deposited using Varying Spinning Times

ARL Equinox 100 X-Ray diffractometer. Figure 4.5 following shows the XRD patterns of Fe:TiO_2 thin films formed through spin coating at different durations from 10 seconds to 60 seconds.

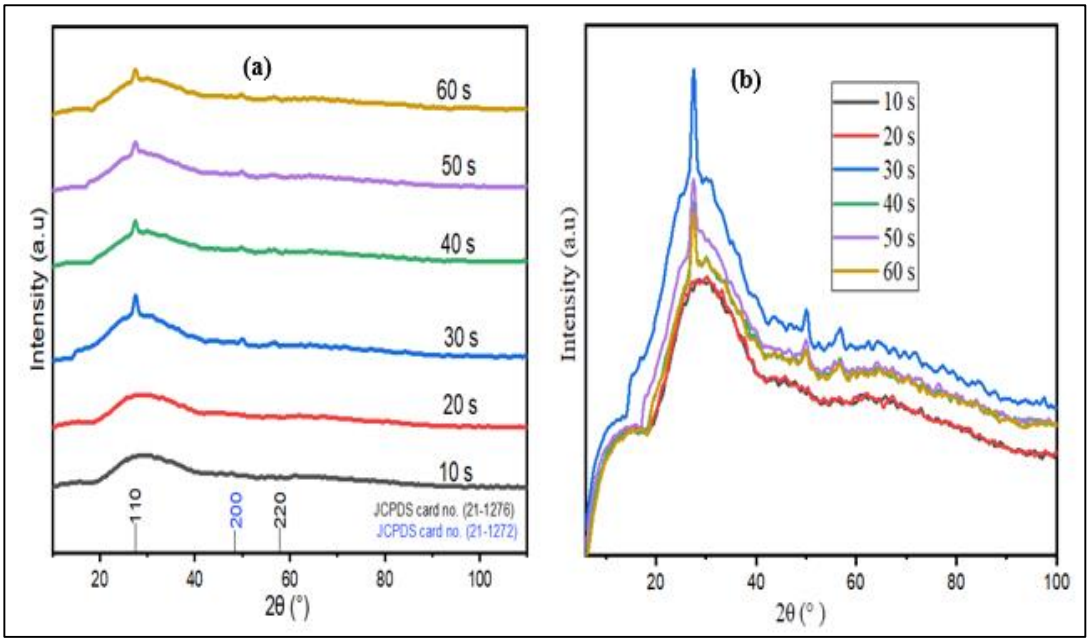


Figure 4.4: XRD patterns of Fe: TiO_2 thin films spin coated using different durations (a) full range XRD pattern, (b) magnified XRD pattern

At shorter spinning times of 10 and 20 S, the diffraction patterns exhibited relatively lower peak intensities and less well-defined diffraction features compared with the longer spinning times. This behaviour suggests a lower degree of crystallinity and less developed crystalline ordering in the films deposited at the shorter spinning durations. The reduced crystallinity may be associated with the shorter time available for the precursor solution to spread and undergo solvent removal during spinning, which can result in a less developed deposited layer prior to subsequent drying and calcination. Similar reports were earlier reported (Zulkefle et al., 2016). With the spinning time extended to 30 S and 40 S, there is a visible improvement in the peak intensity and definition, which indicates a higher level of crystallinity and homogeneity of the film. This implies that such mid-times would give sufficient time to allow sufficient solvent evaporation and uniform distribution of the precursor to facilitate the formation of well-defined phases which is supported by earlier reports (Messemeche et al., 2020). Further extension of spinning time to 50 S and 60 S, however, leads to a decrease in peak intensity and minor broadening of the peaks. Such a deterioration of the quality of film may be connected with high solvent evaporation during spinning and the film dries too soon agreeing with earlier reports (Shanthi et al., 2020). This high rate of drying interferes with good crystallite growth and cause structural defects. Also, over-

spinning decreases the effective deposits of the layer, adding to weaker diffraction signals. Thus, the findings indicate that there is an optimal spinning time between 30 and 40 S which balances between solvent evaporation and film formation. Table 4.2 following summarizes the crystallite size, FWHM and the lattice parameters of Fe:TiO_2 thin films spin coated at different durations.

Table 4.2: Summary of the crystallite sizes, FWHM and the lattice parameters of Fe:TiO_2 thin films spin coated at different durations.

Sample (seconds)	Plane (hkl)	2θ(°)	FWHM (°)	Crystallite size (nm)	dhkl (Å)	Lattice parameter a (Å)
10	110	28.12	2.637	3.105	3.171	4.484
20	110	28.00	2.366	3.460	3.184	4.503
30	110	27.51	1.571	5.206	3.240	4.582
	200	49.78	1.942	4.509	1.830	3.660
	220	57.06	3.057	2.958	1.613	4.562
40	110	27.88	1.592	5.141	3.198	4.522
	200	49.28	4.425	1.975	1.848	3.695
	220	57.09	8.462	1.069	1.612	4.559
50	110	27.49	1.933	4.231	3.242	4.585
	200	50.19	5.115	1.715	1.816	3.632
60	110	27.12	2.038	4.009	3.285	4.646
	200	49.49	4.959	1.764	1.840	3.681
	220	57.18	7.591	1.192	1.610	4.553

The crystallographic characteristics of the Fe:TiO_2 thin films were observed to be greatly affected by the spinning time as revealed in the results. The film at 10 seconds had a relatively wide FWHM of 2.637° for the dominant (110) plane and a small crystallite size of 3.105 nm, which suggested insufficient time for the uniform formation of the film, resulting in poor crystallinity. It was found that the crystallite

size increases from 2.914 nm to 3.460 nm when spinning time was increased to 20 seconds, while the FWHM decreased to 2.366° which implied a slight improvement in the crystal growth and structural ordering. This is supported by earlier reports (Messemeche et al., 2020)

The crystallinity and crystal orientation was improved with further increases to 30 S, yielding the lowest FWHM of 1.571° and the highest crystallite size of 5.206 nm for the (110) plane. Better phase development of the crystals is also supported by the appearance of other diffraction peaks of (200) and (220) planes which also indicates the presence of anatase and rutile phase. This improvement can be attributed to the formation of a uniform precursor layer that resulted in an effective nucleation and grain growth in the following annealing step.

The crystallite size decreased to 5.141 nm with a slight increase in FWHM of the (110) plane from 1.397 to 1.592°, which implies a slight decrease in crystallinity, after 40 seconds. After 50 seconds, the FWHM was further increased to 1.933° and the crystallite size was decreased to 4.231 nm, indicating the increased level of structural disorder which is attributed to excessive spreading of the precursor solution during spin coating. The crystal quality has decreased further during the 60 seconds sample as evidenced by the increase in the FWHM (2.038°) and the crystallite size (4.009 nm). Overall, the film deposited at 30 seconds exhibited the best structural properties, characterized by the smallest FWHM, largest crystallite size and improved phase development. These results indicate that a spinning time of 30 seconds is the optimum condition for achieving high crystallinity and structural uniformity in Fe:TiO_2 thin films. Figure 4.6 following shows the variation of FWHM and crystallite size as a function of the duration of spinning Fe-doped TiO_2 thin films.

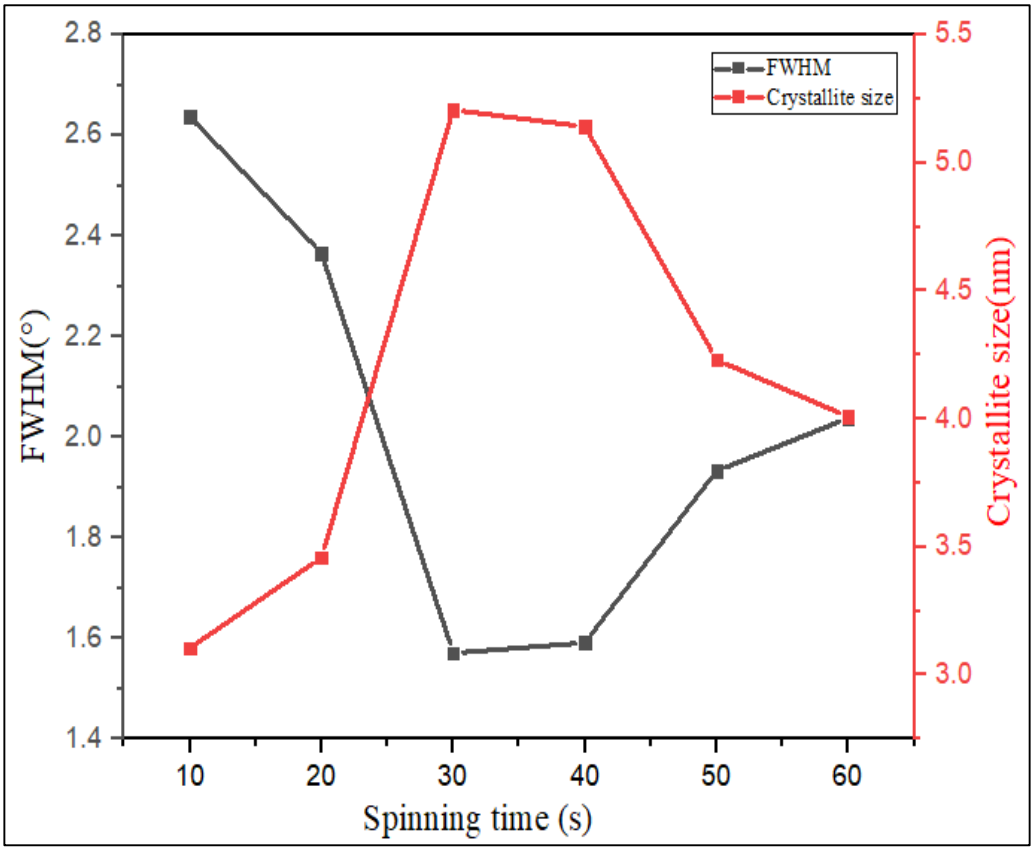


Figure 4.5: Variation of FWHM and crystallite size as a function of the duration of spinning Fe-doped TiO_2 thin films.

The graph demonstrates a definite correlation between FWHM and the crystallite size with the spinning time. From 10 to 30 S, the FWHM decreased from 2.038° to 1.571°. The crystallite size remained the same, varying from 4.009 to 5.206 nm, showing the improvement in the crystallized ordering of Fe: TiO_2 films up to 30 S. This behavior is in line with the known effect of spin coating time on the properties of solution derived thin film. In the study of TiO_2 thin film preparation in this work, it was found that spun film thickness and surface roughness decreased with the increase in spinning time at a constant speed, as reported by (Zulkefle et al., 2016), which implies that the spinning time influences the quantity and distribution of the amount of material left on the substrate.

Likewise, published work on the TiO_2 substrate formed by spin coating has demonstrated that a range of deposition conditions can result in an optimal structural condition, where crystallinity and crystallite size are not necessarily monotonic functions of the deposition condition. In one of the studies, where the spin speed of

the ball was changed, the crystallinity and size of the TiO_2 crystals first rose to an optimum value and then decreased at higher spins (Sharma et al., 2022).

The present results are thus in accord with the general observation that the spin-coating parameters have to be optimized instead of simply increased monotonically. For the conditions used in this study, this time of 30 S was found to be a desirable compromise between the spreading of the precursors, evaporation of the solvent and retention of the material prior to calcination, as indicated by the maximum crystallite size and the lowest FWHM. The FWHM was also found to have rapidly jumped to 2.637° at 40 S. In addition to a decrease in crystallite size to 3.105 nm, it is accompanied by a decrease in crystallite size. The obvious deviation from the trend up to 30 S indicates that the crystallographic development did not improve with increasing spinning time beyond the optimum spinning time. The result is not a direct result of a structural defect or strain, as such, but suggests that coherent crystallite size has decreased and peak broadening has occurred. The relationship between the duration of spinning and the crystallographic properties were shown to be non-linear by the subsequent improvement at 50 S and 60 S. This agrees with published observations of the dependence of film thickness, surface properties, and crystallinity on variations in spin-coating parameters, as the optimum spin-coating condition is different for various deposition systems. In the present study 30 S was chosen as the optimum spinning time since it gave the lowest FWHM and the largest estimated crystallite size for the investigated times.

4.3.2 FTIR Analysis of Fe: TiO_2 Thin Films Deposited using Varying Spinning Times

IR spirit Shimadzu FTIR spectrophotometer was used to examine the functional groups and bonding properties of the Fe:TiO_2 thin films obtained during the spin-coating duration of 10 S to 60 S. The FTIR spectrum in figure 4.7 following showed characteristic absorption features at 763 cm^{-1} and 802 cm^{-1} which are ascribed to Ti - O -Ti lattice vibrations in the rutile phase of TiO_2. The peak at 851 cm^{-1} also confirms the existence of metal-oxygen stretching modes related to doped TiO_2 network (Li et al., 2020). The spectral features emerging at 1530 cm^{-1} and 1700 cm^{-1} are asymmetric carboxylate COO - and C=O stretching bands, respectively, of the remaining organic species or the unreacted hydroxyl groups of the alkoxide precursors in the chemical

solution deposition process. The abrupt and sharp peaks at 3755 cm^{-1} and 3862 cm^{-1} are assigned to the OH vibrations of hydroxyl groups on the TiO_2 surface (Kreft et al., 2020).

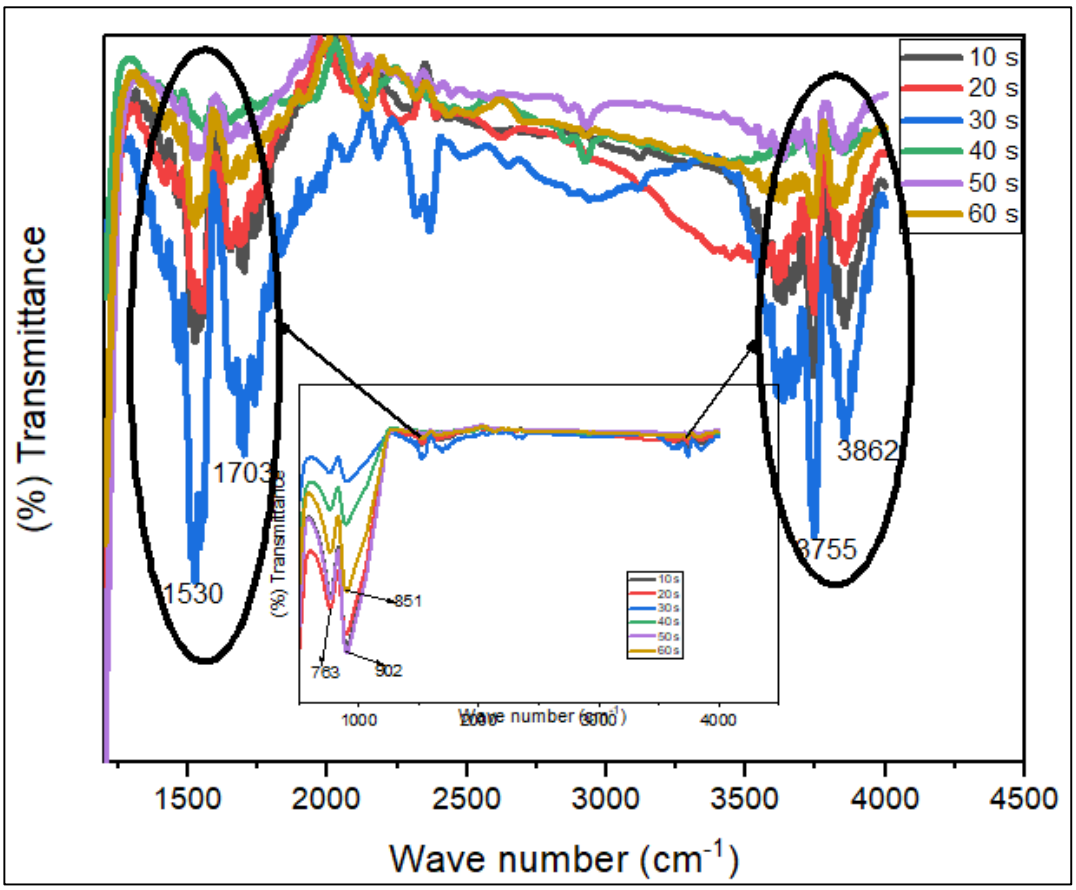


Figure 4.6: FT-IR spectra of Fe: TiO_2 thin films deposited using varying spinning time.

In general, the spinning time (10 to 60 S) only caused slight differences in the relative intensity and transmittance of the FTIR bands, and the characteristic Ti–O–Ti and metal–oxygen vibrations did not shift to significantly different wavenumber positions. This means that the basic bonding structure and functional groups were not significantly changed by the increasing spinning time in the Fe: TiO_2 films. Instead, the small variations in the peak intensity and transmittance can be correlated to the variations in the amount and spread of the precursor material that remains on the substrate with the spinning time, that may affect the effective film thickness and uniformity. Likewise, the bands related to C—O/C=O and O—H did not show strong dependence on spinning time, as long as the spinning time was varied under the

conditions used. Hence, the main effect of the spinning time on the deposited coating was on the physical properties, such as the film thickness and film uniformity, of the Fe: TiO_2 films, and the chemical bonding environment and the characteristic functional group of the Fe: TiO_2 films did not change significantly.

4.3.3 UV–Vis Analysis of Fe: TiO_2 Thin Films Deposited using Varying Spinning Times

Evolution one plus UV–Vis spectrophotometer was further employed to examine the effect of spin-coating duration on the optical properties of Fe:TiO_2 thin films. The films were deposited at varying spinning times ranging from 10 S to 60 S and their absorbance spectra were recorded over the wavelength range of 300–900 nm. The forbidden energy gaps were estimated using plots derived from the absorption data. Figure 4.8 presents (a) the absorbance spectra and (b) the corresponding plots of $(\alpha h\nu)^{1/2}$ versus photon energy ($h\nu$) for the different spinning durations, with the extracted band gap values indicated.

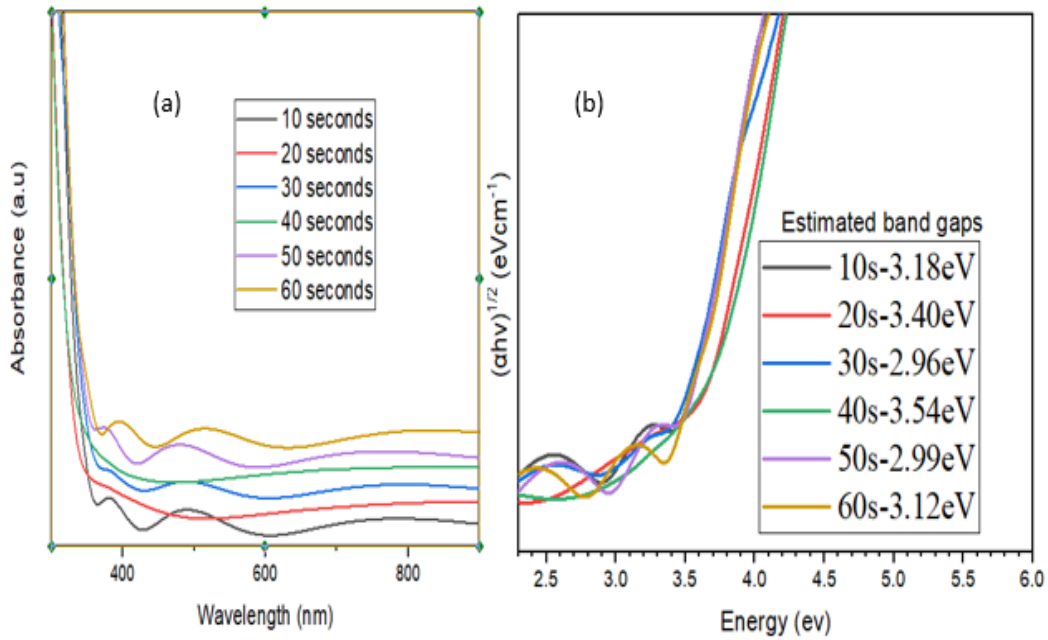


Figure 4.7: (a) the absorbance as a function of wavelength (b) the plots of $(\alpha h\nu)^{1/2}$ versus photon energy $(h\nu)$ for the different spinning durations

The light related characteristics of Fe:TiO_2 thin films as a function of spin coating time is shown in figure 4.8. The absorption is strong in all the samples in the UV region

and this is a common characteristic to TiO_2 based materials. The difference in absorbance intensity as spinning times increased suggests that the spinning time had an impact on precursor retention on the substrate, leading to changes in film thickness and uniformity (Lin et al., 2012). These differences in response to incident light and absorbance of the Fe: TiO_2 films were due to these variations. These observed changes thus imply that the spinning time affected the physical and microstructural evolution of the films, and the amount of absorbance was dependent on the characteristics of the deposited film.These optical band gap values were obtained from the Tauc plots and reveal considerable variation for the different coating durations. The forbidden energy gap rises from 3.18 eV at 10 S to 3.40 eV at 20 S, decreases sharply to 2.96 eV at 30 S, rises again to 3.54 eV at 40 S and then decreases to 2.99 eV and 3.12 eV for the 50 S and 60 S coatings, respectively.

The lack of a systematical increase or decrease suggests that there are several factors that influence the optical behavior of the films which are affected by the spin time. For shorter spin durations, incomplete removal of the solvent or relatively thick coatings can lead to the possible generation of defect states, which can increase the band gap. The significant drop at 30 S and 50 S indicates higher densities of localized electronic states in the forbidden energy gap, which may be due to structural disorder, oxygen vacancy or Fe-related impurity content (Rasim et al., 2023). The higher band gap values measured at the 20 S and especially the 40 S, on the other hand, suggest better film uniformity and lower defect density, which favor sub-band gap transitions and lead to an optical response at higher energies. The film obtained in the spinning time of 40 S has the highest band gap (3.54 eV), indicating that the sample has the most uniform structure among the samples investigated (Cadatal et al., 2022) In summary, the results show that spin-coating time plays a pivotal role in film nucleation and growth, defect generation and optoelectronic characteristics of Fe: TiO_2 ultrathin layers and it is a crucial parameter for optimizing the thin films.

4.4 Fe: TiO_2 Thin Films Coated using a Varying Number of Layers

Fe: TiO_2 coatings were successfully deposited using the spin-coating technique with varying numbers of coating layers and their structural and optical properties were systematically investigated to evaluate the effect of layer buildup on film performance.

4.4.1 XRD Analysis of Fe:TiO_2 Thin Films Coated using a Varying Number of Layers

The structural evaluation of the coated layers was performed via ARL Equinox 100 X-Ray diffractometer. Figure 4.9 following shows the XRD patterns of Fe:TiO_2 thin films (a) full range pattern and (b) magnified XRD pattern prepared with different numbers of deposited layers ranging from one to five and annealed at 450 °C for 2 hours. The patterns are used to examine the impact of layer thickness on the crystallinity, phase formation and preferred orientation of the coating.

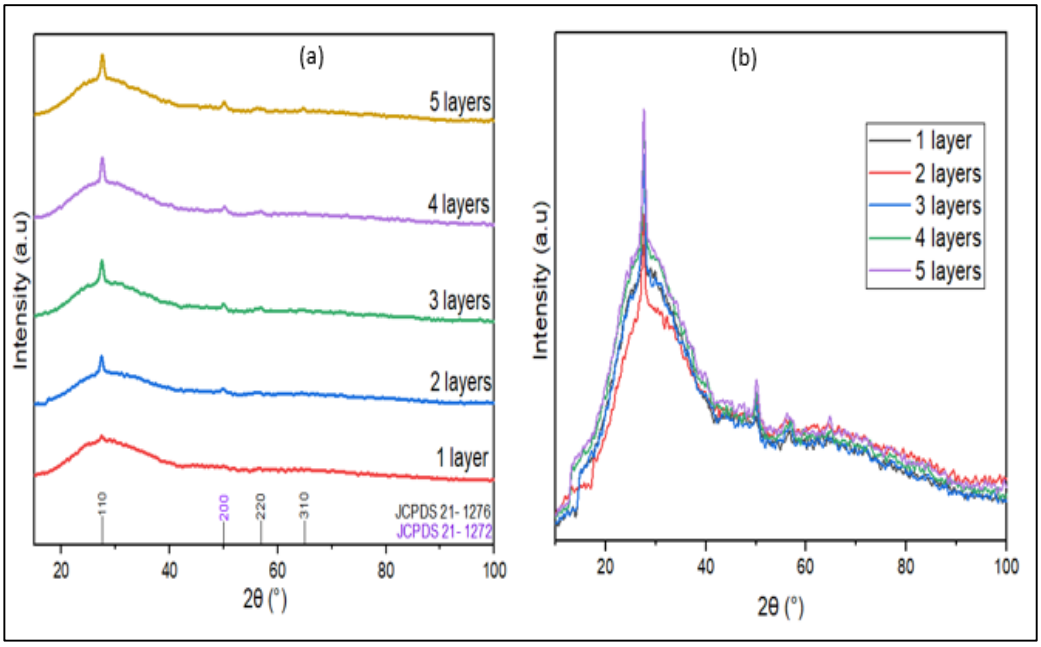


Figure 4.8: XRD patterns of Fe: TiO_2 thin films prepared with different numbers of deposited layers (a) full range XRD pattern (b) magnified XRD pattern

The XRD patterns in figure 4.9 reveal that the Fe: TiO_2 thin films have a mixed-phase structure of both rutile and anatase phases. All the samples exhibit the diffraction peak at $2\theta \approx 27°$, corresponding to the (110) plane, which indicates the occurrence of rutile phase. The diffraction peak of the (200) plane is seen in the 2-, 3-, 4- and 5-layer films, which indicates the existence of the anatase phase and the formation of a mixed-phase TiO_2 structure. Other reflections of the (220) crystal plane are found in 3-, 4-and 5-layer films and the (301) peak comes out in the 5-layer film, which shows that as the number of layers increased, the crystal structure gradually became more perfect and the development of the crystal structure continued. These new diffraction peaks

indicate that the crystal growth and stability of the phase scaled proportionally with film thickness. Moreover, the diffraction peaks of 5-layer sample are relatively sharper and more intense than that of other films, suggesting to improve crystallinity, crystallite growth and reduce structural disorder. The presence of several clear diffraction planes in the 5-layer film indicates that there is an increase in crystal ordering and a good phase development. The obtained results indicate that a greater number of the spin-coating layers resulted in sufficient material for effective nucleation and grain growth during annealing, where the 5-layer film presented the most favorable structure among all the samples. Table 4.3 following summarizes the crystallite size, FWHM and the lattice parameters of Fe: TiO_2 thin films of varying number of layers.

Table 4. 3: Summary of the crystallite sizes, FWHM and the lattice parameters of Fe:TiO_2 thin films of varying number of layers.

Sample (No. of layers)	Plane (hkl)	$2\boldsymbol{\theta}$(°)	FWHM (°)	Crystallite size (nm)	dhkl (Å)	Lattice parameter a (Å)
1	110	27.96	2.485	3.294	3.294	4.509
2	110	27.28	1.914	4.271	3.266	4.619
	200	49.31	5.013	1.744	1.847	3.693
3	110	27.51	1.923	4.253	3.240	4.582
	200	49.78	1.670	5.244	1.830	3.660
	220	56.91	3.091	5.410	1.617	4.573
4	110	27.33	1.981	4.127	3.261	4.611
	200	49.34	1.195	7.315	1.846	3.691
	220	56.62	5.046	1.788	1.624	4.594
5	110	26.92	1.528	5.345	3.309	4.680
	200	49.78	2.542	3.445	1.830	3.660
	220	56.78	5.810	1.177	1.620	4.582
	301	65.11	8.761	1.076	1.431	4.680

Table 4.3 shows that the crystallinity, crystallite size, lattice parameters and microstructural properties of the Fe doped TiO_2 thin films were significantly affected by the number of spin-coating layers. The XRD profiles confirmed that all the samples had a mixed phase of TiO_2, observed by the presence of a dominant peak of rutile (110) and anatase (200), indicating a mixed phase TiO_2 structure throughout the samples. The general trend was that the crystallite size increased with the number of layers in the film with value ranging from 3.294 nm in the 1-layer film to 5.345 nm in the 5-layer film for the rutile (110) plane. This is also correlated by a reduction in FWHM from 2.485° to 1.528° signifying improvement in crystallinity, a decrease in lattice strain and an improvement in grain growth which is in line with existing literature (Rajeswari et al., 2021). The lessened peak broadening with increasing number of layers implies that the thicker coatings gave more favorable conditions for crystal nucleation/growth during the annealing process. In addition, the occurrence of higher-index planes (220) and (301), especially in the thicker films, indicates better polycrystallinity and better structural ordering. The 5-layer sample showed the best crystal quality and the most stable structure, with the biggest crystallite size and the smallest FWHM values and the diffraction pattern was the most distinct. The results show that the structural properties of the Fe:TiO_2 thin films improve with increasing number of layers and that the sample obtained after 5 layer deposition is the best one for crystallinity and crystal growth. Figure 4.10 shows the variation of FWHM and crystallite size as a function of the number of deposited layers of Fe: TiO_2 thin films.

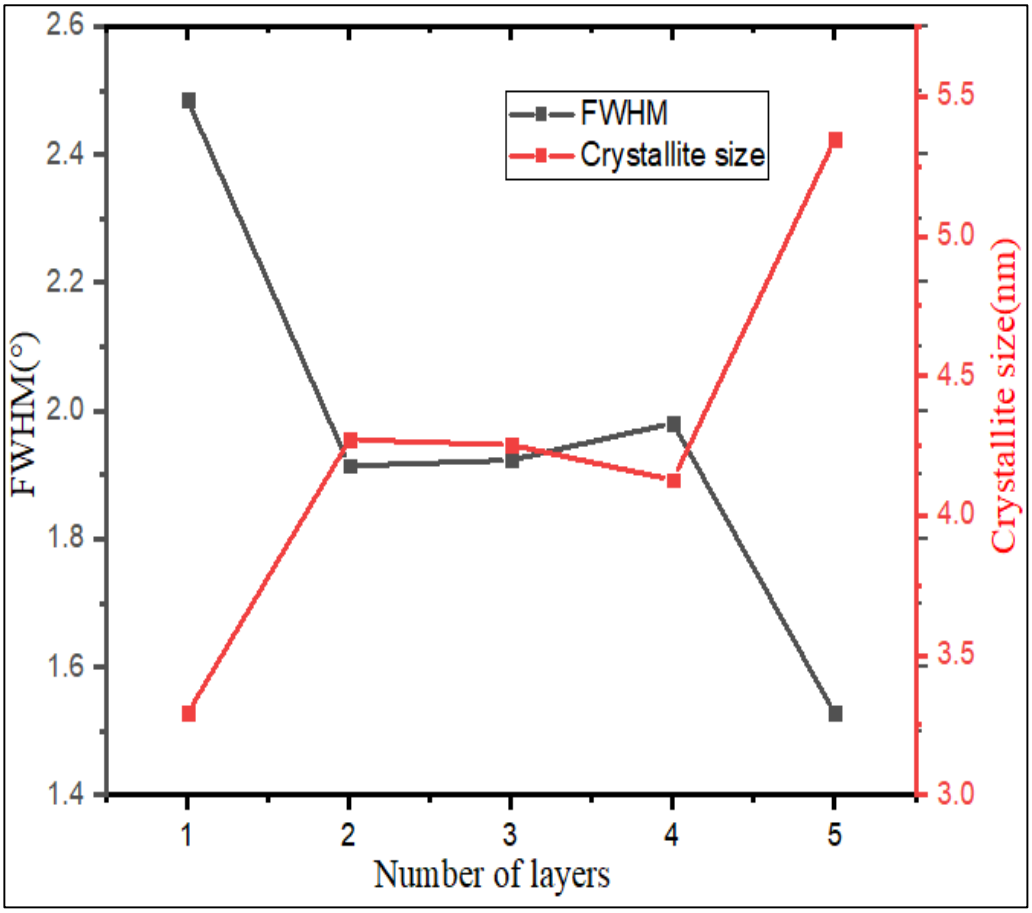


Figure 4.9 Variation of FWHM and crystallite size as a function of the number of deposited layers of Fe: TiO_2 thin films

The variation of FWHM and crystallite size with the number of layers deposited further substantiates the profound microstructural dependence of Fe: TiO_2 thin film on the film thickness. There was an inverse relation between the crystallite size and FWHM with the narrow peaks showing better crystallinity and larger crystallite sizes. This is clearly visible in the rutile reflection (110) where the FWHM of the film reduces gradually from 2.485° to 1.528° and the crystallite size increases from 3.294 nm to 5.345 nm respectively for 1-layer film and 5-layer film. This behavior suggests that the more layers the grains are spin coated, the greater the grain size is grown and the lesser the lattice imperfections during annealing. Thicker films also show other diffraction peaks, (220) and (301), which is an additional confirmation of the improved polycrystallinity and structural development.

The difference of calculated d-spacing and lattice parameters is small, indicating that there is residual strain in the TiO_2 lattice that may be caused by the incorporation of

Fe and thickness dependence. This is supported by earlier reports (Shymanovska et al., 2022) The lattice parameters, however, are very close to those of the standard tetragonal structure of TiO_2, indicating only minor distortions of this crystal structure. Overall, the 5-layer film shows the highest structural quality, as is reflected in the lowest FWHM, largest crystallite size and most well-defined diffraction features. The results indicate that the more layers that have been deposited, the more crystalline and ordered the structure would be; the 5-layer coating was determined to be the optimum. The coexistence of anatase and rutile phases is favorable for optoelectronic and photocatalytic applications because of the better charge separation and the less electron–hole recombination. Similar relationships between crystallite size, diffraction-peak broadening, structural characteristics and the existence of anatase and rutile have been reported for Fe-doped TiO_2 thin films (Ruan et al., 2022).

4.4.2 FTIR Analysis of Fe: TiO_2 Thin Films Coated using a Varying Number of Layers

IR spirit Shimadzu FTIR spectrophotometer was used to identify the characteristic functional groups and bonding vibrations present in the Fe: TiO_2 thin films deposited using one to five coating layers. The FTIR spectra presented in figure 4.11 exhibited characteristic absorption bands in the 737–743 cm^{-1} region, which are associated with metal–oxygen vibrations of the TiO_2 lattice. Similar Ti–O/Ti–O–Ti vibrations have been reported in Fe-doped TiO_2 materials. The absorption feature around 900 cm^{-1} may be associated with Ti–O–Fe bonding resulting from modification of the Ti–O–Ti network following Fe incorporation.

Previous FTIR investigations of Fe-doped TiO_2 have reported changes in the Ti–O vibration region following Fe incorporation and attributed these changes to modifications of metal–oxygen bonding and possible formation of Ti–O–Fe bonds (Bakre et al., 2016) (Mragui et al., 2023). Additional absorption bands at 1280 and 1532 cm^{-1} may be related to vibrational modes of residual organic species originating from the precursor system, while the band at 1737 cm^{-1} can be associated with C=O stretching vibrations. The absorption band at 2925 cm^{-1} is attributable to aliphatic C–H stretching vibrations. The high-wavenumber absorption at 3746 cm^{-1} is associated with O–H stretching from surface hydroxyl groups. Similar O–H-related bands and adsorbed-water vibrations have been reported for Fe-doped TiO_2 materials,

confirming the presence of hydroxylated surfaces following synthesis (Zhang et al., 2002) (Wahyuni et al., 2023).

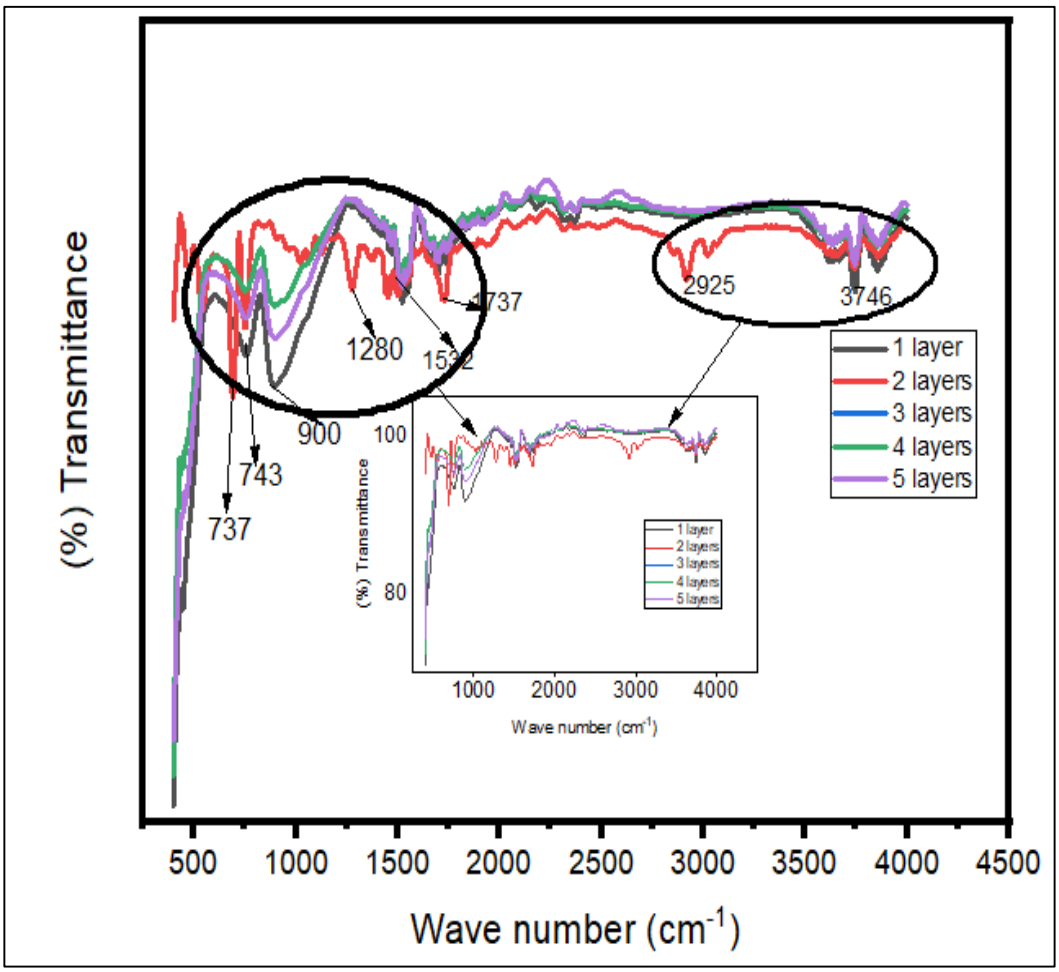


Figure 4.10: FT-IR spectra of Fe: TiO_2 thin films with varying number of deposited layers

It was noteworthy that there was a close similarity and overlap of the overlaid spectra of films with various numbers of layers, across the entire wavenumber range, implying that the chemical composition, bonding environment and uniformity of doping were consistent independent of the number of layers deposited. This reproducibility implies that the number of added layers is the main factor that affects the film thickness without impeding the integrity of the structure and functional groups of the Fe:TiO_2 material which agrees to earlier reports (Mercy et al., 2026).

In general, The FTIR spectra of the different coatings showed only slight differences as the number of coating layers varied from one to five, with the characteristic Ti–O–Ti, Ti–O–Fe, C–H, C=O and O–H absorption bands still present in the different films.

The similarity in position of the main absorption bands clearly shows that the chemical bonding and functional groups did not change significantly with the number of layers. The relative absorption intensity differences, however, could relate to the deposition of more material and film thickness changes at higher deposition, as more layers were added. The amount of coating layers thus had the main effect on the amount of material that produces infrared absorbing effect, but did not affect much the nature of the chemical bonds in the Fe: TiO_2 network. The presence of these bands of Ti–O–Ti and Ti–O–Fe through all coating thicknesses also suggests that the same bonding environment was preserved when the film thickness increased. Thus, an increase in the number of layers caused significant changes in physical thickness of the films, but caused only small changes in the functional groups and bonding properties of the films.

4.4.3 UV-Vis spectroscopy Analysis of Fe: TiO_2 Thin Films Coated using a Varying Number of Layers

To evaluate the influence of number of deposited layers on the optical properties of Fe:TiO_2 thin films, Evolution one plus UV–Vis spectrophotometer was used on samples prepared with varying numbers of spin-coated layers, 1–5 layers. The absorbance spectra were recorded in the wavelength range of 300–900 nm and the corresponding optical band gaps were estimated using Tauc plots derived from the absorption coefficient. Figure 4.12 shows (a) the absorbance as a function of wavelength and (b) the plots of $(\alpha h\nu)^{1/2}$ versus photon energy ($h\nu$) for the different layer numbers. The extracted band gap values are also indicated for comparison.

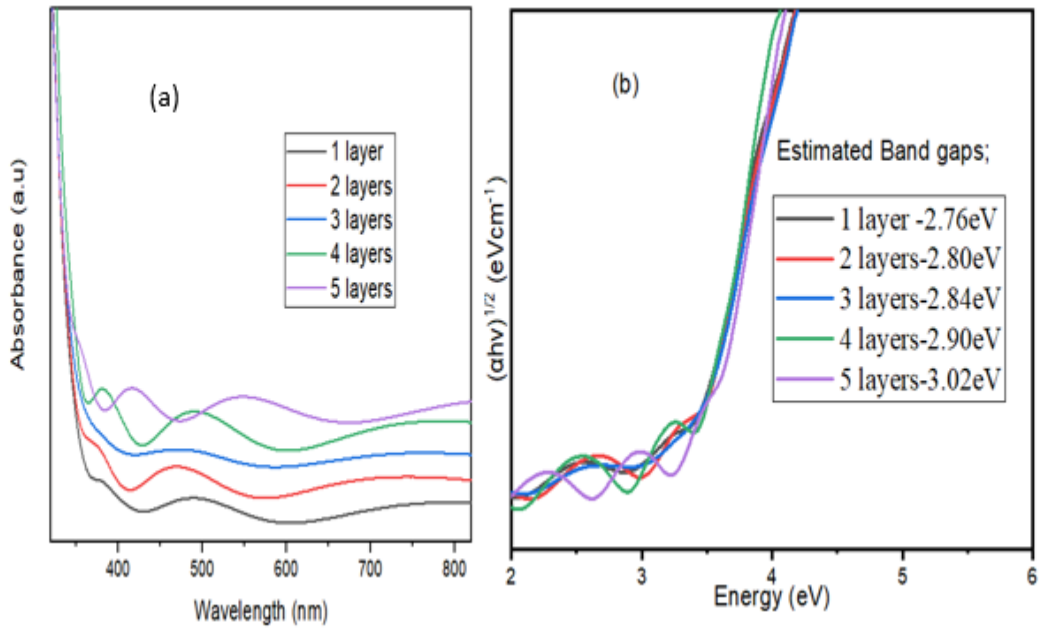


Figure 4.11: (a) the absorbance as a function of wavelength (b) the plots of $(\alpha h\nu)^{1/2}$ versus photon energy $(h\nu)$ for the different layer numbers

The optical properties of Fe:TiO_2 thin films as a function of the number of coating layers is shown in figure 4.12. The absorbance spectra show that all samples have strong absorbance in the UV region and the overall absorbance decreases with increasing number of layers. This is the expected behaviour since adding layers to the film increases the film thickness, which means that a higher percentage of the photons travelling through the film will be absorbed by the material. The Tauc plots reveal that the photon energy threshold of the single-layer coating (2.76 eV) is lower than that of the five-layer film (3.02 eV). The progressive band gap widening suggests a blue shift in the optical absorption edge as the number of the layers increase. This indicates that the thicker films have better structural quality and lower density of defect states. The slightly smaller band gap seen in the single-layer film could be due to a greater number of grain boundaries, which would contain surface defects and Fe induced impurity states, which would create electronic levels in the forbidden energy band. The films are more continuous and compact with each deposition in order to minimize structural imperfections and minimize transitions that occur as a result of defects. Hence, there is a gradual rise in optical band gap from 2.76 eV to 3.02 eV. The results suggest that the quality of films improves as the number of layers deposited increases and the optical properties of films approach the optical properties of intrinsic TiO_2 which is

supported by the existing literature (Timoumi et al., 2023). Hence, the number of layers is also a good parameter to regulate the light absorption and band gap energy of Fe:TiO_2 thin films.

4.5 Stability of Fe: TiO_2 Thin Films over Twenty-Eight Days

To evaluate the long-term structural stability of the optimized Fe:TiO_2 thin film, XRD measurements were carried out ARL Equinox 100 X-Ray diffractometer immediately after synthesis (day 1) and subsequently at weekly intervals over a period of twenty-eight days under ambient laboratory conditions. Monitoring the diffraction patterns over time provides information on whether prolonged storage induces structural changes such as phase transformation, lattice distortion, crystallinity loss or crystallite growth. Since the structural integrity of semiconductor thin films directly influences their optical and electronic performance, stability assessment is an important criterion in determining their suitability for practical photovoltaic applications (Sassi et al., 2024) . Figures 4.13 and 4.14 show a photograph of an optimized thin film and the resulting XRD diffractograms respectively.



Figure 4.13: A photograph of an optimized Fe:TiO_2 thin film

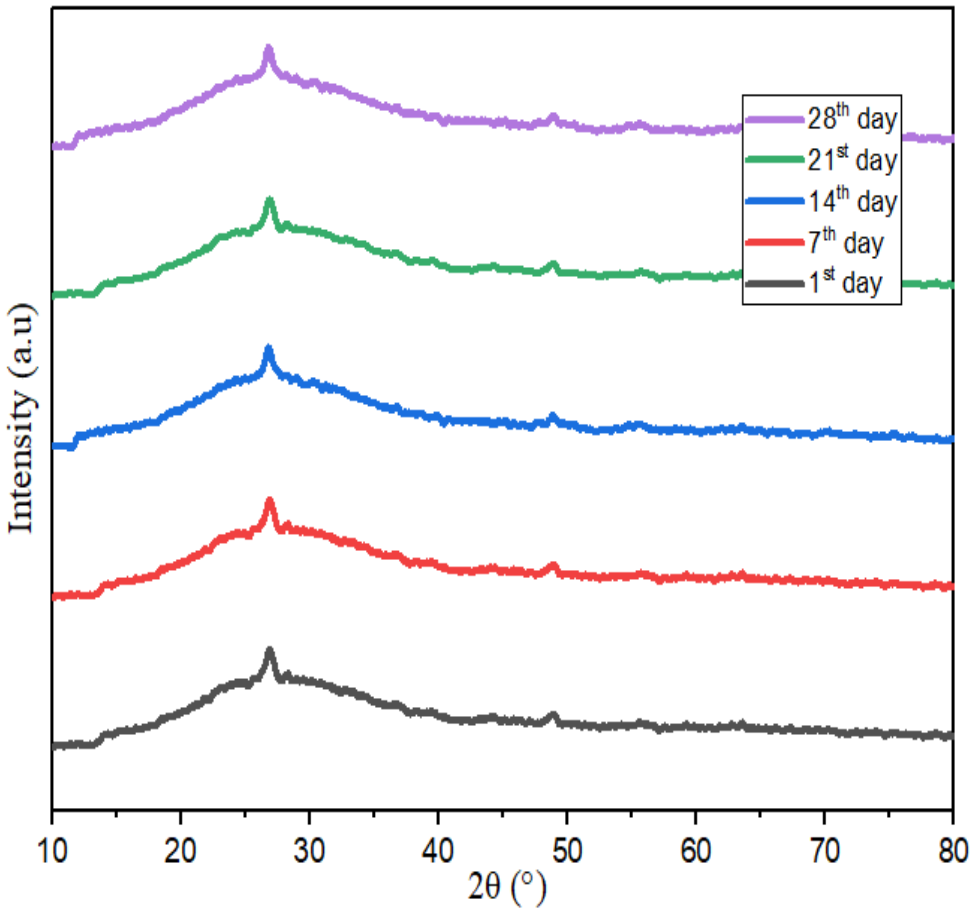


Figure 4.14: XRD patterns of the optimized Fe: TiO_2 thin film monitored over a period of twenty-eight days at intervals of one week

Figure 4.14 demonstrates that the optimized Fe: TiO_2 thin film maintained its crystalline structure throughout the twenty-eight-day monitoring period. The dominant diffraction peak corresponding to the rutile (110) plane remained clearly visible in all the diffractograms, while no additional peaks associated with impurity phases or degradation products were detected. The persistence of the characteristic diffraction peak indicates that the crystalline phase remained unchanged during storage, suggesting that the incorporation of Fe into the TiO_2 lattice did not compromise the structural stability of the film. This is supported by the existing literature (Yin et al., 2023). Although the diffraction peak exhibited a slight reduction in intensity with increasing storage time, the peak position remained essentially unchanged, indicating that no significant lattice expansion or contraction occurred. The same trend was earlier reported by (Khima et al., 2024). The slight decrease in intensity and minor peak broadening may be associated with small variations in crystallinity or microstructural strain during storage. However, these changes were

insufficient to cause a detectable phase transformation. The retention of the diffraction peak throughout the monitoring period therefore demonstrates that the optimized Fe: TiO_2 thin film possesses good structural stability under ambient conditions, making it suitable for applications that require prolonged structural integrity.

Table 4. 4: XRD Stability Analysis of Optimized Fe: TiO_2 Thin Film Over 28 Days

Characterization days	2θ (°)	FWHM (°)	Crystallite Size (nm)
1st	27.33	1.629	5.018
7th	27.32	1.680	4.866
14th	27.31	1.641	4.981
21st	27.31	1.712	4.775
28th	27.30	1.681	4.863

The numerical values presented in Table 4.4 further confirm the structural stability observed from the XRD patterns. The diffraction angle (2θ) changed only slightly from 27.33° on day 0 to 27.30° after twenty-eight days, representing a negligible shift of only 0.03°. Such a small variation falls within the experimental uncertainty of XRD measurements and therefore does not indicate any significant modification of the crystal lattice. This observation confirms that the optimized Fe:TiO_2 thin film maintained its crystal structure throughout the storage period.

Similarly, the FWHM exhibited only minor fluctuations, varying between 1.629° and 1.712°. Since FWHM is inversely related to crystallite size, these small variations suggest only slight changes in crystallinity rather than structural degradation (Park et al., 2021). The corresponding crystallite size remained relatively constant, ranging from 5.018 nm on day 0 to 4.863 nm after twenty-eight days, with the minimum value of 4.775 nm recorded on day 21. The overall variation in crystallite size was less than 5%, indicating that the nanocrystalline structure remained essentially unchanged during storage. The combined behaviour of the diffraction angle, FWHM and crystallite size demonstrates that the optimized Fe:TiO_2 thin film possesses excellent

structural stability under ambient laboratory conditions. The absence of significant changes in these structural parameters suggests that the film is resistant to phase degradation and maintains its crystallographic integrity over time. Such stability is desirable for solar cell applications because it ensures that the photoactive layer can retain consistent structural properties during storage and operation, thereby contributing to reliable device performance.

4.6 Chapter Summary

In this chapter, the structural, chemical and optical properties of Fe: TiO_2 thin films, obtained by sol-gel spin coating technique, have been described. The effects of precursor volume, spinning time and number of coating layers were studied. The result indicated that the crystallite size was around 4.11 nm and 5.21 nm for the precursor volume of 1.0 mL and spinning time of 30 S, respectively. The optical band gap increased from one to five layers of coatings, from 2.76 eV to 3.02 eV, with 5 layers providing the best overall properties. FTIR confirmed the presence of Ti–O–Ti and Ti–O–Fe bonds and UV–Vis analysis indicated strong absorption in the UV region. The stability study also revealed minor changes in the structural parameters during the course of the investigation for 28 days, which indicates good structural stability of the Fe: TiO_2 thin films under the investigated conditions.

CHAPTER FIVE
CONCLUSION AND RECOMMENDATIONS

5.1 Conclusion

Based on the findings of this study, the following conclusions were made:

i. Effect of precursor solution volume

The precursor solution volume significantly influenced the structural and optical properties of the Fe: TiO_2 thin films. Among the investigated volumes, 1.0 mL produced the optimum film, exhibiting the largest crystallite size (4.107 nm) and a reduced full width at half maximum (1.992°), indicating improved crystallinity. FTIR analysis confirmed the formation of Ti–O–Ti and Ti–O–Fe bonds, while UV–Vis analysis showed that the precursor solution volume affected the optical band gap, demonstrating that precise control of the deposited solution volume is essential for obtaining high-quality Fe: TiO_2 thin films.

ii. Effect of spinning time

Spinning time had a significant effect on the crystallographic and optical properties of the deposited films. A spinning time of 30 s produced the optimum thin film with the largest crystallite size (5.206 nm), the lowest FWHM (1.571°) and the lowest optical band gap (2.96 eV). The reduced band gap is attributed to Fe-induced impurity energy levels within the TiO_2 band structure, which enhanced visible-light absorption and improved the suitability of the films for photovoltaic applications.

iii. Effect of the number of coating layers

The number of deposited layers influenced the crystallinity and optical behaviour of the Fe: TiO_2 thin films. Increasing the number of coating layers improved the structural quality of the films, with five coating layers producing the optimum film. FTIR spectra confirmed the preservation of the TiO_2 network with successful Fe incorporation, while UV–Vis analysis showed that the optical band gap varied with film thickness, demonstrating that the number of coating layers is an important parameter in optimizing thin-film performance.

iv. Structural stability of Fe: TiO_2 thin films

The optimized Fe: TiO_2 thin films exhibited good structural stability over the 28-day storage period. XRD analysis showed only slight variations in diffraction peak position, crystallite size and FWHM, indicating that the crystalline structure remained stable with no significant structural degradation. These results demonstrate that the optimized Fe: TiO_2 thin films possess good durability and are suitable for long-term photovoltaic applications.

Overall, the study demonstrated that optimization of the spin-coating deposition parameters, together with 3 mol% Fe doping, significantly improved the structural and optical properties of TiO_2 thin films. The optimized films exhibited improved crystallinity, reduced optical band gap, successful Fe incorporation and good structural stability, making them promising window-layer materials for photovoltaic applications.

5.2 Recommendations

In view of the findings obtained in this study, the following recommendations are made to support the optimization and practical application of Fe: TiO_2 thin films in photovoltaic devices.

5.2.1 Recommendation from the study

Based on the findings of this study, the following recommendations are made:

i. The optimized fabrication conditions identified in this study (1.0 mL precursor solution volume, 30 s spinning time, five coating layers and 3 mol% Fe doping) should be adopted as a baseline for testing Fe: TiO_2 thin films intended for photovoltaic applications, as they produced improved crystallinity, reduced optical band gap and good structural stability.
ii. Careful control of spin-coating deposition parameters should be maintained during thin-film fabrication because slight variations in precursor solution volume, spinning time and coating layers were found to significantly influence the structural and optical properties of the films.
iii. Fe: TiO_2 thin films should be considered for use as window-layer materials in thin-film solar cells due to their improved visible-light absorption, good

crystallinity and demonstrated structural stability over the 28-day evaluation period.

5.2.2 Proposed future research

Based on the scope and findings of this study, the following areas are recommended for future research:

i. Investigate the long-term stability of the optimized Fe: TiO_2 thin films over periods longer than 28 days under different environmental conditions, such as humidity, temperature variations and continuous light exposure, to evaluate their durability for practical photovoltaic applications.
ii. Test complete thin-film solar cells incorporating the optimized Fe: TiO_2 films as window layers and evaluate key photovoltaic performance parameters, including power conversion efficiency, short-circuit current density, open-circuit voltage and fill factor.
iii. Investigate the combined influence of Fe doping concentration and optimized spin-coating parameters to establish the optimum balance between crystallinity, optical band gap, charge transport and photovoltaic performance.
iv. Employ advanced characterization techniques such as scanning electron microscopy (SEM), transmission electron microscopy (TEM), atomic force microscopy (AFM)and photoluminescence (PL) spectroscopy to correlate surface morphology, microstructure and charge-carrier recombination with the structural and optical properties of the films.
v. Investigate alternative substrates, transparent conductive oxides and annealing atmospheres to determine their influence on the crystallographic, optical and electrical properties of Fe: TiO_2 thin films and their suitability for different photovoltaic device architectures.

REFERENCES

Al-Amin, K., Kawsar, M., Mamun, M. T. R. B., & Sahadat Hossain, M. (2025). Fourier transform infrared spectroscopic technique for analysis of inorganic materials: a review. *Nanoscale advances*, *7*(21), 6677–6702. https://doi.org/10.1039/d5na00522

Al-Ezzi, A. S., & Ansari, M. N. M. (2022). Photovoltaic Solar Cells: A Review. *Applied System Innovation*, *5*(4), 67. https://doi.org/10.3390/asi5040067

Amudhavalli, B., Mariappan, R., & Prasath, M. (2022). Synthesis chemical methods for deposition of ZnO, CdO and CdZnO thin films to facilitate further research. *Journal of Alloys and Compounds*, *925*, 166511. https://doi.org/10.1016/j.jallcom.2022.166511

Arifin, N. M., Mhd Noor, E. E., Mohamad, F., Mohamad, N., & Mohamed Muzni, N. H. (2024). Enhancing the Properties of Nanostructure TiO_2 Thin Film via Calcination Temperature for Solar Cell Application. *Energies*, *17*(14), 3415. https://doi.org/10.3390/en17143415

Arunmetha, S., Dhineshbabu, N. R., Sakthipandi, K., & Jayavel, R. (2024). Exploring the impact of Fe^{3+} ions on TiO_2 nanostructures to enhance photocatalytic efficiency. *Journal of Materials Science: Materials in Electronics*, *35*(27), 1793. https://doi.org/10.1007/s10854-024-13566-5

Auf, d., M., & Di Carlo, A. (2019). Analytic approximations for solar cell open circuit voltage, short circuit current and fill factor. *Solar Energy*, *187*, 358–367. https://doi.org/10.1016/j.solener.2019.05.056

Adeyinka, Adekanmi & Mbelu, Onyedika & Adediji, Yaqub & Yahya, Daniel. (2023). a-review-of-current-trends-in-thin-film-solar-cell-technologies. 17.

Baishya, K., Ray, J. S., Dutta, P., Das, P. P., & Das, S. K. (2018). Graphene-mediated band gap engineering of WO_3 nanoparticle and a relook at Tauc equation for band gap evaluation. *Applied Physics A*, *124*(10), 704. https://doi.org/10.1007/s00339-018-2097-0

Bakre, P. V., Volvoikar, P. S., Vernekar, A. A., & Tilve, S. G. (2016). Influence of acid chain length on the properties of TiO_2 prepared by sol-gel method and LC-MS

studies of methylene blue photodegradation. *Journal of Colloid and Interface Science*, *474*, 58–67. https://doi.org/10.1016/j.jcis.2016.04.011

Ballif, C., Haug, FJ., Boccard, M. *et al.* Status and perspectives of crystalline silicon photovoltaics in research and industry. *Nat Rev Mater* **7**, 597–616 (2022). https://doi.org/10.1038/s41578-022-00423-2

Bogdanov, D., Ram, M., Aghahosseini, A., Gulagi, A., Oyewo, A. S., Child, M., Caldera, U., Sadovskaia, K., Farfan, J., De Souza Noel Simas Barbosa, L., Fasihi, M., Khalili, S., Traber, T., & Breyer, C. (2021). Low-cost renewable electricity as the key driver of the global energy transition towards sustainability. *Energy*, *227*, 120467. https://doi.org/10.1016/j.energy.2021.120467

Bojtor, A., Krisztián, D., Korsós, F., Kollarics, S., Paráda, G., Kollár, M., Horváth, E., Mettan, X., Márkus, B. G., Forró, L., & Simon, F. (2024). Dynamics of Photoinduced Charge Carriers in Metal-Halide Perovskites. *Nanomaterials*, *14*(21), 1742. https://doi.org/10.3390/nano14211742

Bonkerud, J., Zimmermann, C., Weiser, P. M., Vines, L., & Monakhov, E. V. (2021). On the permittivity of titanium dioxide. *Scientific Reports*, *11*(1), 12443. https://doi.org/10.1038/s41598-021-92021-5

Butt, M. A. (2022). Thin-Film Coating Methods: A Successful Marriage of High-Quality and Cost-Effectiveness—A Brief Exploration. *Coatings*, *12*(8), 1115. https://doi.org/10.3390/coatings12081115

Cadatal-Raduban, M., Pope, J., Olejníček, J., Kohout, M., Harrison, J. A., & Hasan, S. M. R. (2022). Ultraviolet-C Photoresponsivity Using Fabricated TiO_2 Thin Films and Transimpedance-Amplifier-Based Test Setup. *Sensors*, *22*(21), 8176. https://doi.org/10.3390/s22218176

Chandra, P, T., Podder, J., & Paik, L. (2022). Effect of Fe doping on the microstructure, optical and dispersion energy characteristics of TiO_2 thin films prepared via spray pyrolysis technique. *Results in Optics*, *8*, 100235. https://doi.org/10.1016/j.rio.2022.100235

Chaudhari, M. N. (2021). Thin film Deposition Methods: A Critical Review. *International Journal for Research in Applied Science and Engineering Technology*, *9*(VI), 5215–5232. https://doi.org/10.22214/ijraset.2021.36154

Chaudhary, K. T. (2021). Thin Film Deposition: Solution Based Approach. In *Thin Films*. IntechOpen. https://doi.org/10.5772/intechopen.94455

Cisternas, E., Aguilera-del-Toro, R., Aguilera-Granja, F., & Vogel, E. E. (2024). Effect of Substitutional Metallic Impurities on the Optical Absorption Properties of TiO_2. *Nanomaterials*, *14*(14), 1224. https://doi.org/10.3390/nano14141224

Dai, Z., & Giustino, F. (2024). Identification of large polarons and exciton polarons in rutile and anatase polymorphs of titanium dioxide. *Proceedings of the National Academy of Sciences*, *121*(48), e2414203121. https://doi.org/10.1073/pnas.2414203121

Depla, D., Mahieu, S., & Greene, J. E. (2010). Sputter Deposition Processes. In *Handbook of Deposition Technologies for Films and Coatings* (pp. 253–296). Elsevier. https://doi.org/10.1016/B978-0-8155-2031-3.00005-3

Dinnebier, R. E., & Billinge, S. J. L. (2019). *The Bragg equation derived*. *H*, 2–23. https://doi.org/10.1107/97809553602060000935

Doan, N. S., Huh, J., Mac, V. H., Kim, D., & Kwak, K. (2020). Probabilistic Risk Evaluation for Overall Stability of Composite Caisson Breakwaters in Korea. *Journal of Marine Science and Engineering*, *8*(3), 148. https://doi.org/10.3390/jmse8030148

Dolgonos, A., Mason, T. O., & Poeppelmeier, K. R. (2016). Direct optical band gap measurement in polycrystalline semiconductors: A critical look at the Tauc method.*Journal of Solid State Chemistry*, *240*, 43–48. https://doi.org/10.1016/j.jssc.2016.05.010

Dong, X., Mamat, M., Baikeli, Y., Liu, G., & Xiaerding, F. (2024). Effect of Fe doping on crystalline phase, structure and photocatalytic properties of TiO_2 thin films. *Optical Materials*, *150*, 115196. https://doi.org/10.1016/j.optmat.2024.115196

Efaz, E. T., Rhaman, M. M., Imam, S. A., Bashar, K. L., Kabir, F., Mourtaza, M. E., Sakib, S. N., & Mozahid, F. A. (2021). A review of primary technologies of

thin-film solar cells. *Engineering Research Express*, *3*(3), 032001. https://doi.org/10.1088/2631-8695/ac2353

El-Shafei, R., Hegazy, H., & Acharya, B. (2021). A Review of Antiviral and Antioxidant Activity of Bioactive Metabolite of Macroalgae within an Optimized Extraction Method. *Energies*, *14*(11), 3092. https://doi.org/10.3390/en14113092

Estrada-Flores, S., Martínez-Luévanos, A., Perez-Berumen, C. M., García-Cerda, L. A., & Flores-Guia, T. E. (2020). Relationship between morphology, porosity and the photocatalytic activity of TiO_2 obtained by sol–gel method assisted with ionic and nonionic surfactants. *Boletín de La Sociedad Española de Cerámica Vidrio*, *59*(5), 209–218. https://doi.org/10.1016/j.bsecv.2019.10.003

Fatima, Q., Haidry, A. A., Zhang, H., El Jery, A., & Aldrdery, M. (2024). A critical review on advancement and challenges in using TiO_2 as electron transport layer for perovskite solar cell. *Materials Today Sustainability*, *27*, 100857. https://doi.org/10.1016/j.mtsust.2024.100857

Foo, S., Thambidurai M, Senthil Kumar P, Yuvakkumar R, Huang Y, Dang C. *Recent review on electron transport layers in perovskite solar cells*. *Int J Energy Res*. 2022; 46(15): 21441-21451. doi:10.1002/er.7958

Foyshal, M., Ferdousy, J., Mahbubur, M., Rachona, A. M., Kabir, M. F., Shahid, M. H., & Rahman, M. (2025). Iron-Doped Titanium Dioxide Nanoparticles with Enhanced Ferromagnetic Properties for Spintronic Applications. *BioNanoScience*, *15*(3), 344. https://doi.org/10.1007/s12668-025-01963-x

Fricano, A., Tavormina, F., Pignataro, B., Vetri, V., & Ferrara, V. (2025). Progress and Prospects of Biomolecular Materials in Solar Photovoltaic Applications. *Molecules*, *30*(15), 3236. https://doi.org/10.3390/molecules30153236

Gapale, S A Arote, B M Palve, R Y Borse, Influence of precursor solution concentration on the structural, optical and humidity sensing properties of spray-deposited TiO_2 thin films[J]. *J. Semicond.*, 2018, 39(12): 122003. doi: 10.1088/1674-4926/39/12/122003.

Ghobadi, N. (2013). Band gap determination using absorption spectrum fitting procedure. *International Nano Letters*, *3*(1), 2. https://doi.org/10.1186/2228-5326-3-2

Ghosh, S., Saha, S., Moyeen, A. A., Mahmood, A. A., & Islam, M. B. (2025). Tailoring the structural and optical properties of TiO_2 thin films: A study of undoped, N-doped and Fe-doped variants via sol-gel spin coating. *Next Materials*, *8,* 100757. https://doi.org/10.1016/j.nxmate.2025.100757

Giannouli, M. (2021). Current Status of Emerging PV Technologies: A Comparative Study of Dye-Sensitized, Organic and Perovskite Solar Cells. *International Journal of Photoenergy*, *2021*, 1–19. https://doi.org/10.1155/2021/6692858

Giechaskiel, B., & Clairotte, M. (2021). Fourier Transform Infrared (FTIR) Spectroscopy for Measurements of Vehicle Exhaust Emissions: A Review. *Applied Sciences*, *11*(16), 7416. https://doi.org/10.3390/app11167416

Gürakar, S., Ot, H., Horzum, S., & Serin, T. (2020). Variation of structural and optical properties of TiO_2 films prepared by DC magnetron sputtering method with annealing temperature. *Materials Science and Engineering: B*, *262,* 114782. https://doi.org/10.1016/j.mseb.2020.114782

Hassan, Q., Viktor, P., J. Al-Musawi, T., Mahmood Ali, B., Algburi, S., Alzoubi, H. M., Khudhair Al-Jiboory, A., Zuhair Sameen, A., Salman, H. M., & Jaszczur, M. (2024). The renewable energy role in the global energy Transformations. *Renewable Energy Focus*, *48*, 100545. https://doi.org/10.1016/j.ref.2024.100545

Hiroi, Z. (2022). Inorganic Structural Chemistry of Titanium Dioxide Polymorphs. *Inorganic Chemistry*, *61*(22), 8393–8401. https://doi.org/10.1021/acs.inorgchem.2c00945

Imran, M., Saeed, Z., Pervaiz, M., Mehmood, K., Ejaz, R., Younas, U., Nadeem, H. A., & Hussain, S. (2021). Enhanced visible light photocatalytic activity of TiO_2 co-doped with Fe, Co and S for degradation of Cango red. *Spectrochimica Acta Part A: Molecular and Biomolecular Spectroscopy*, *255*, 119644. https://doi.org/10.1016/j.saa.2021.119644

Kääriäinen, M.-L., Kääriäinen, T. O., & Cameron, D. C. (2009). Titanium dioxide thin films, their structure and its effect on their photoactivity and photocatalytic properties. *Thin Solid Films*, *517*(24), 6666–6670. https://doi.org/10.1016/j.tsf.2009.05.001

Kaiyum, M. A., Kabir, M. H., Ali, M. M., & Rahman, M. S. (2021). Effects of Iron Doping on Properties of TiO_2 Thin Film Prepared by Spin Coating Method. *Journal of Surface Investigation: X-ray, Synchrotron and Neutron Techniques*, *15*(6), 1225-1231.

Kamoun, O., Gassoumi, A., Kouass, S., Alhalaili, B., Vidu, R., & Turki-Kamoun, N. (2020). An Investigation on the Synthesis of Molybdenum Oxide and Its Silica Nanoparticle Composites for Dye Degradation. *Nanomaterials*, *10*(12), 2409. https://doi.org/10.3390/nano10122409

Kant, N., & Singh, P. (2022). Review of next generation photovoltaic solar cell technology and comparative materialistic development. *Materials Today: Proceedings, First International Conference on Design and Materials*, *56*, 3460–3470. https://doi.org/10.1016/j.matpr.2021.11.116

Kayani, Z. N., Wahid, I., Saddiqe, Z., Riaz, S., Waseem, S., & Naseem, S. (2020). Tailoring of optical, biological and magnetic properties of nanocrystalline Fe doped TiO_2 thin films. *Materials Research Express*, *6*(12), 1250h2. https://doi.org/10.1088/2053-1591/ab6b5a

Kesornkhup, S., Tuantranont, A., Lomas, T., Sriprachuabwong, C., & Wasapinyokul, K. (2021). Accuracy of Swanepoel Method in Calculation of Polymer Film Thicknesses. *Acta Physica Polonica A*, *140*(2), 113–121. https://doi.org/10.12693/APhysPolA.140.113

Khetta, O. B., Attaf, A., Derbali, A., Saidi, H., Bouhdjer, A., Aida, M. S., khetta, Y. B., Messemeche, R., Nouadji, R., Rahmane, S., & Djehiche, N. E. (2022). Precursor concentration effect on the physical properties of transparent titania (Anatase- TiO_2) thin films grown by ultrasonic spray process for optoelectronics application. *Optical Materials*, *132*, 112790. https://doi.org/10.1016/j.optmat.2022.112790

Khima, N., Chelouche, A., Challali, F., Djouadi, D., Djermoune, A., Luce, M., Cricenti, A., Becerril, D., Bellucci, S., & Touam, T. (2024). TiO_2 sol–gel thin

films: Effect of acidic and basic pH on physical characteristics. *Journal of Sol-Gel Science and Technology*, *112*(1), 277–288. https://doi.org/10.1007/s10971-024-06519-1

Kochylas, I., Gardelis, S., Likodimos, V., Giannakopoulos, K. P., Falaras, P., & Nassiopoulou, A. G. (2021). Improved Surface-Enhanced-Raman Scattering Sensitivity Using Si Nanowires/Silver Nanostructures by a Single Step Metal-Assisted Chemical Etching. *Nanomaterials*, *11*(7), 1760. https://doi.org/10.3390/nano11071760

Kreft, S., Wei, D., Junge, H., & Beller, M. (2020). Recent advances on TiO_2-based photocatalytic CO_2 reduction. *EnergyChem*, *2*(6), 100044. https://doi.org/10.1016/j.enchem.2020.100044

Kumar, A., Gupta, S. K., Dhamaniya, B. P., Pathak, S. K., & Karak, S. (2023). Understanding the origin of defect states, their nature and effects on metal halide perovskite solar cells. *Materials Today Energy*, *37*, 101400. https://doi.org/10.1016/j.mtener.2023.101400

Lee, T. D., & Ebong, A. U. (2017). A review of thin film solar cell technologies and challenges. *Renewable and Sustainable Energy Reviews*, *70*, 1286–1297. https://doi.org/10.1016/j.rser.2016.12.028

Lettieri, S., Pavone, M., Fioravanti, A., Santamaria Amato, L., & Maddalena, P. (2021). Charge Carrier Processes and Optical Properties in TiO_2 and TiO_2-Based Heterojunction Photocatalysts: A Review. *Materials*, *14*(7), 1645. https://doi.org/10.3390/ma14071645

Li, J., Zhang, Q., Liu, J., Yu, M., Ma, H., Yang, J., Ye, S., Ramirez Reina, T., & Liu, J. (2020). In-situ formation of carboxylate species on TiO_2 nanosheets for enhanced visible-light photocatalytic performance. *Journal of Colloid and Interface Science*, *577*, 512–522. https://doi.org/10.1016/j.jcis.2020.05.054

Lin, C. Y. W., Channei, D., Koshy, P., Nakaruk, A., & Sorrell, C. C. (2012). Effect of Fe doping on TiO_2 films prepared by spin coating. *Ceramics International*, *38*(5), 3943–3946. https://doi.org/10.1016/j.ceramint.2012.01.047

Lourduraj, S., & Williams, R. V. (2017). Effect of iron doping on structural and optical properties of TiO_2 thin film by sol–gel routed spin coating technique. *Journal*

of Advanced Dielectrics, *07*(04), 1750024. https://doi.org/10.1142/S2010135X17500242

Mammadov, N. S., Ganiyeva, N. A., & Aliyeva, G. A. (2022). Role of renewable energy sources in the world. *Journal of Renewable Energy, Electrical and Computer Engineering*, *2*(2), 63-67.

Manickam, K., Muthusamy, V., Manickam, S., Senthil, T. S., Periyasamy, G., & Shanmugam, S. (2020). Effect of annealing temperature on structural, morphological and optical properties of nanocrystalline TiO_2 thin films synthesized by sol–gel dip coating method. *Materials Today: Proceedings, Advanced Materials for Clean Energy and Health Applications (AMCEHA) , University of Jaffna, Jafna, Sri Lanka, 6-8 February, 2019*, *23*, 68–72. https://doi.org/10.1016/j.matpr.2019.06.651

Mercy, J., M. D., Josephine Prabha, A., Bansura Banu, K., & Naveen Marshal, V. J. B. (2026). Transition metal-doped one-dimensional TiO_2: A synergistic experimental and DFT study for photocatalytic applications. *Results in Surfaces and Interfaces*, *22*, 100701. https://doi.org/10.1016/j.rsurfi.2025.100701

Mesoudy, A. E., Machon, D., Ruediger, A., Jaouad, A., Alibart, F., Ecoffey, S., & Drouin, D. (2023). Band gap narrowing induced by oxygen vacancies in reactively sputtered TiO_2 thin films. *Thin Solid Films*, *769*, 139737. https://doi.org/10.1016/j.tsf.2023.139737

Messemeche, R., Saidi, H., Attaf, A., Benkhetta, Y., Chala, S., Azizi, R., & Nouadji, R. (2020). Elaboration and characterization of nano-crystalline layers of transparent titanium dioxide (Anatase- TiO_2) deposited by a sol-gel (spin coating) process. *Surfaces and Interfaces*, *19*, 100482. https://doi.org/10.1016/j.surfin.2020.100482

Min, H. (2021). Thin Films Deposited By Spin Coating Technique: Review. *Pakistan Journal of Chemistry*, *11*, 38–47. https://doi.org/10.15228/2021.v11.i03-4.p07

Mohammad, B. A. (2015). Types of Solar Cells and Application. *American Journal of Optics and Photonics*, *3*(5), 94. https://doi.org/10.11648/j.ajop.20150305.17

Moumen, A., Kumarage, G. C. W., & Comini, E. (2022). P-Type Metal Oxide Semiconductor Thin Films: Synthesis and Chemical Sensor Applications. *Sensors*, *22*(4), 1359. https://doi.org/10.3390/s22041359

Mragui, A. E., Aadnan, I., Zegaoui, O., & Silva, J. C. G. E. da. (2023). Physico-chemical characterization and photocatalytic activity assessment under UV-A and visible-light irradiation of iron-doped TiO_2 nanoparticles. *Arabian Journal of Chemistry*, *16*. https://doi.org/10.1016/j.arabjc.2023.105331

Muniz, F. T. L., Miranda, M. R., Morilla dos Santos, C., & Sasaki, J. M. (2016). The Scherrer equation and the dynamical theory of X-ray diffraction. *Acta Crystallographica Section A: Foundations and Advances*, *72*(3), 385–390. https://scripts.iucr.org/cgi-bin/paper?S205327331600365X

Mustafa, H. A. M., & Jameel, D. A. (2021). Modeling and the main stages of spin coating process: A review. *Journal of Applied Science and Technology Trends*, *2*(02), 119–123. https://doi.org/10.38094/jastt203109

Nair, P. B., V.B.Justinvictor, Daniel, G. P., Joy, K., Ramakrishnan, V., Kumar, D. D., & Thomas, P. V. (2014). Structural, optical, photoluminescence and photocatalytic investigations on Fe doped TiO_2 thin films. *Thin Solid Films*, *550*, 121–127. https://doi.org/10.1016/j.tsf.2013.10.112

Oviedo, A. M., Truong Thi, H., Van, Q. C., & Nguyen, H. H. (2023). Physicochemical properties of Fe-doped TiO_2 and the application in Dye-sensitized solar cells. *Optical Materials*, *137*, 113587. https://doi.org/10.1016/j.optmat.2023.113587

Prasad, R. D., Teli, B., Prasad, R. S., Prasad, R. B., Prasad, S. R., Sinha, P., ... & Guo, Z. (2024). A review on thin film technology and nanomaterial characterization techniques. *ES Materials and Manufacturing*, *25,* 1198.

Priyalakshmi D., K., Goswami, P., & Chaturvedi, H. (2022). Fabrication of nanocrystalline TiO_2 thin films using Sol-Gel spin coating technology and investigation of its structural, morphology and optical characteristics. *Applied Surface Science*, *591*, 153226. https://doi.org/10.1016/j.apsusc.2022.153226

Racovita, A. D. (2022). Titanium Dioxide: Structure, Impact and Toxicity. *International Journal of Environmental Research and Public Health*, *19*(9), 5681. https://doi.org/10.3390/ijerph19095681

Rajeswari, R., Venugopal, D., Dhayal Raj, A., Arumugam, J., John Sundaram, S., & Kaviyarasu, K. (2021). Effect of doping concentration for the properties of Fe doped TiO_2 thin films applications. *Materials Today: Proceedings, NANOSMATAFRICA-2018*, *36*, 468–474. https://doi.org/10.1016/j.matpr.2020.05.109

Rasim Mohammed, H., & Mohammed Hadi Shinen, D. (2023). Study the optical properties of Titanium dioxide Nano films. *Materials Today: Proceedings, International Virtual Conference on Sustainable Materials (IVCSM-2k20)*, *81*, 459–463. https://doi.org/10.1016/j.matpr.2021.03.613

Rhatta, N., Gn, K., Gundanna, S. K., & Bhatta, U. M. (2020). Effect of thermal annealing on structural and electrical properties of TiO_2 thin films. *Thin Solid Films*, *710*, 138262. https://doi.org/10.1016/j.tsf.2020.138262

Ruan, X., Cui, X., Cui, Y., Fan, X., Li, Z., Xie, T., Ba, K., Jia, G., Zhang, H., Zhang, L., Zhang, W., Zhao, X., Leng, J., Jin, S., Singh, D. J., & Zheng, W. (2022). Favorable Energy Band Alignment of TiO_2 Anatase/Rutile Heterophase Homojunctions Yields Photocatalytic Hydrogen Evolution with Quantum Efficiency Exceeding 45.6%. *Advanced Energy Materials*, *12*(16), 2200298. https://doi.org/10.1002/aenm.202200298

Ruzgar, S., & Pehlivanoglu, S. A. (2020). The effect of Fe dopant on structural, optical properties of TiO_2 thin films and electrical performance of TiO_2 based photodiode. *Superlattices and Microstructures*, *145*, 106636. https://doi.org/10.1016/j.spmi.2020.106636

Sadia, S. I., Shishir, M. K. H., Ahmed, S., Aidid, A. R., Islam, M. M., Rana, M. M., Al, -Reza Sharif Md, & Alam, M. A. (2024). Crystallographic biography on nanocrystalline phase of polymorphs titanium dioxide (TiO_2): A perspective static review. *South African Journal of Chemical Engineering*, *50*(1), 51–64. https://doi.org/10.1016/j.sajce.2024.07.005

Sahadat, H., Md., & Ahmed, S. (2023). Easy and green synthesis of TiO_2 (Anatase and Rutile): Estimation of crystallite size using Scherrer equation, Williamson-Hall plot, Monshi-Scherrer Model, size-strain plot, Halder- Wagner Model. *Results in Materials*, *20*, 100492. https://doi.org/10.1016/j.rinma.2023.100492

Sassi, S., Bouich, A., Hajjaji, A., Khezami, L., Bessais, B., & Soucase, B. M. (2024). Cu-Doped TiO_2 Thin Films by Spin Coating: Investigation of Structural and Optical Properties. *Inorganics*, *12*(7), 188. https://doi.org/10.3390/inorganics12070188

Sharma, N., & Kumar, R. (2022). Effect of spin speed on the properties of TiO_2 thin films. *Materials Today: Proceedings, International Conference on Materials, Mechanics, Mechatronics and Manufacturing*, *62*, 6615–6618. https://doi.org/10.1016/j.matpr.2022.04.614

Shanthi, J., Aishwarya, S., & Swathi, R. (2020). Enhanced optical & structural properties by potassium iodide doping on spin coated TiO_2 thin films. *Chemical Data Collections*, *29*, 100494. https://doi.org/10.1016/j.cdc.2020.100494

Shuhadah, A., Rosli, Z. M., Juoi, J. M., Johari, N. D., Suzaim, F. H., & Moriga, T. (1). Influence Of Water And Precursor Molarity On The TiO_2 Thin Films Deposited From Solventless Sol-Gel. *Journal Of Advanced Manufacturing Technology (JAMT)*, *12*(1(4), 125-134. Retrieved from https://jamt.utem.edu.my/jamt/article/view/4903

Shymanovska, V. V., Khalyavka, T. A., Manuilov, E. V., Gavrilko, T. A., Aho, A., Naumov, V. V., & Shcherban, N. D. (2022). Effect of surface doping of TiO_2 powders with Fe ions on the structural, optical and photocatalytic properties of anatase and rutile. *Journal of Physics and Chemistry of Solids*, *160*, 110308. https://doi.org/10.1016/j.jpcs.2021.110308

Simon, A. H. (2025). Sputter processing. In *Handbook of Thin Film Deposition* (pp. 93–140). Elsevier. https://doi.org/10.1016/B978-0-443-13523-1.00011-9

Sobczyk-Guzenda, A., Owczarek, S., Szymanowski, H., Volesky, L., Walkowiak, B., Miszczak, S., & Gazicki-Lipman, M. (2015). Iron doped thin TiO_2 films synthesized with the RF PECVD method. *Ceramics International*, *41*(6), 7496–7500. https://doi.org/10.1016/j.ceramint.2015.02.071

Thomas, S., Kalarikkal, N., Oluwafemi, O. S., & Wu, J. (Eds.). (2019). *Nanomaterials for solar cell applications*. Elsevier.

Timoumi, A., Alameer, O. O., & Alamri, S. N. (2023). Intensive study of coating multilayer TiO_2 nanoparticles thin films used for optoelectronics devices. *Results in Materials*, *18*, 100390. https://doi.org/10.1016/j.rinma.2023.100390

Vaiciulis, I., Girtan, M., Stanculescu, A., Leontie, L., Habelhames, F., & Antohe, S. (2012). On titanium oxide spray deposited thin films for solar cells applications. *Proceedings of the Romanian Academy - Series A (Mathematics, Physics, Technical Sciences, Information Science)*, *13*(4), 335–342.

Wahyuni, E. T., Lestari, N. D., Cinjana, I. R., Annur, S., Natsir, T. A., & Mudasir, M. (2023). Doping TiO_2 with Fe from iron rusty waste for enhancing its activity under visible light in the Congo red dye photodegradation. *Journal of Engineering and Applied Science*, *70*(1), 9. https://doi.org/10.1186/s44147-023-00178-9

Wang, Y.-H., Rahman, K. H., Wu, C.-C., & Chen, K.-C. (2020). A Review on the Pathways of the Improved Structural Characteristics and Photocatalytic Performance of Titanium Dioxide (TiO_2) Thin Films Fabricated by the Magnetron-Sputtering Technique. *Catalysts*, *10*(6), 598. https://doi.org/10.3390/catal10060598

Waweru, G. S., Kiprotich, S., & Waithaka, P. (2024). *Structural and optical properties of Fe doped* TiO_2 *nanoparticles: Investigation of effects of different doping concentration*. https://hdl.handle.net/10625/63241

Xu, S., Zhang, L., Wang, B., & Ruoff, R. S. (2021). Chemical vapor deposition of graphene on thin-metal films. *Cell Reports Physical Science*, *2*(3). https://doi.org/10.1016/j.xcrp.2021.100372

Yin, Y., Huang, C., Luo, X., & Xu, B. (2023). Iron behavior during the continuous phase transition of iron-doped titanium dioxide determined via high-temperature in-situ X-ray diffraction, rietveld refinement and density functional theory studies. *Journal of Materials Research and Technology*, *23*, 2426–2439. https://doi.org/10.1016/j.jmrt.2023.01.159

Yunus, Y., Mahadzir, N. A., Mohamed Ansari, M. N., Tg Abd Aziz, T. H., Mohd Afdzaluddin, A., Anwar, H., Wang, M., & Ismail, A. G. (2022). Review of the Common Deposition Methods of Thin-Film Pentacene, Its Derivatives and

Their Performance. *Polymers*, *14*(6), 1112. https://doi.org/10.3390/polym14061112

Zerrouk, I., Bensouici, F., Benyakhlef, M., & Boultif, A. (2026a). Synthesis and characterisation of Fe-doped TiO2 films on soda–lime glass: Effect of pure TiO_2 interlayer as a diffusion barrier toward photocatalytic applications. *Thin Solid Films*, *844*, 140958. https://doi.org/10.1016/j.tsf.2026.140958

Zhang, J.-Y., Boyd, I. W., O'Sullivan, B. J., Hurley, P. K., Kelly, P. V., & Sénateur, J.-P. (2002). Nanocrystalline TiO2 films studied by optical, XRD and FTIR spectroscopy. *Journal of Non-Crystalline Solids*, *303*(1), 134–138. https://doi.org/10.1016/S0022-3093(02)00973-0

Zulkefle, M. A., Rahman, R. A., Yusof, K. A., Abdullah, W. F. H., Rusop, M., & Herman, S. H. (n.d.). *Spin Speed and Duration Dependence of TiO_2 Thin Films pH Sensing Behavior*. https://doi.org/10.1155/2016/9746156

APPENDICES

Appendix 1: Research authorization

MURANG'A UNIVERSITY OF TECHNOLOGY
Office of the Director, Postgraduate Studies
E-mail: bps@mut.ac.ke
Website: www.mut.ac.ke
P.O. Box 75-10200
Murang'a, Kenya

Ref: MUT/ARP/PGS/19/2020 /VOL.1 **Date:** 4th May, 2026

Ms. Sharon Chemutai-AS402/5134/2024,
School of Pure and Applied Sciences,
Murang'a University of Technology,
P.O. Box 75-10,200
Murang'a.

Dear Ms. Chemutai,

RE: APPROVAL OF RESEARCH PROPOSAL AND SUPERVISORS.

I am pleased to inform you that the Directorate of Postgraduate Studies on 25th February, 2026 considered and approved your Master research proposal entitled ***"Synthesis Characterization of Iron-Doped Titanium Dioxide Thin Films."*** and appointed the following as supervisors:

1. Dr. John Njagi - Murang'a University of Technology
2. Dr. Jatani Ungula - Kenya Methodist University

You may now proceed with your data collection subject to obtaining research permit from NACOSTI, if required. You should also begin consulting your supervisors and submit through them quarterly progress reports to the Director Postgraduate Studies through your CoD and School Dean. Progress Reports forms can be accessed in the Student Portal.

It is the policy and regulations of the University that you observe deadlines. The guidelines on Postgraduate supervision can be accessed in the post graduate Handbook.

Your responsibilities as a student will include, among others;

i. Maintain regular consultation with your supervisor(s), at least once a month
ii. Submit quarterly reports on time, through your supervisors, CoD, Dean and to the Director of Postgraduate Studies;

iii. Ensure quality work all through;
iv. Present your research findings at 2-3 seminars/conferences prior to thesis examination.
v. Publish one article from your research findings in a refereed journal prior to thesis examination.

For any further clarification please contact the undersigned.

Yours Sincerely,

Prof. Geoffrey Muchiri, PhD
Director, Postgraduate Studies
GM/MMK

DIRECTORATE OF POSTGRADUATE STUDIES
MURANG'A UNIVERSITY OF TECHNOLOGY
05 MAY 2026
P. O. Box 75 - 10200, MURANG'A
Tel: 0771463515, Email: info@mut.ac.ke

Copy to:
1. Registrar, Academics, Research and Students Affairs
2. Dean, School of Pure and Applied Sciences

Appendix 2: Publication

This thesis has produced the following paper

Sharon, C., Njagi, J., Ungula, J., Kiprotich, S. (2026). Effect of Precursor Solution Volume on Structural and Optical Properties of Iron Doped Titanium Dioxide Thin Films Prepared by Spin Coating. *Advances in Materials*, *15*(3), 91-98. https://doi.org/10.11648/j.am.20261503.12